Investigating the cellular mechanisms underlying Yap-dependent choroid fissure closure in zebrafish.

Niccolo Fioritti

University College London
Department of Cell and Developmental Biology

PhD Supervisors:
Professor Stephen Wilson, Dr Isaac Bianco

A thesis submitted for the degree of
Doctor of Philosophy

March 2021

Declaration

I, Niccolo Fioritti, confirm that the work presented in this thesis is my own. Where information has been derived from other sources, I confirm that this has been indicated in the thesis.

Abstract

Coloboma is a clinical condition in which failure of choroid fissure closure during development leads to defects in the mature eye. Coloboma is one of the main causes of visual impairments in humans and it can be both syndromic and isolated. Mutations in the *YAP* gene, a key regulator of tissue and organ shape and size, cause coloboma both in humans and zebrafish by largely unknown mechanisms. In zebrafish, Yap and its homologue Taz have been shown to be critical in the specification of the retina pigment epithelium (RPE). This study investigates potential cellular mechanisms of Yap-mediated choroid fissure closure using the *yap*^{nl13} zebrafish coloboma mutant, focusing on the RPE.

Firstly, we investigated the specificity of *yap*^{nl13} phenotype. Although *yap* is broadly expressed in the zebrafish embryo, the phenotype of *yap*^{nl13} is specific to the eye. Using RT-PCR and qRT-PCR experiments we assessed and excluded the presence of eye specific alternative *yap* isoforms that could correlate with the specificity of the phenotype.

Secondly, we aimed to understand whether the *yap*^{nl13} mutation affected the specification and proliferation of the RPE. Confocal time-lapse experiments revealed that both specification and proliferation of the RPE are not affected in *yap*^{nl13} zebrafish mutant.

Finally, we aimed to understand if the *yap*^{nl13} mutation impairs mechanotransduction in the developing RPE. Yap is a key effector in mechanotransduction and is critical for the maintenance of cell and tissue mechano-homeostasis. Immunohistochemistry experiments coupled with morphological analysis of the RPE cells suggested an impairment in actomyosin contractility in the *yap*^{nl13} mutant. Decreasing cell contractility, using both chemical and genetic manipulation of myosin, increases the frequency of coloboma in *yap*^{nl13} mutants whereas increasing cell contractility rescues the phenotype.

This work highlights the role of Yap in generating the tissue tension required for optic cup fusion. We suggest that the *yap*^{nl13} mutation results in an RPE-specific

downregulation of cell contractility which affects the correct folding of the optic cup resulting in failure of choroid fissure closure.

Impact Statement

In this work I provide new information about the role of the gene *yap* in eye morphogenesis with a focus on its function in choroid fissure closure. Mutation of the *yap* gene is causative of coloboma both in human and in zebrafish. Coloboma arises when the choroid fissure fails to fuse during the development of the eye, and it is one of the main causes of congenital visual impairment and blindness in human. Although failure in the fusion of the choroid fissure represents a major cause of visual impairment, the cellular and molecular mechanisms underlying this process are still poorly understood. The data gathered in this work provides a possible mechanism for the formation of coloboma phenotype in *yap* mutants.

The observations performed on the *yap*^{nl13} zebrafish mutant provide a specific example of the role of this gene in the regulation of the mechanical forces during eye morphogenesis. While Yap has been identified as critical in cell tension, its role in the regulation of mechanotransduction in the context of the eye has not been previously explored. This work identifies *yap* as a key gene ensuring the correct regulation of the mechanical properties of the RPE tissues during eye morphogenesis.

Furthermore, the incomplete penetrance of the *yap*^{nl13} zebrafish mutant provides a sensitised background facilitating the discovery and the screening of genes involved in RPE genesis and ocular diseases. This will help to broaden our understanding of the complex genetics underlying congenital eye defects.

Acknowledgements

Writing the acknowledgements does feel a bit weird: some sort of final sigh, both catching breath from the thesis-writing, and an emotional sigh for a journey that comes to an end. Even more odd is writing them during this pandemic which made everything a bit weirder and more intense: I'll take this as an excuse for these acknowledgments being much longer (and possibly cheesier) that I expected. Thank you in advance for indulging me.

The following pages are the result of the direct and indirect effort of many people: some of you helped me daily in the lab, some of you helped me out of the lab, some of you (poor you!) managed to do both! I owe to all of you, for helping me reaching this point, for your teaching and for your support.

I'd firstly like to thank both Steve and Gaia for giving me the possibility to start this PhD and for your scientific guidance. Thank you, Steve, for welcoming me in this beautiful lab and for having made this group as beautiful and creative as it is. Thank you, Gaia, for the patience needed for supervising me and coping with my brain, as scattered as my bench. I learned a lot in these years, and I want to thank you a huge lot for this.

I'm incredibly glad of having had the chance to meet the whole first floor family: it is a beautiful and rich environment and you all are the best group of people I could hope to be surrounded by. I am thankful to each one of you for having helped me in many a way during my PhD. A huge thank you to:

Yama and Isaac for your supervision on my PhD; Eirinn for introducing me to the joys and pains of python and electronics; Gareth for your jokes and your lab tips; Asaph for your stories and for all the time you spent trying to explain me more on AI; Giulia for our endless chat on books, science, life, the universe and everything both in front of coffees and in the office (ergh... still sorry to everyone who's reading this and suffered from the continuous chatter...); Leo for your bench help, wisdom and for the calm you transmitted. Lisa my PhD sister: I'm happy we shared our journey and again congrats! Of course, thanks for the… "faff"! Joanna another of my PhD sisters, for the patience to listen to my paranoias and all of

your suggestions. I'm missing you hissing in the corridors; Anya for our chats, the boardgames, the zombies killed together and the (a few times too many) beers! Chintan, my desk mate! Thank you for coping with my (mostly useless) interruptions and for my "as engineer, do you think that…" questions; Ingrid for always irradiating me with your happiness and joy. I miss your positivity! Masa for all the tips on biomechanics and immunos. And thanks for the hospitality in your office while I was using imaris; Paride for the help on grasping stats. I cannot wait to be hearing your guitar live again! Hannah for all our weird exchanges on science, merging into books then music, theatre, philosophy…! Shannon for your enthusiasm and positive energy that still resonates in me; Sabine for all the game nights you organized; Sumi, thank you for being so incredibly kind every time I asked for any help in the lab; Tom for the huge wisdom shared on everything! I insist: you should definitely start a podcast! Diz for showing me around the lab and always helping me whenever I needed the hardest things to find. A special thank you to Declan for having adopted me as the "little brother you do have", thank you for the support, the patience to listen to my babbling mind and the wisdom you shared, together with the beers and walks. And to Ana for the direction and the needed tough love. If ever I managed to be organized (or just slightly less chaotic) I probably owe it to you -bench-wise, desk-wise, life-wise…- Oh. And thank you for never having bitten me.

A huge thank you for my London family: Renato and Ruth: having you guys as my home for most of my PhD has been incredible and I'm so, so glad for all of our time together filled with food, talks, music, laughter and wisdom. You've been an amazing support: love you guys!

Of course, a thank you to my far friends who supported me: Teo, Barla, Sara, Chiara, Mela, Gio, Paul. The time we managed to spend together or talking to you has been critical for keeping me sane (or as sane as I get anyway) during this journey: thank you for sharing the joys and pains of this PhD together and been there even if we're far. Garbs: this line has been added on purpose for you after yesterday's skypub: an extra thank you for having read the pre-alpha version of some of these chapters (I hope I can return the favour soon!). And the "climbing crew" who also listened to my fish-related frustrations as I fell from the heights:

Eva (thanks a huge lot for the patience of proof-reading all those pages!), Aaron, Graham, Jo, Alex, Mira, Pav, Alison and Clive…The evenings together made this far land home.

Thank you, Franco for having shown me this zebrafish sea in the first place and for our talks on books, science and life.

Thank you to my family, who believed in me enough for me to arrive here and supported me all the way through, since the very beginning: it has been a long journey… I love you and I miss you! Thanks for being there anytime I need help, to support me or celebrate my successes (or my failures!) with me.

And finally, thank you Ros: thank you for your incredibly accurate proof reading (I'm leaving an annoyingly misplaced bold full stop here, just for you**.**). But mostly thank you for your huge patience and for being next to me all this time, for all the cheering up when needed and the celebrations at every chance we had. I'm so glad you're with me here and I couldn't have done it without you.

Tomorrow I'll probably freak out realizing all the wise and witty things I've always wanted to write in my acknowledgements and the names of the people I didn't mention. If, for some reason, you didn't find your name here, I deeply apologize. If you'll ever read these lines and resent the absence of your name: text me and I'll owe you a beer. Or whatever you fancy. But now it's late, and my sparse and random neurons cry for rest.

So long, and thanks for all the fish.

Table of Contents

Table of Figures

Chapter 1.

Introduction

1.1 The development of the eye.

The development of the eye is strongly evolutionarily conserved across vertebrates (Lamb et al., 2007; Sinn and Wittbrodt, 2013; Treisman, 2004). The first step in eye development is the specification of the eye field. The single central eye field subsequently splits into two symmetrical anlagen which evaginate distally generating the optic vesicles (OV). At the end of its evagination the distal-most part of the optic vesicle invaginates generating a bilayered structure, the optic cup (OC), in which the outer retinal pigment epithelium (RPE) enwraps the neuroretina (NR) (Chow and Lang, 2001).

1.1.1 Establishment of the eye field.

The eye field is located in the rostral part of the neuroectoderm and gives origin to the eye structure. Its molecular signature is the expression of genes encoding eye-field transcription factors (EFTFs), including *Pax6, Six3, Opx2*, and *Rx*. Mutation or inactivation of each of the EFTFs leads to eye phenotypes in all vertebrate species. Conversely, overexpression of EFTFs genes can be sufficient to expand the optic field (Chow *et al.*, 1999; Loosli, Winkler and Wittbrodt, 1999; Bernier *et al.*, 2000; Loosli *et al.*, 2001; Zuber *et al.*, 2003; Bailey *et al.*, 2004)**.**

One of the early-acting transcription factors required for the specification of the eye field is Otx2. Otx2 is critical for the specification of the forebrain and its loss results in lack of forebrain and midbrain in mouse (Acampora *et al.*, 1995; Matsuo *et al.*, 1995). Expression of *Otx2* is also required for the neuroectoderm to become competent for the development of ocular tissues. Indeed, deficiency of *Otx1* and *Otx2* gene expression leads to eye defects in a dosage dependent manner (Martinez-Morales *et al.*, 2001). The requirement of *Otx2* for eye structure competence has been observed by ectopic expression of the EFTFs: EFTFs expression is sufficient to drive the formation of ectopic eye tissues only in the anterior region of the neural plate, where *Otx2* is expressed (Loosli, Winkler and Wittbrodt, 1999; Chuang and Raymond, 2002; Zuber *et al.*, 2003).

Otx2 expression domain is caudally restricted by Wnt activity, which is, in turn, rostrally inhibited. Reduction of Wnt/β-catenin anterior inhibition results in the

expansion of the caudal diencephalic and midbrain territory at the expense of eye and telencephalic tissue. Conversely, ectopic inhibition of the Wnt/β-catenin pathway is sufficient to expand caudally the telencephalon and eyes domains (Heisenberg *et al.*, 2001; van de Water *et al.*, 2001; Houart *et al.*, 2002). This can be also observed in the *masterblind* (*mbl*) zebrafish mutant in which loss of rostral inhibition of Wnt activity results in expansion of the caudal diencephalon at the expenses of both the telencephalon and the eye field (Heisenberg *et al.*, 2001; Wilson and Houart, 2004; Stigloher *et al.*, 2006).

Alteration of Wnt/β-cateni rostral inhibition at early stages of anterior neural plate (ANP) patterning affects both the telencephalon and the eye field as at this developmental stage these domains are not yet segregated (Stigloher *et al.*, 2006). The establishment of the eye field and its segregation from the telencephalon requires the expression of the eye field determinant *rx3* (Loosli *et al.*, 2003; Stigloher *et al.*, 2006; Sinn and Wittbrodt, 2013). Loss of Rx3 activity is sufficient to result in lack of eye development in zebrafish (Loosli *et al.*, 2003; Stigloher *et al.*, 2006). The role of *rx3* and its homologues in the establishment of the eye field is conserved across vertebrates and it has been described in Xenopus, Medaka and mouse (Loosli *et al.*, 2001; Tucker *et al.*, 2001; Zuber *et al.*, 2003; Fish *et al.*, 2014).

Once established, the eye field domain is restricted anteriorly by the telencephalon and caudally be the diencephalon. Caudally the activation of Wnt non-canonical pathway restricts the activity of the Wnt/β-catenin pathway to the diencephalon. In particular, it was observed in zebrafish that Wnt11 and the eye field specific Wnt receptor Fzd5 are required for the establishment of its boundary with the diencephalon (Cavodeassi *et al.*, 2005). In zebrafish, the establishment of the anterior boundary of the eye field domain is dependent on Bmp activity originating at the rostral margin of the ANP. Here, Bmp restricts rostrally *rx3* activity while promoting telencephalic fate of the anterior region of the ANP (Bielen and Houart, 2012).

The expression of *rx3* in the eye field domain is critical for the maintenance of the cohesion and of the segregation of the eye field. It was observed in zebrafish that *rx3* is required for the regulation of *eph* and *ephrin* expression in the eye field and

in the surrounding anterior neural plate (Cavodeassi, Ivanovitch and Wilson, 2013). Ephrin and Eph are membrane proteins regulating cell-cell interaction often responsible for the repulsive behaviour between different cellular domains (Pasquale, 2008). In absence of functional *rx3,* the signalling from Eph/ephrin is disrupted, resulting in loss of eye field boundaries and of the segregation of its cells. Disruption of the segregation of the eye field due to loss of Eph/Ephrin activity resulted in misregulation of eye field splitting and optic vesicle evagination (Pasquale, 2008).

1.1.2 Splitting of the eye field and optic vesicle evagination.

Once specified, the single central eye field becomes split into two symmetrical retinal primordia. Failure in the separation of the eye field leads to cyclopia as the consequence of the development of a single central retinal primordium. The physical division of the eye field relies on TGF-β and FGF signalling originated from the axial mesoderm underlying the eye field (Rebagliati *et al.*, 1998; Varga, Wegner and Westerfield, 1999; Sinn and Wittbrodt, 2013). These factors induce migration of cells from the prospective hypothalamus from the posterior region of the eye field dividing it into two symmetrical regions (Varga, Wegner and Westerfield, 1999; Wilson and Houart, 2004; Sinn and Wittbrodt, 2013). Simultaneously, Shh secretion from the ventral midline inhibits the expression of *pax6* in the medial region of the eye fields, splitting its expressing domain in two (Chiang *et al.*, 1996; Roessler *et al.*, 1996). A nice example for the role of Shh in the suppression of *pax6* comes from studies performed in *Astyanax mexicanus* (Yamamoto, Stock and Jeffery, 2004). In this species there are two populations, one with eyes - the surface one - and one which does not develop eyes - the cave one. In the cave population overexpression of *shh* from the prechordal plate inhibits *pax6* expression, obliterating the eye field. This overexpression is sufficient to induce eye regression in embryos of the surface population. The role of Shh for eye field splitting is highly conserved. In mammals, loss of Shh signalling is causative of cyclopia as observed both in mouse and human (Chiang *et al.*, 1996; Roessler *et al.*, 1996).

As the eye field is split into two eye primordia, the process of evagination of the optic vesicle takes place **(Fig. 1.0).** In amniotes, at the moment of optic vesicle evagination, the cells of the eye vesicle are organised as a polarised cuboidal epithelium: changes in shape of the neuroepithelium drive the lateral evagination of the neural tube ventricle originating the optic vesicle **(Fig. 1.0 A).** Conversely, in teleosts the optic vesicle originates from the dense mass of the eye field **(Fig. 1.0 B)**. In this class, at the moment of its evagination, the eye field is comprised of two different cell populations which are required for the progression of the optic vesicle morphogenesis (Ivanovitch et al., 2013). In zebrafish, the cells at the margin of the eye field are organised into a pseudostratified neuroepithelium prior to the epithelialization of the surrounding neural tissue. As the marginal cells of the eye fields organise into an epithelium, the cells in the inner eye field, which are initially mesenchymal, undergo mesenchymal to epithelial transition (MET) and intercalate in the eye field pseudostratified epithelium. The intercalation process of the inner mass of the eye field in the peripheral eye field neuroepithelium leads to the formation of a virtual ventricle within the optic vesicle. This process coupled with the thickening of the forming eye neuroepithelium leads to the lateral evagination of the optic vesicle.

The whole process of epithelization of the eye field and formation of the optic vesicle is strongly reliant on extracellular matrix (ECM) deposition. Deposition of ECM around the eye field is required for the acquisition of neuroepithelial characteristics by the peripheral cells of the eye field. The ECM is in fact a critical signal inducing and maintaining the polarisation and the organisation of the eye field neuroepithelium (Ivanovitch et al., 2013). In absence of both Laminin and the apical polarity protein Pard6 the epithelization of the eye field fails and the whole optic vesicle evagination is compromised. This indicates that the formation of the neuroepithelium from the eye field is required for its evagination.

As the optic vesicle evaginates, the naso-temporal axis of the eye is established. The main determinants for of the nasal and temporal neuroepithelium are *foxg1* and *foxd1* respectively (Picker *et al.*, 2009; Hernández-Bejarano *et al.*, 2015). The origin of the naso-temporal patterning of the optic cup relies on its exposure to both Fgf signalling from the dorsal forebrain and Shh signalling from the ventral

forebrain during evagination. During the evagination of the optic vesicle and the following formation of the optic cup, the eye primordia rotate by 90°, moving the original dorsal region of the eye in the final nasal position (Fig. 1.2 B). Once the *foxg1* and *foxd1* expressing domains are established by Fgf and Shh signalling respectively, the boundary between them is sustained by their mutual repression (Hernández-Bejarano *et al.*, 2015). Indeed, inhibition of Fgf activity expands the temporal domain while loss of Hh activity expands caudally the nasal domain.

During the evagination of the optic vesicle, the patterning of the retina takes place resulting in the differentiation of the retina pigment epithelium (RPE) and of the neuroretina **(Fig. 1.0 C)**. At the beginning of optic vesicle evagination the ocular neuroepithelium is bipotential as the presumptive RPE is competent to develop in neuroretina and the presumptive neuroretina has the potency to differentiate into RPE. As the optic vesicle approaches the surface ectoderm, its most distal region acquires neuroretinal identity, while the tissue adjacent to the prospective neuroretina, in the dorsal region of the optic cup, acquires RPE identity. (Fuhrmann, 2010). The initial determinant of the RPE is *mitf*, which is initially expressed across the whole optic vesicle (Nguyen and Arnheiter, 2000): inhibition of *mitf* results in the differentiation of the neuroretina, while sustained *mitf* expression coupled with *otx2* are required for the specification of the RPE (See paragraph 1.2). The earliest neuroretina specific gene is the homeobox gene *Vsx2/Chx10*. Chx10- together with Sox10 are responsible for the inhibition of Mitf activity in the distal region of the eye neuroepithelium allowing its differentiation into neuroretina. FGF derived from the surface ectoderm has been identified as the main signal responsible for the repression of *Mitf* in the prospective neuroretina (Hyer, Mima and Mikawa, 1998; Fuhrmann, 2010): removal of the surface ectoderm adjacent to the optic vesicle resulted in loss of neuroretina specification and expansion of the RPE domain. Conversely, ectopic induction of FGF secretion across the optic vesicle was sufficient to induce neuroretina specification. The study also highlighted that, in absence of cues from FGF, the neuroepithelium of the optic vesicle remains bipotent and displays both neuroretina and RPE phenotypes. However, it was shown that FGF is not sufficient to induce the transdifferentiation of RPE into neuroretina in cultured optic vesicle (Horsford et al., 2005). Experiments on mammalian optic vesicle

culture showed that abolishment of *Chx10/Vsx2* expression results in ectopic expression of *Mitf,* leading to a RPE-like identity in the neuroretina (Horsford et al., 2005). It has furthermore been shown that, when *Chx10/Vsx2* is mutated, FGF signalling fails to maintain neuroretina specification and it transdifferentiates into RPE. Thus overall, the neuroretina determination relies on the proximity of the optic vesicle to the surface ectoderm which, through FGF signalling mediated by *Chx10/Vsx2,* inhibits *Mitf* expression and generates a distal neuroretina domain.

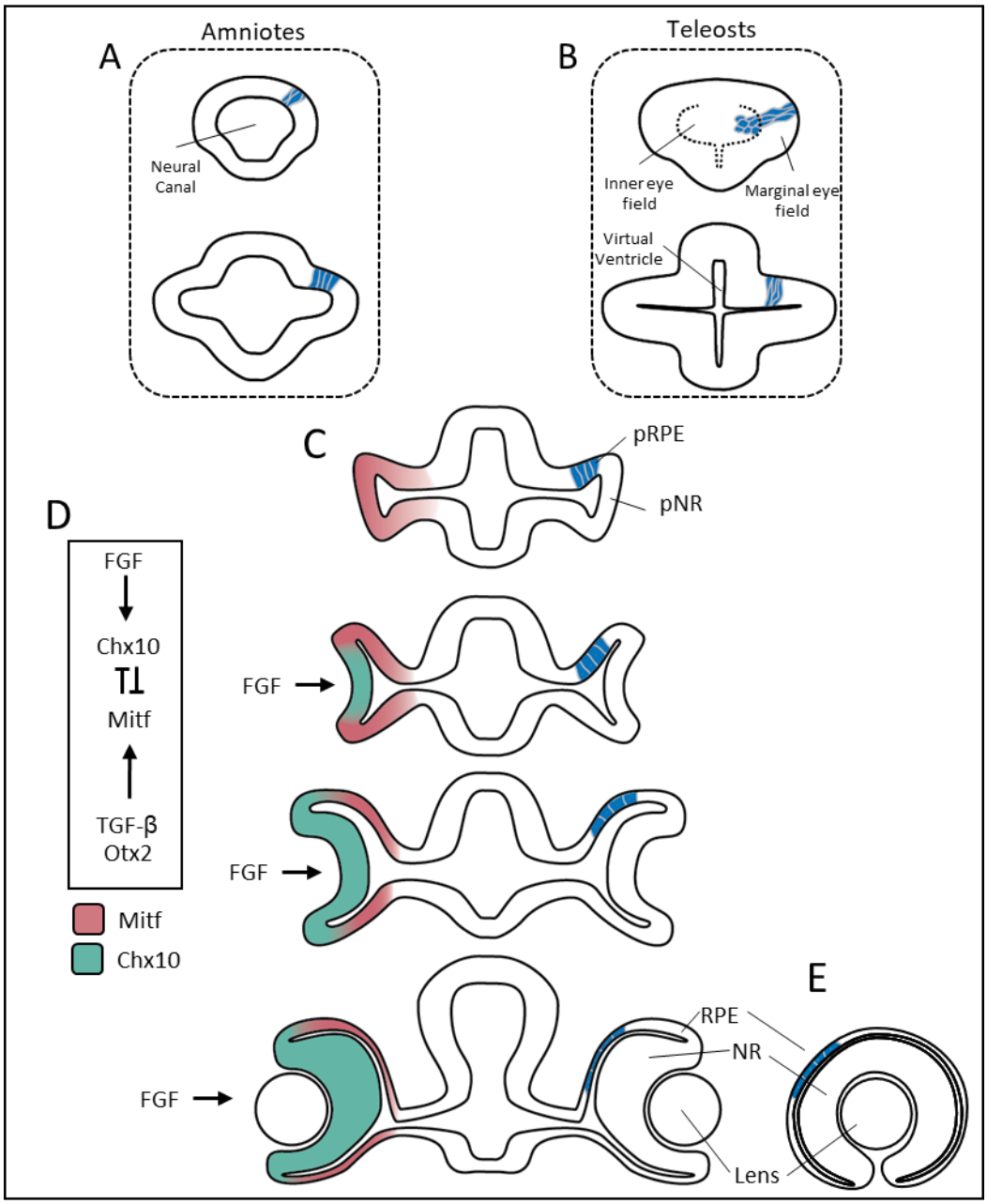

Figure 1.0| The development of the vertebrate eye.
A| In amniotes the formation of the OV results from the lateral evagination of the neural tube (Adapted from: Martinez-Morales, Cavodeassi and Bovolenta, 2017). **B|** In teleosts the OV originates from the cavitation of the mesenchymal inner eye field undergoing epithelization. **C|** During the evagination of the OV and the following invagination of the OC the RPE stretches, from a pseudostratified epithelium to cuboidal. In teleosts the stretching of the RPE continues resulting in squamous epithelium (Adapted from: Moreno-Marmol, Cavodeassi and Bovolenta, 2018). **D|** The OV initially expresses *Mitf* induced both by *Otx2* from the eye field and by TGF-β, from the periocular mesenchyme. The expression of *Mitf* is inhibited at the beginning of OV invagination in the prospective neuroretina by *Chx10*, induced by FGF signalling from the surface ectoderm. **E|** Lateral view of the invaginating optic cup.

1.1.3 Invagination of the optic cup.

Once the domains of the RPE and neuroretina are determined and the evaginating optic vesicle touches the overlying surface ectoderm, it begins to invaginate. The invagination of the optic vesicle will result in a bilayered structure, the optic cup (OC) in which the outermost layer, the RPE, enwraps the neuroretina.

The process of epithelial folding occurring during optic cup invagination has been observed and described during multiple different morphogenetic events: for instance in *Drosophila* gastrulation and in vertebrate neural tube closure (Khan *et al.*, 2014; Nikolopoulou *et al.*, 2017; Visetsouk *et al.*, 2018; Ko, Kalakuntla and Martin, 2020). Epithelial folding is driven by morphological changes in cells: in this process, cells acquire a specific “wedge shape” morphology as they constrict the apical or basal surface. This polar constriction is dependent on the contractility of the circumferential actomyosin belt, and relies on the adhesion to the ECM to transmit the generated mechanical tension at a tissue level (Pearl, Li and Green, 2017; Wen, Wang and Shibata, 2017; Krueger *et al.*, 2018). During optic cup folding, neuroretina cells undergo both basal and apical constriction depending on their position on the optic cup (Martinez-Morales, Cavodeassi and Bovolenta, 2017) **(Fig. 1.1 A,B)**.

The basal constriction of the neuroepithelium driving optic cup morphogenesis was firstly described in the medaka *ojoplano* (*opo*) mutant (Martinez-Morales *et al.*, 2009). The *opo* medaka mutant is characterised by disruption in optic cup folding while the patterning of the eye neuroepithelium is unaltered. Observations on the *opo* mutant revealed that actin deposition in the basal region of the neuroepithelium was reduced. This reduction was coupled with reduction of adhesion molecules (integrins and paxillin) anchoring the neuroepithelium to the ECM. Interestingly, reduction of integrin molecules alone was sufficient to phenocopy the *opo* phenotype, revealing that the loss of cell adhesion to the ECM is required for optic cup folding. Morphological analysis of the nuclei in the *opo* mutant neuroepithelium revealed that the eye phenotype is due to a reduction in cell tension generation. In particular, while in wild type embryos retinal nuclei appeared to be elongated in response to the cell’s tensional state, nuclei in the

opo mutant did not show such elongation. As nuclear shape reflects the mechanical tension transmitted through the ECM, loss of nuclei deformation in the *opo* mutant indicated an inefficient transmission of mechanical forces to the basal lamina due to lack of cell adhesion. This study highlighted that the basal constriction of the neuroretina is required to generate the force to invaginate the optic cup. It furthermore elucidates that the adhesion to the basal lamina is necessary for the force generated at a cellular level to be exerted at a tissue level.

The role of basal shrinkage in driving optic cup invagination has been furthermore explored in zebrafish (Nicolás-Pérez *et al.*, 2016; Sidhaye and Norden, 2017). Analyses on tissue contractility revealed an increment of myosin foci in the basal neuroepithelium which actively pulls upon the basal lamina. Similar to what observed in the *opo* mutant, downregulation of the ECM component *lamc1* resulted in loss of optic cup invagination. These data confirmed both the active role of the neuroretina in the invagination of the optic cup and the requirement of ECM in the transmission of forces generated by this tissue. The accumulation of tension at the basal margin of the neuroretina was furthermore tested directly: laser-induced cuts at the basal lamina of the neuroretina were sufficient to reduce the invagination of the optic cup. This demonstrated that the integrity of the basal ECM is required for the transmission of the force generated by the shrinking neuroretina forcing the invagination of the optic cup.

Together with basal constriction, cells of the optic cup's neuroepithelium undergo apical constriction at the hinge region between the inner and outer optic cup **(Fig. 1.1 B)**. Similar to the basal constriction, the apical constriction of the hinge cells is reliant on actomyosin contractility and is an active behaviour. It has been proposed that the change in shape of the hinge cells, coupled with force generated by the tangential expansion of the neuroretina, are sufficient to drive the optic cup invagination (Eiraku *et al.*, 2011; Eiraku, Adachi and Sasai, 2012). Studies on 3D in vitro culture suggested the "relaxation-expansion" model: in this model, the invagination of the optic cup is driven by the difference in tissue tension between the RPE (stiffer) and the neuroretina (softer). As the optic vesicle evaginates, the distal region of the expanding neuroepithelium reduces its myosin phosphorylation levels and becomes softer. The tangential expansion of the

neuroretina is thus confined by the stiffer RPE: in this situation, the apical contractility of the hinge cells is sufficient to induce a bias towards the inward bending of the neuroretina. Once this bias is initiated, the expansion of the neuroretina against the resisting force from the RPE continues driving the neural retina involution (See chapter 4; **Fig 4.0**). This model has been partly investigated in the mouse system (Carpenter *et al.*, 2015). This study showed that inhibition of Wnt signalling reduced both the number of cells at the hinge region of the optic cup and the number of RPE cells. Wnt inhibition furthermore reduced the level of myosin-mediated tension at the interface of the RPE and neuroretina. At an organ level these reductions give rise to a poorly invaginated optic cup with lack of choroid fissure closure (See paragraph 1.1.4). While this study suggested that the stiffness of the RPE is critical for optic cup invagination, it also revealed the role of the extension of the RPE domain. The study in fact suggests a “bimetallic strip” model as a mechanism driving the invagination of the optic cup: in this model the optic cup curvature originates from the difference in surface between the larger and stiffer RPE and the smaller neuroretina (Carpenter *et al.*, 2015).

In teleosts, as the optic cup invaginates, the neuroretina dramatically increases its basal surface (Heermann *et al.*, 2015): by the end of optic cup invagination, the neural retina surface has almost a 5-fold increase of its area compared to its surface at the beginning of the process. While basal constriction can model the morphological changes of the optic cup, it is not sufficient to explain the increase of surface of the neuroretina. Live confocal imaging experiments performed on zebrafish identified epithelial flow as the main mechanism feeding the expanding neuroretina during optic cup invagination **(Fig. 1.1 D)** (Picker *et al.*, 2009; Heermann *et al.*, 2015). In particular, neuroepithelial cells from both the temporal and medial portion of the optic vesicle, averting the surface ectoderm, flow around the nasal and temporal rim of the optic cup. The last cells taking part into the epithelial flow during optic cup invagination will form the RPE. The imaging also revealed that most of the rim involution movement took place in the most nasal and temporal region of the optic cup. Furthermore, the epithelial flow was not affected in embryos treated with cell proliferation inhibitor (Aphidicolin), indicating that this movement is independent by cell division (Heermann *et al.*, 2015).

Epithelial flow in the optic cup invagination has been so far correlated with repression of BMP signalling: the study analysed the patterning of the BMP antagonist *follistatin* (*fsta*) and *bambi*a (*bambi*) which were mainly expressed in the nasal and temporal region of the optic cup. This pattern corresponded to the regions where the epithelial flow is most prominent, suggesting that inhibition of BMP signalling is required for cell mobilization. Accordingly, pan-ocular expression of BMP4 resulted in arrest of the epithelial flow: in this situation, the prospective neuroretina did not migrate in the distal region of the optic cup and remained in the prospective RPE domain. The cells which did not take part in the rim flow remaining in the medial region of the optic cup did not lose their identity and differentiated in ectopic neuroretina. At organ level, arrest of the epithelial flow due to overexpression of BMP resulted in lack of choroid fissure closure (Heermann *et al.*, 2015).

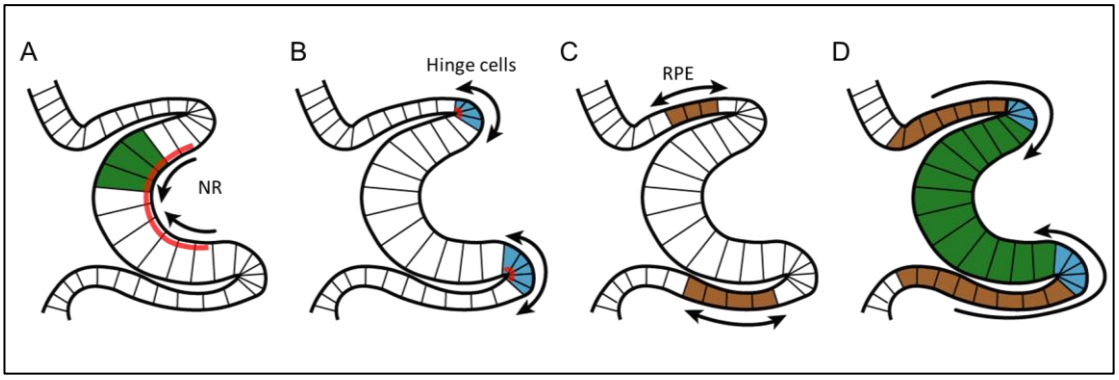

Figure 1.1| Tissue movements during eye development.
A| Apical constriction in the neuroretina (NR) driven by apical accumulation of myosin (in red). **B|** Basal constriction at the hinge cells driven by basal accumulation of myosin (in red). **C|** Stretching of the retina pigment epithelium (RPE) **D|** The simultaneous occurrence of apical and basal constriction together with the stretching of the RPE drives the epithelial flow movements during eye development (black arrows indicating the rim involution movements) (Adapted from: Eiraku, Adachi and Sasai, 2012)

While the bending of the neuroretina and the epithelial flow take place simultaneously, they are not mechanistically dependent on each other. In the *opo* mutant, where the invagination of the optic cup is impaired, there is not ectopic neuroretina, suggesting that the epithelial flow occurs even in absence of bending of the optic cup (Martinez-Morales *et al.*, 2009; Heermann *et al.*, 2015). It is

conversely suggested that the epithelial flow is impacted by external factors. One possibility lies in the active role of the RPE: during optic cup invagination the RPE stretches from a cuboidal to a squamous epithelium (Moreno-Marmol, Cavodeassi and Bovolenta, 2018). It is still unclear whether these changes in RPE cell shape are the result of a passive process due to the bending of the optic cup or whether RPE cells have an active role in regulating its shape. If the latter was the case, the active expansion of the RPE could be the force driving the epithelial flow.

1.1.4 Choroid fissure closure.

The invagination of the optic cup occurs asymmetrically, from dorsal to ventral, and this leaves a transient opening in its ventral region: the choroid or optic fissure (CF, OF). The formation of the choroid allows the population of periocular mesenchyme cells (POM) to colonise the intraocular region and give origin to the retinal vasculature and allows the axons from the retina to leave the eye (Gage *et al.*, 2005; Hartsock *et al.*, 2014; Bazin-Lopez *et al.*, 2015; James *et al.*, 2016). As development continues, the choroid fissure fuses, giving continuity to the neuroretina and the RPE.

The establishment of the dorsoventral asymmetry in the optic vesicle is critical for the correct morphogenesis/invagination of the optic cup and ultimately for the formation of the choroid fissure. Similarly to the rest of the brain, the original dorsoventral polarity of the eye is strongly reliant on ventral Shh signalling and dorsal Bmp signalling (Macdonald *et al.*, 1995; Adler and Belecky-Adams, 2002; Wilson and Houart, 2004; Yang, 2004; Lupo *et al.*, 2005; Wilson and Maden, 2005). In the dorsal eye, the Bmp signalling induces the transcriptional activation of members of the *Tbx* gene family (Veien *et al.*, 2008). Conversely, the ventral Shh gradient leads to the formation of an expression domain of the *Vax* and *Pax* gene families (**Fig. 1.2 A,B**; Ekker *et al.*, 1995; Macdonald *et al.*, 1995; Barbieri *et al.*, 1999; Lupo *et al.*, 2005; Kim and Lemke, 2006). Similarly, experiments performed *in vitro* showed that embryonic stem cell-derived eye organoids are able to independently generate this dorsoventral polarity (Hasegawa, Truman and Nose, 2016). In these organoids Bmp signalling was spontaneously activated

within the optic cup leading to the resolution of *Tbx5* and *Vax2* dorsal and ventral eye domains respectively. From these experiments it also emerged that BMP is the major regulator of D-V polarity stem-cell derived eye organoids, while Shh has a marginal role in the optic cup polarization. Furthermore, the optic cups in which the dorsoventral polarity was established were able to invaginate asymmetrically and generate a choroid fissure-like structure (Hasegawa, Truman and Nose, 2016).

Loss of dorsoventral patterning can conversely lead to a symmetric invagination of the optic cup and failure in the formation of choroid fissure. Indeed, in eye organoids lacking of dorsoventral patterning, the invagination of the optic cup occurred symmetrically and did not lead to the formation of the choroid fissure (Eiraku et al., 2011). Furthermore, disruption of Bmp signalling from the ventral optic vesicle has been proven to be required for the formation of the choroid fissure (Morcillo et al., 2006). In mouse, disruption of *Bmp7* resulted in lack of expression of eye ventral determinants *Pax2, Vax2* and *Vax1* and concomitant absence of choroid fissure formation. Correct dorsoventral patterning is not only required for the formation of the choroid fissure but also for its closure. In many cases disruption of the dorsoventral axis in the eye leads to defects in choroid fissure fusion - a condition known as coloboma. Coloboma associated with loss of dorsoventral patterning has been observed in several model systems (Barbieri *et al.*, 1999; Lupo *et al.*, 2005; Zhou *et al.*, 2008). For example, in mouse the loss of Wnt receptor Lrp6 resulted in the disruption of the dorsalizing signalling from *Bmp4* and dorsal expansion of Vax2 expression domain accompanied by loss of Tbx5 expression (Zhou *et al.*, 2008). Ultimately, the disruption of the dorsoventral patterning of the optic cup in the Lrp6 KO mouse resulted in severe eye coloboma.

Experiments performed in zebrafish showed that the formation of the choroid fissure occurs spontaneously in isolated optic cups once the naso-temporal and dorsoventral patterning of the optic vesicle are established (Gestri et al., 2018). The development of explanted optic vesicle onto the yolk of host embryos occurred normally with exception of the choroid fissure fusion, which never occurred. However, where the explant was performed during early stages of eye

development (12ss), choroid fissure formation was less consistent, suggesting that the patterning of the optic vesicle is established prior to the 12ss stage.

While the correct patterning of the eye is critical for the formation of the choroid fissure, it is not sufficient for its fusion. The experiments performed on heterotopic eye transplants showed that while the optic cup morphogenesis occurred normally in explanted optic vesicle, no transplanted eyes showed fusion of the choroid fissure (Gestri et al., 2018). Given that the optic vesicles are isolated by the periocular mesenchyme (POM) surrounding the eye, one possibility is that the lack of choroid fissure fusion is due the lack of signalling from the POM cells**.** POM cells are a cell population which has dual origin deriving both from the neural crest cells and from the mesoderm. This cell population is critical for the development of different tissues including ciliary body muscles, extraocular muscles and the eye vasculature and are furthermore required for the generation of signalling driving optic cup patterning and differentiation (Fuhrmann, Levine and Reh, 2000; Gage *et al.*, 2005; Gestri, Link and Neuhauss, 2012; Williams and Bohnsack, 2015)**.**

The role of POM cells in choroid fissure closure has been observed both in mouse and zebrafish. Mutations in the POM-specific genes, such as *Pitx2*, *lmx1b*, *foxc1*, *tfap2a* lead to the disruption of eye patterning, expansion of the *vax1* and *vax2* expression domains, disruption of the ventral retina and failure in choroid fissure closure (Evans and Gage, 2005; Berry *et al.*, 2008; McMahon *et al.*, 2009; Lupo *et al.*, 2011). These studies highlighted how POM is required for the choroid fissure closure through the establishment and maintenance of the ventral patterning of the optic cup. However, a study performed in zebrafish has been able to decouple the role of POM in choroid fissure closure from their role in ventral retina patterning (Lupo *et al.*, 2011). Abrogation of retinoic acid receptor signalling (RAR) led to failure in choroid fissure closure and disruption of ventrally expressed genes. Expression analyses performed on embryos in which RAR signalling was inhibited allowed the identification of two distinct groups of genes regulated by RAR, one of which is expressed in the ventral retina and one in the POM. Knock-down of POM specific RAR signalling targets resulted in coloboma phenotype without affecting the patterning of the ventral retina. These evidences

supported the fact that POM cells are required for choroid fissure fusion also in a process which is independent from their role in maintenance of the optic cup dorsoventral patterning.

One of the key features of choroid fissure closure is that, differently from other epithelial fusions, the nasal and temporal margin of the choroid fissure approach each other via the basal membrane. As the basal surface of the RPE is in contact with the basal lamina, at the moment of choroid fissure closure the extracellular matrix composing the lamina needs to be dissolved. This allows the two margins of the choroid fissure to get in direct contact, repolarise and fuse (James *et al.*, 2016; Bernstein *et al.*, 2018; Gestri *et al.*, 2018). Failure in the degradation of the basal membrane lining the choroid fissure is in fact sufficient to drive failure of its fusion and lead to coloboma (Tsuji *et al.*, 2012).

POM cells have a critical role in choroid fissure fusion for their role in the degradation of its basal membrane **(Fig. 1.2 E, F, G)**. While the absence of mesoderm-derived POM does not impair choroid fissure closure, disruption of genes specific to neural-crest-cell-derived POM leads to eye morphogenesis defects and coloboma (McMahon *et al.*, 2009; Sedykh *et al.*, 2017). This suggested that neural-crest-cell-derived POM are conversely essential for choroid fissure fusion. Indeed in isolated optic cup, in complete absence of POM cells, the choroid fissure fails to fuse, indicating that this cell population is required for this process (Gestri et al., 2018). The direct observation of POM cell behaviour in choroid fissure closure has been mostly performed on zebrafish (Gestri et al., 2018; James et al., 2016). In this model it was observed that motility of POM cells is required for basal lamina degradation at the level of the choroid fissure**.** In the choroid fissure area, foci of high actomyosin activity within the population of mesoderm-derived POM cells were in fact observed in regions of higher degradation of the choroid fissure basal lamina. Moreover, POM-specific inhibition of cell motility in the *talin1* loss of function mutant was sufficient to impair basal lamina degradation in the choroid fissure resulting fusion failure and coloboma. The study furthermore addressed the role of the POM-derived hyaloid vasculature in choroid fissure fusion by observation of the *cloche* zebrafish mutant. In the *cloche* mutant, that completely lacks the hyaloid vasculature, the

breakdown of the basal lamina and choroid fissure fusion occurs, even though delayed. Thus, while the hyaloid vasculature and the mesodermal-derived POM population facilitate the choroid fissure basal membrane degradation, the neural-crest-cell-derived POMs are actively contributing to this process.

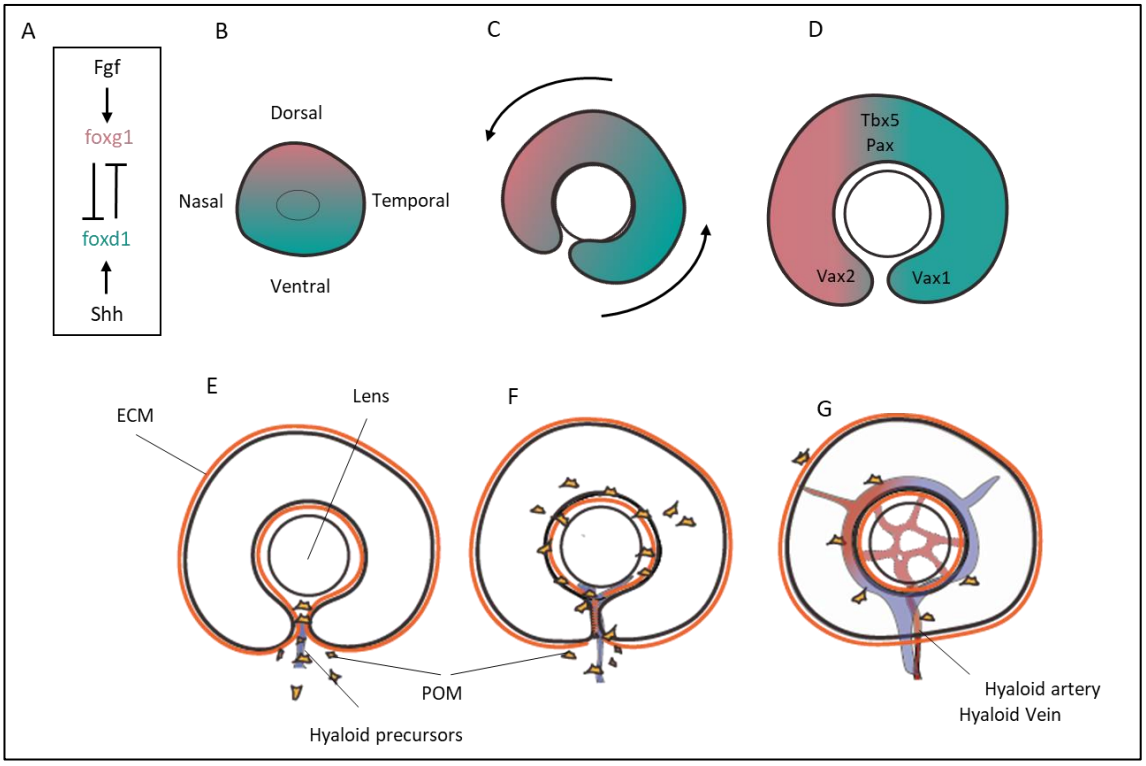

Figure 1.2 Establishment of the zebrafish eye patterning and the role of POM in choroid fissure closure
A,B| The original dorsoventral patterning is established in the optic vesicle under the influence of dorsal Fgf and ventral Shh signals. **C|** During development the eye rotates in a pinwheel motion, moving the dorsal foxg1 domain in the nasal position of the eye, and foxd1 in the temporal position. **D|** Established dorsoventral and nasotemporal eye patterning. **E|** As development proceeds, the choroid fissure is colonized by POM cells. **F|** POM cells contribute to the degradation of the basal memrbane (ECM) in the choroid fissure allowing the two fissure's margin to come in contact and fuse **G.**

1.2 The Retinal Pigment Epithelium.

Across the whole animal kingdom photoreceptors are preserved from exposure to the toxic effects of excess photons through a pigmented tissue acting as a "photon sink". In vertebrates, this pigmented tissue constitutes the outermost layer of the eye: the retinal pigment epithelium (RPE, **Fig1**). Indeed, one of the

most noticeable features of the RPE is its high pigmentation, which contributes to its function in protection of the photoreceptors and names this tissue.

In all vertebrates, the RPE is a single layered epithelium. However, the RPE differs in the morphology of its cells as in teleosts the RPE is a squamous epithelium while in amniotes it is a cuboidal epithelium. Morphologically RPE cells show apical processes which extend and interdigitate with the outer segments of the photoreceptors (Altunay, 2000)**.** The basal surface of the RPE is characterised by a number of cells folding that act to increase the cell surface area thus facilitating the exchange with the adjacent choriocapillaris vasculature. The RPE acts in fact as a buffer between the photoreceptors and the choriocapillaris plexus allowing the solute exchange between these two tissues. The direct interface between the RPE and the choriocapillaris plexus is represented by the Bruch's membrane, the basal membrane of the RPE.

1.2.1 Development of the RPE

The first molecular determinant for the RPE is the basic helix-loop-helix (bHLH) transcription factor Mitf which, together with Otx2, is required for the specification and maintenance of the RPE (Hodgkinson *et al.*, 1993; Matsuo *et al.*, 1995; Martinez-Morales *et al.*, 2001; Westenskow, Piccolo and Fuhrmann, 2009). Similar to the other eye determinants, the role of Mitf is strongly conserved across vertebrates**.** Although they are expressed prior to RPE melanization, *Mitf* and *Otx2* are required for the expression of pigment genes and loss of Mitf results in loss of pigmentation and in transdifferentiation of the RPE into neuroretina (Bumsted and Barnstable, 2000). Evidence from mouse studies indicates that *Mitf* is initially expressed across the whole optic vesicle (Nguyen and Arnheiter, 2000). Once the optic vesicle gets in contact with the surface ectoderm, ectodermal FGF signalling induces the expression of the neuroretina determinant *Vsx2. Vsx2* inhibits *Mitf* in the distal region of the optic vesicle initiating the differentiation of the neuroretina **(Fig. 1)** (Yun *et al.*, 2009; Zou and Levine, 2012).

Once induced, RPE identity is maintained by a number of upstream factors that regulate the expression of *Mitf* and *Otx2*. One of these factors is the Wnt/βcatenin

signalling (Westenskow, Piccolo and Fuhrmann, 2009): upon deletion of βcatenin, the RPE loses its epithelial organisation, and it transdifferentiates into neuroretina as indicated by downregulation of *Mitf* and *Otx2* and upregulation of *Vsx2* expression. However, while both *Otx2* and βcatenin are sufficient to drive the expression of *Mitf* in the optic vesicle, neither of these factors alone is sufficient to induce *Mitf* transcription (Westenskow *et al.*, 2010). Studies in chick showed that *β-catenin* and *Otx2* were able to drive RPE transdifferentiation of the neuroretina in optic vesicle only when these factors were co-expressed. *Otx2* acts in fact as a competence factor allowing βcatenin signalling to induce *Mitf* expression.

Sonic Hedgehog (Shh) is an important signalling factor for the differentiation, maturation and maintenance of the RPE. Experiments in chick showed that inhibition of Shh signalling resulted in disruption of the ventral RPE paired with loss of the RPE marker *Otx2*, thus indicating loss of RPE cell identity (Zhang and Yang, 2001). In *Xenopus*, inhibition of Hh signalling after eye field separation did not disrupt the neuroretina while it inhibited the differentiation of the RPE (Perron *et al.*, 2003). In particular, the study observed that Hh signalling is received by RPE precursors where it induces their maturation and the Hh signalling is furthermore sustained. Inhibition of Hh signalling resulted in loss of RPE cells and pigmentation without, however, leading to transdifferentiation into neuroretina.

Some of the factors required for the maintenance of *Mitf* expression in the RPE, such as signalling from the TGFβ and Wnt/βCatenin pathways, are derived from the extraocular tissues (i.e. extraocular mesenchyme and surface ectoderm) (Westenskow, Piccolo and Fuhrmann, 2009; Steinfeld *et al.*, 2013). Studies in chick highlighted the role of the surface ectoderm in the induction of the RPE during early optic vesicle evagination (Steinfeld *et al.*, 2013): the surface ectoderm provides BMP signalling which induces *Mitf* expression in the evaginating optic vesicle. BMP signalling is furthermore stabilised by a simultaneous contribution of *Wnt* from the dorsal surface ectoderm ultimately sustaining *Mitf* expression.

Together with the surface ectoderm, the extraocular mesenchyme is critical for the maintenance of *Mitf* expression in the RPE through TGFβ signalling

(Fuhrmann, Levine and Reh, 2000). Experiments on optic vesicle explants cultured in absence of extraocular mesenchyme showed loss of *Mitf* and Mitf-target genes (such as the matrix metalloproteinase MMP115 which is required for melanin synthesis) in the RPE. These experiments furthermore indicated that extraocular mesenchyme not only maintains RPE identity, but also restricts the neuroretina domain: absence of extraocular mesenchyme resulted in ectopic expansion of the neuroretina marker *Chx10*. The absence of extraocular mesenchyme could be compensated by Activin, indicating TGFβ as the main contributor for RPE sustenance from this tissue.

Once specified, the RPE undergoes major changes in cell shape. While at the moment of its specification it consists of a pseudostratified epithelium, during the development of the RPE its cells stretch and become cuboidal. In amniotes the mature RPE maintains the cuboidal morphology while in teleosts its stretching continues ultimately resulting in a squamous epithelium. It has not been clarified whether the invagination of the optic cup drives the stretching of the PRE or whether the morphological changes of this epithelium is an active process (Moreno-Marmol et al., 2018) (See chapter 4).

1.2.2 Function of the RPE

The mature RPE has a variety of functions (Boulton and Dayhaw-Barker, 2001). It constitutes the outer-retinal barrier: as such one of its roles is the regulation of the transport of ions and metabolites across the epithelium. Such transport is highly regulated and occurs through junctional protein complexes both in the apical and basal domains of the RPE cells (Boulton and Dayhaw-Barker, 2001; Strauss, 2005; Díaz-Coránguez, Ramos and Antonetti, 2017) (See chapter 4). The RPE has also a key role in the transport, storage and processing of retinoids which are required to sustain the visual cycle. It has the role of absorbing retinol from the bloodstream, converting it into retinal and transporting it to the photoreceptors (Raymond and Jackson, 1995; Boulton and Dayhaw-Barker, 2001; Strauss, 2005). Another main function of the RPE is the protection from phototoxicity and free radicals. Indeed, the high metabolic rate of the RPE makes it prone to the generation of reactive oxygen species (ROS). Furthermore, the constant exposure to light contributes to the generation of ROS. Melanin can thus

act as a photon sink, protecting both the RPE cells themselves and absorbing extra photons in order to protect the photoreceptors.

The RPE is furthermore critical for many aspects of eye development such as cell differentiation and morphogenesis. As previously mentioned, the RPE contributes to the generation of the mechanical forces driving the invagination of the optic vesicle and the folding of the optic cup. The RPE is also required for the development and maintenance of the underlying neuroretina (Raymond and Jackson, 1995). Experiments performed in mouse showed that ablation of the RPE during early eye development resulted in disorganization of the neuroretina and regression of the eye. While ablation of the RPE in later developmental stages allowed the development of the eye, the laminar structure of the neuroretina was disrupted. The direct correlation between sustenance of the underlying neuroretina and RPE was made evident in eye regions where the ablation of the RPE was incomplete. Exclusively in the region in which the RPE was intact, the underlying neuroretina showed healthy lamination and structure while it was disrupted in all the other regions of the eye (Longbottom *et al.*, 2009). The communication between RPE and neuroretina is critical for the regulation of the neuroretina proliferation. In particular, the presence of Gap junctions at the interface of these two tissues allows the release of proliferative signals from the RPE (Pearson *et al.*, 2005; Tibber, Becker and Jeffery, 2007). One of the mechanisms through which the RPE sustains the regulation of neuroretina proliferation is through the release of soluble ATP driven by Ca^{2+} waves. The RPE has been observed releasing ATP from the apical region, facing the neuroretina: secreted ATP drives neuroretina proliferation through purinergic signalling (Pearson *et al.*, 2005). Loss of RPE Gap junction proteins is furthermore sufficient to impair this mechanism of neuroretina mitosis regulation, revealing that this mechanism is indeed essential for its development.

The RPE also ensures the integrity of the photoreceptors' outer segments and their development. In mouse retina culture the RPE is required for the maintenance of photoreceptors outer segments (Ogilvie *et al.*, 1999). However, the outer segment development was not altered if the RPE was not continuous across the culture. This indicated that the RPE ensures correct outer segment

development through diffusible factors. The role of the RPE in the development of photoreceptor outer segments has been observed also *in vivo. Mitf* mutation in mouse not only results in the disruption of the RPE but also resulted in impaired development of rod photoreceptor outer segments (Bumsted, Rizzolo and Barnstable, 2001).

1.3 Eye defects: microphthalmia anophthalmia and coloboma.

Defects in the complex development of the eye can lead to a wide range of ocular phenotypes (Skalicky *et al.*, 2013; Williamson *et al.*, 2014; Reis and Semina, 2015; Deml *et al.*, 2016; Harding and Moosajee, 2019). Disruptions of early developmental stages of the eye result in microphthalmia, anophthalmia and coloboma (MAC) which are amongst the most common congenital eye defects in humans. Microphthalmia defines the phenotype in which the eye is smaller in volume than the population mean, which can lead to diverse degrees of visual impairment to blindness. Anophthalmia identifies the complete loss of all the ocular tissues during development, including optic nerve and chiasm (Harding and Moosajee, 2019). Clinically, anophthalmia also includes severe cases of microphthalmia, where the eye is formed but it regresses into non-functional cystic tissues. Ocular coloboma is the failure of closure of the choroid fissure. Similar to the previously described ocular phenotypes, coloboma has a range of severity as it can involve a variety of tissues including the iris, the retina and the RPE and can result in impaired vision.

Many of the mutations causative of MAC in humans involve genes directly responsible for eye development such as *OTX2 VSX2, RAX, PAX6* or members of the signalling pathways involved in this process as *BMP4,7* and *ALDH1A3, STRA6, RARB.* As these genes and their role are highly conserved amongst vertebrates, mutation of the same genes causes similar phenotypes in a variety of animal systems. However, the same mutation can lead to different phenotypes in different individuals. This suggests that while individual mutations have been identified as causative of MAC, for these mutations to result in ocular developmental defects the presence of sensitizing factors is required (Reis and Semina, 2015). MAC are to be in fact considered a phenotype spectrum rather

than individual phenotypes (Harding and Moosajee, 2019; Young *et al.*, 2019). This is due to the number of environmental factors and genetic background in which the mutation takes place, providing differentially sensitised backgrounds for eye development (Harding and Moosajee, 2019). While many of the mutations causative of MAC in humans affect genes involved in eye development, up to a third of MAC cases occur in association with other non-ocular developmental defects.

Congenital coloboma is reported to be one of the main causes of visual impairment in human (Gregory-Evans *et al.*, 2004). While the term coloboma groups all the consequences of the impairment in choroid fissure closure, it can be classified depending on the severity of the phenotype and the tissues involved. Iris coloboma groups the cases in which the RPE is resulting in the typical "keyhole" pupil. Conversely, in chorioretinal coloboma both the NR and the RPE and choroid are affected, generally in the posterior segment of the eye. In severe cases the lack of fusion of the choroid fissure can affect the optic nerve (Gregory-Evans *et al.*, 2004)

Causes of coloboma can be both genetic and environmental. Drugs administration during pregnancy has been identified as a possible cause underlying coloboma. In particular thalidomide and alcohol assumption during pregnancy appear to be causative for a range of eye defects including coloboma (Miller and Strömland, 1999; Gregory-Evans *et al.*, 2004). Similarly, vitamin A deficiency has been proposed as a cause of ocular coloboma (Hornby, Ward and Gilbert, 2003; Gregory-Evans *et al.*, 2004). Rarely, cases of coloboma are reported in association with maternal viral infections, however in these cases the causation has to be confirmed (Gregory-Evans *et al.*, 2004).

While environmental causes can be causative for isolated incidence of coloboma, a portion of the identified cases has been identified correlated with genetic abnormalities. A number of chromosomal aberrations have been identified to be causative of both syndromic or isolated coloboma in human. Interestingly those aberrations show overlap with genes known to be associated with coloboma including *SHH, CH10* , *FGF, PAX*, *VAX* and *YAP1*.(Gregory-Evans *et al.*, 2004; Williamson *et al.*, 2014; Eckert *et al.*, 2017). Indeed, most of the genes that have

been correlated with syndromic or isolated coloboma in human, are critical for eye morphogenesis and patterning.

1.4 Yap and the Hippo pathway.

1.4.1 The Hippo pathway

The tuning of cell proliferation, cell death and differentiation is critical for the accurate development of tissues and organs. The Hippo pathway and its effector Yap have been identified as the key elements in such regulatory processes (See chapter 3). The Hippo pathway has been firstly described in *Drosophila* through screenings for over-proliferation phenotype which allowed to identify the role of this pathway in the regulation of tissue growth (Xu *et al.*, 1995; Camargo *et al.*, 2007; Pan, 2007).

Further studies identified the role of this pathway in the integration of multiple stimuli representing the cell's environment. The Hippo pathway is responsible for the integration of stimuli such as oxidative stress, cell polarity, cell crowding, cell adhesion, substrate stiffness and mechanical stresses (Pan, 2007; Dupont *et al.*, 2011; Halder, Dupont and Piccolo, 2012; Piccolo, Dupont and Cordenonsi, 2014; Hansen, Moroishi and Guan, 2015; Davis and Tapon, 2019)**.**

Since its isolation, the Hippo pathways has been identified as responsible for the regulation of cell number in a variety of developing tissues including lungs, brain, liver, bone vasculature and heart (Jiang *et al.*, 2009; Lian *et al.*, 2010; Fitamant *et al.*, 2015; Lange *et al.*, 2015; Lu, Finegold and Johnson, 2018) (See chapter 3). Yap transcriptional activity is furthermore critical in the regulation of cell fate. In a number of cases, Yap transcriptional activity sustains cell pluripotency while reduction of its activity results in cell differentiation. Examples for the role of Yap in cell fate determination are that in mammary glands, pancreas and kidneys, Yap transcriptional activity maintains the cells as non-specified (Lian *et al.*, 2010; Chen *et al.*, 2014; Gao *et al.*, 2014; Panciera *et al.*, 2016; McNeill and Reginensi, 2017). Yap thus integrates information from the cell's environment to trigger the cellular fate switch in response to cell-cell adhesion, tensile state and ECM stiffness indicating tissue maturity (See chapter 3).

The core structure of the Hippo pathway is conserved across all metazoans and it consists of a phosphorylation cascade ultimately converging on Yap (Davis and Tapon, 2019; Hansen et al., 2015; Piccolo et al., 2014). The first protein in the Hippo pathway cascade is Mst1/2. Phosphorylated Mst1/2 subsequently phosphorylates LATS1/2 which, in turn, is directly responsible for the phosphorylation of Yap. The phosphorylated state of Yap mediates its transcriptional activity through regulation of its nuclear shuttling. Upon phosphorylation Yap is inhibited by cytoplasm retention through binding of the protein 14-3-3, or by proteasomal degradation. Conversely, when the Hippo pathway is inactive, Yap remains in a dephosphorylated state and it is free to translocate in the nucleus where it binds the transcription factor TEAD promoting the transcription of its downstream target genes (Piccolo, Dupont and Cordenonsi, 2014; Hansen, Moroishi and Guan, 2015). This core mechanism for Yap phosphorylation represents a hub for the integration of a variety of stimuli transduced by independent pathways ultimately converging on the Hippo cascade. The signalling converging on the Hippo pathway transduces information relative to the environment and to the tissue organization: in epithelia, Yap transcriptional activity is in fact correlated to factors as cell polarity, cell-cell adhesion and cell-ECM adhesion (Piccolo, Dupont and Cordenonsi, 2014; Hansen, Moroishi and Guan, 2015; Rausch and Hansen, 2020).

Cell polarity is one of the upstream regulators of the Hippo pathway. Information regarding apico-basal polarity is transduced to the core Hippo cascade through the tight-junctions (TJ) protein complex (Genevet and Tapon, 2011; Fulford, Tapon and Ribeiro, 2018; Liu *et al.*, 2018). Many of the proteins composing the TJ complex are known to directly interact with Mst and Lats proteins: TJ proteins can act as scaffolds assembling the Hippo core kinase and promoting the phosphorylation of Yap. Indeed, interference with the apical-basal determinants can lead to the transcriptional activation of the Yap protein as consequence of disruption of the Hippo kinase core (Schroeder and Halder, 2012). For example, experiments show that the apical protein Zonula Occludens 2 (ZO2) can directly regulate Yap activity. ZO2, is in fact able to drive Yap sequestration to the cytosol by generating, and binding, the Lats1-Yap complex (Liu *et al.*, 2018).

Junctional proteins are furthermore relevant in the regulation of Yap in response to cell-cell adhesion stimuli. These stimuli are transduced to the Hippo pathway through the adherens junctions (AJ) components providing a mechanism for the cell to sense and respond to cell crowding and density (Borghi *et al.*, 2012; Yang *et al.*, 2015; Hirata, Samsonov and Sokabe, 2017; Dutta *et al.*, 2018; Fulford, Tapon and Ribeiro, 2018). The regulation of Yap activity of the AJ relies on the conformational changes of its components upon tensile strain: in particular, mechanical tension induces unfolding of Vinculin. Once the conformation of this protein has changed, these components of the AJ are able to bind LATS inhibiting its phosphorylative function (Dutta *et al.*, 2018; Ibar *et al.*, 2018). Conversely, α-catenin, another critical component of AJ, has been found to be able to stabilize the complex of Yap and 14-3-3, preventing Yap dephosphorylation and sustaining its sequestration to the cytoplasm (Dobrokhotov *et al.*, 2018).

ECM composition is another important regulator for Yap activity as its nuclear translocation has been observed being directly correlated with cell-spreading and substrate stiffness (Dupont *et al.*, 2011; Nukuda *et al.*, 2015; Dobrokhotov *et al.*, 2018)**.** The transduction of mechanical proteins into cellular signals is reliant on focal adhesion (FA) proteins cluster which includes talins, vinculins and paxilins (Klapholz and Brown, 2017; Rausch and Hansen, 2020). While FA proteins are critical to sense mechanical information from the cell substrate, focal adhesion kinase (FAK) transduces this information downstream. In particular, FAK is in fact responsible for the inhibition of LATS in presence of stiff ECM, resulting in Yap nuclear localisation (Rausch and Hansen, 2020)**.**

The hippo pathway can furthermore integrate extracellular biochemical signals (Guo and Zhao, 2013). In particular, activation of G-protein-coupled receptors (GPCRs) on the cell surface is able to activate downstream Yap transcriptional activity. The signalling from GPCRs converges on RhoGTPase and F-Actin remodelling, which are, in turn, regulators of Yap activity. Yap transcriptional activity can be regulated directly by the actomyosin cytoskeleton, thus relaying information on the mechanical state of the cell (Davis and Tapon, 2019). While

the exact molecular mechanisms through which the cytoskeleton regulates Yap activity have to be yet elucidated, it is known that polymerised actin (F-actin) has a major role in increasing Yap transcriptional activity. Loss of actin depolymerization proteins can increase Yap transcriptional activity while induction of actin depolymerization reduces its activity. The Amot family is suggested to be playing a role in cytoskeletal-mediated Yap regulation in a Hippo independent manner (Chan *et al.*, 2011; Mana-Capelli *et al.*, 2014). Amot proteins are F-actin binding proteins which can be localised at TJ and AJ. Amot can bind and sequester Yap to the TJ, inhibiting its transcriptional activity. Actin competes with Yap-Amot binding, providing a mechanism through which Yap activity can be regulated in response of actin polymerization.

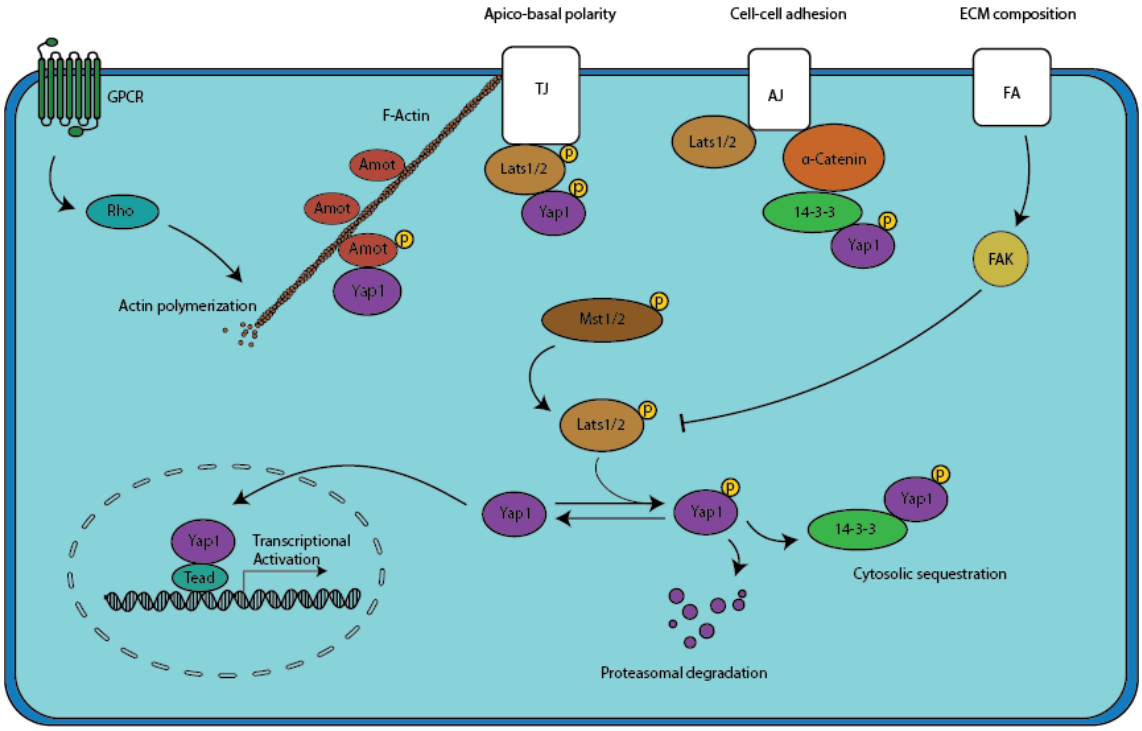

Figure 1.3| Regulation of Yap phosphorylation.
Yap phosphorylation is regulated by the core Hippo pathway involving Mst and Lats. The core Hippo pathway is regulated upstream by cell polarity signalling transduced through the tight junction complex (TJ). TJ are able to stabilize the Lats-Yap complex promoting its phosphorylation. Cell-cell adhesion signalling is transduced to the Hippo pathway through the apical junction complex (AJ). The AJ is able to sequester Lats upon tension. It can conversely stabilize the complex of phosphorylated Yap and 14-3-3 sustaining its sequestration in the cytosol. Focal adhesion (FA) is responsible for the inhibition of Lats in response to ECM stiffness changes. Finally, GPCR can regulate the transcriptional activity Rho-mediated regulation of actin polymerization. Actin polymerization can regulate Yap phosphorylation through unknown mechanisms and competing for the binding of Amot, which, in turn, can sequester Yap to the cytosol.

1.4.2 Yap function in eye development.

Yap is critical in the development of the eye in most animals studied. Its role in eye development covers the maintenance of the pool of retinal progenitor cells, regulation of cell differentiation and proliferation (Lian *et al.*, 2010; Asaoka *et al.*, 2014; Williamson *et al.*, 2014; Cabochette *et al.*, 2015; Miesfeld *et al.*, 2015).

One of the roles of Yap in eye development is the maintenance of the retinal progenitor pools through the regulation of their cell cycle. It was observed in mouse that Yap is expressed early in development in the eye tissues being strongly expressed in the retinal progenitor cells (Williamson *et al.*, 2014; Kim *et al.*, 2016). In these cells, loss of Yap resulted in reduced proliferation coupled with suppression of G to S phase cell cycle transition. Indeed the role in retinal progenitor maintenance has also been observed in *Xenopus* (Cabochette *et al.*, 2015)**.** In this model Yap controls the pool of retinal progenitor cells also in the post-embryonic retinal growth: overexpression of *Yap* led to eye overgrowth as a consequence of continued cell proliferation and survival**.** Conversely, *Yap* knock-down resulted in decreased cell survival and proliferation leading to the generation of eyes smaller than the wild-type. However, by restoring *Yap* activity in the eye in late embryogenesis, the normal size of the eye could be recovered. The role of Yap in post-embryonic retinal growth has been linked to its function in maintaining the proliferative state in retinal progenitor cells: loss of Yap resulted in slowed cell cycle kinetics in retinal progenitor cells resulting in the reduction of both the cellular progenitor pool and their differentiation into mature retinal cells.

Together with its role in the maintenance of the retinal cell progenitor pool, Yap has a role in the maintenance of differentiated ocular tissues. In particular, it was observed in the mouse model that loss of *Yap* led to loss of RPE differentiation and trans-differentiation into neuroretina (Kim *et al.*, 2016). In particular, absence of *Yap* led to ectopic expansion of neuroretina markers (such as Chx10) paired with loss of the RPE determinant *Mitf*. *Yap* is also responsible for the maintenance of the mature neuroretina. In *Yap* conditional KO mice, it was observed a reduction of neuroretina cell number and laminar thinning of this tissue: loss of Yap-mediated anti-apoptotic signalling was identified being

responsible for the increase of cell death in the neuroretina. Together with the survival of the neuroretina, *Yap* has also a critical role in the regulation of the polarity of its cells. Together with hypocellularity, the neuroretina of Yap CKO mice underwent major disruption of the laminar organization showing irregular folded morphology and irregular thickness. Such disorganisation has been observed being the consequence of lack of Yap-mediated maintenance of cell polarity in the neuroretina tissue, leading to the disruption of apical polarity complexes. If this is a consequence of the lack of the RPE or if this is due to a direct effect of Yap in the neuroretina needs however to be addressed with the use of tissue specific KO.

The role of Yap in the regulation of the balance between retinal progenitor cell proliferation and differentiation has been confirmed also in the zebrafish model (Asaoka *et al.*, 2014). It was observed that expression of constitutively active Yap led to the downregulation of photoreceptor specific genes such as *otx*, *crx* and *rhodopsin*, indicating a lack of retinal differentiation. The study furthermore identified a direct interaction between Yap and Rx1 (through the Yap WW protein-protein interaction domains), providing a mechanism for Yap-mediated control of retina specification: the study proposes that, when the Hippo pathway is inactive, Yap promotes TEAD-mediated transcription of proliferation genes. Simultaneously, de-phosphorylated Yap binds and sequesters Rx1 inhibiting its activation of photoreceptor specific genes. Yap activity can in this way sustain the undifferentiated state of the retinal progenitor cells. Conversely, upon Hippo pathway activation (and consequent Yap phosphorylation), the Rx1-mediated transactivation of photoreceptors genes is upregulated driving the maturation of photoreceptors cells.

In zebrafish, mutation in the *yap* gene leads to loss of RPE, indicating that Yap has a role also in the differentiation and maintenance of this tissue (Miesfeld *et al.*, 2015). In this study two *yap* mutant alleles were observed: yap^{mw48} and yap^{nl13}. In the yap^{mw48} mutant areas lacking the RPE were observed across the eye. In these regions the neuroretina progenitors were not covered by the RPE. However, the retina tissue was properly layered and the photoreceptor structures

were maintained even in region were the RPE was not present. The inclusion of a single mutant *taz* allele in a homozygous *yap*^{mw48} background resulted in higher severity in the RPE loss. The loss of RPE in consequence of *yap* mutation was linked directly to the lack of expression of Tead target genes: driving the expression of *yap* lacking the Tead binding domain resulted in loss of RPE development, indicating that Yap-mediated activation of Tead is required for the correct development of the RPE. While the RPE was disrupted, neither proliferation nor apoptosis were altered in this tissue, indicating a role of Yap early in the specification of the RPE. Indeed, differently from control cells, cells from a *yap*^{wm48} / *taz*$^{-/-}$ donor grafted into wild type embryos, fail to contribute to the formation of the RPE. This confirmed that *yap* together with *taz* are required to drive the specification of progenitor cells to acquire RPE fate. Other observations on the role of *yap* in eye development in the zebrafish model have been performed on the *yap*^{nl13} mutant. This mutant shows a coloboma phenotype without any other overt defects (See chapter 2.1).

1.5 Aims of the thesis

Coloboma is one of the main causes of congenital visual impairment in humans. However, little is known on the mechanisms driving the process of choroid fissure closure and how impairments of these mechanisms lead to coloboma. While many of the morphogenetic events driving eye development have been studied in detail, the mechanisms underlying the fusion of the choroid fissure are only recently beginning to be understood.

Genome wide studies revealed that mutations in the *YAP* gene can be causative of coloboma in human, providing information on the relevance of this gene in choroid fissure fusion (Williamson *et al.*, 2014). This has been shown in the *yap*^{nl13} zebrafish allele as well (Miesfeld *et al.*, 2015). However, the mechanisms through which *YAP* is involved in choroid fissure closure, and the mechanistic causes underlying the coloboma phenotype upon mutation of this gene are not yet defined. The zebrafish model provides a very insightful system to observe development processes *in vivo:* embryo accessibility allows the study of

developmental events which are precluded in other well studied vertebrate systems.

Previous studies performed by this laboratory on the *yap*^{nl13} allele showed that the coloboma phenotype in *yap*^{nl13} is due to the lack of functional *yap* in the RPE (See chapter 2). However, the nature of RPE defects resulting in a coloboma phenotype have not yet been investigated. *yap* encodes a co-transcriptional factor critical in development due to its role in the regulation of cell differentiation, cell proliferation and mechanotransduction. Considering the known functions of *yap*, this work aims to understand which developmental events are misregulated in the RPE as consequence of the *yap*^{nl13} mutation. Understanding the mechanisms underlying the coloboma phenotype of *yap*^{nl13} mutants will provide insights on the role of *yap* for choroid fissure closure.

To do so, the following aims have been set out:

1. Despite the fact that *yap* is broadly expressed in different domains of the embryos, the *yap*^{nl13} phenotype is eye specific. Thus, I investigate possible mechanisms for the eye specificity of the *yap*^{nl13} zebrafish mutant.

2. Given the role of *yap*^{mw48} in promoting RPE specification and the general requirement for Yap in regulating cell proliferation. I investigated the effects of the *yap*^{nl13} mutation on the specification and proliferation of the RPE.

3. The YAP/TAZ/Hippo pathway has been extensively studied for its ability to sense and respond to changes in mechanical forces-such as stretching and compressing. I thus investigate whether the *yap*^{nl13} mutation impairs the mechanotransduction and the mechanical properties of the RPE.

Chapter 2.

Yap transcriptional activity is reduced specifically in the eye in *yap*^{nl13} zebrafish mutants.

2.1 Introduction

yap is broadly expressed during zebrafish development: in early stages *yap* is transcribed ubiquitously in the embryo. *Yap* transcripts are detectable through *in situ* hybridization already in the zygote: the presence of *yap* RNA prior to mid-blastula transition suggests maternal contribution of early *yap* transcripts (Jiang *et al.*, 2009). As development proceeds, *yap* transcription localises in the notochord, brain, eyes, and branchial arches (Jiang et al. 2009).

A number of studies have revealed how Yap is critical for the development of a large variety of tissues and organs (Camargo et al., 2007; Varelas, 2014; Zhao et al., 2010). Knockdown experiments showed that downregulation of *yap* leads to developmental delays in gastrulation, cardiogenesis, hematopoiesis and somitogenesis (Morin-Kensicki *et al.*, 2006; Hu *et al.*, 2013). Furthermore, a decrease of Yap activity leads to disruption of the whole body axis and to ventralization of the zebrafish embryo (Hu et al., 2013). The broad role of *yap* is also reflected by the phenotype of the *yap* medaka mutant *hirame* (*hir*). Indeed, medaka *hir* mutant embryos show disruption of the body axis: the whole embryo flattened due to loss of cell tension, which leads to the collapse of multiple tissues including the neural tube, somites and eyes (Porazinski et al., 2015).

Despite the extensive role of *yap* in development and its broad expression pattern in the zebrafish embryo, the *yap*^{nl13} phenotype in the zebrafish larva is specific to the eye. Similarly, the first study which correlated a mutation in *YAP* to a coloboma phenotype in humans described how coloboma phenotype can be both syndromic and isolated. The study reported two cases of families carrying *YAP* mutation: while in one of the families coloboma is paired with hearing loss, intellectual disability, haematuria and orofacial clefting, in the other family coloboma is not associated with any other phenotype (Williamson *et al.*, 2014). The study suggested that the variability of the phenotype in the two families could be traced back to the presence of different alternative transcripts, ameliorating the syndromic effect of *YAP* mutation in one of the two study cases.

The hypothesis of splicing-mediated regulation of *yap* tissue-specific transcriptional activity has been the object of several studies. The large number of existing *yap* isoforms (8 in humans and 2 in zebrafish) suggested that different *yap* isoforms could have non-redundant functions (Gaffney et al., 2012; Hoshino et al., 2006; Hu et al., 2013). Supporting this hypothesis, the first in-depth study on *YAP* alternative splicing in human (Gaffney *et al.*, 2012) found that while most of the 8 isoforms were expressed at different levels across the majority of the human tissues, one of the alternative *YAP* variants was completely missing in leukocytes. This finding suggested the existence of a tissue-specific regulation of splicing events. The study furthermore revealed that the relative abundance of *YAP* isoforms varies significantly in different tissues corroborating the hypothesis of tissue-specific alternative splicing in *YAP*.

Two main *yap* isoforms have been identified both in mammals and in zebrafish. The two main identified isoforms differ in the fact that they harbour one or two WW domains, respectively (Iglesias-Bexiga *et al.*, 2015). The WW domains are wide-spread modules regulating protein-protein interaction, allowing Yap to form dimers and complexes with other co-transcriptional factors, transcriptional enhancers and repressors. Since Yap has no intrinsic DNA-binding domain, its function as transcriptional regulator is critically reliant on the WW modules to mediate its association with other transcription factors. It has been shown that the two WW domains of Yap have different protein binding specificity and that the presence of tandem WW domains further alters the selectivity of protein-protein interactions (Finch-Edmondson et al., 2016). As a consequence, the presence of a single or two WW domains in the Yap protein mediates the association of Yap with different partners, resulting in the modulation of Yap's transcriptional activity (Iglesias-Bexiga *et al.*, 2015; Chen *et al.*, 2019). Alternative splicing can modulate Yap's transcriptional activity by modification of the C-terminal transactivation domain. It has been found that some of the Yap isoforms generate Yap proteins with a shorter TAD sequence. In particular, alternative splicing events can partly disrupt the leucine zipper of the Yap's transactivation domain, strongly affecting the protein's transcriptional activity (Finch-Edmondson et al., 2016).

Overall, it appears that alternative splicing can finely modulate the transcriptional potency of Yap both by directly affecting its transactivation domain and by modulation of its interaction with specific partners. The presence of differently enriched *yap* isoforms in different tissues furthermore indicates that *yap* splicing events occur with various frequencies across multiple tissues. Since distinct isoforms have variable transcriptional potency and different protein-protein interaction preferences, this provides a possible mechanism for *yap* tissue specific regulation. Although it has not yet been verified, it is plausible that the tissue-specific relative abundance of *yap* isoforms could lead to preferential association with tissue-specific partners resulting in tissue-specific Yap transcriptional function.

Yap transcriptional activity is strongly reliant on its cooperation with Taz, a co-transcriptional factor homologous of Yap. Yap and Taz have high protein sequence similarity (around 60% in humans (Kanai *et al.*, 2000; Plouffe *et al.*, 2018)) resulting in very similar protein structure and domains: Taz harbours a TEAD binding domain followed by a single WW domain and a C-terminal transactivation domain. The high structural similarity between Yap and Taz is matched by functional redundancy of the two proteins as, like Yap, the main partner of Taz is the transcriptional factor TEAD.

The functional overlap between Yap and Taz has been often described both *in vitro* and *in vivo* (Gao *et al.*, 2014; Varelas, 2014; Plouffe *et al.*, 2018; Tang *et al.*, 2018). For example, a recent study in zebrafish reported an overlapping role of Yap and Taz in the establishment of left-right asymmetry (Fillatre *et al.*, 2019). In this study it has been observed that while downregulation of *taz* leads to mild defects in laterality, the downregulation of both *yap* and *taz* exacerbates this phenotype. Similarly, the penetrance of laterality defects in *taz* homozygous mutants is increased in embryos carrying a single *yap* mutated allele.

Similarly, in the retinal pigment epithelium (RPE), a redundancy between *taz* and *yap* functions has been reported the zebrafish yap^{mw48} mutant (Miesfeld et al., 2015). yap^{mw48} mutant embryos are characterised by reduction of RPE cells. This reduction in yap^{wm48} mutant embryos is the consequence of defects in RPE specification, while proliferation and apoptosis are unaltered in yap^{mw48} mutant.

RPE. Like *yap*^{nl13}, the penetrance of the *yap*^{mw48} mutation is temperature dependent: the phenotype of *yap*^{mw48} is fully rescued when embryos are raised at 20°C. However, this is abolished when a single mutant *taz* allele is added to a *yap*^{mw48} homozygous background. Furthermore, the phenotype of *yap*^{mw48}, *taz*$^{+/-}$ embryos raised at 28°C is exacerbated compared to embryos carrying *yap*^{mw48} mutation alone as embryos show complete loss of RPE cells. Conversely, embryos homozygous for *taz* mutation show no developmental defect. Overall these observations indicated an overlapping role of *yap* and *taz* in the specification and development of the RPE (Miesfeld et al., 2015).

Considering the evidence for the overlapping roles of *yap* and *taz* in *yap*^{mw48}, we sought to understand whether the reported redundancy of *taz* is also responsible for the incomplete penetrance of *yap*^{nl13} in mutant embryos raised at 28°C. Alternatively, given that *yap*^{nl13} leads to the formation of different *yap* splice variants, we investigated whether the phenotype could be due to the presence of a specific isoform. Indeed, it has been shown that temperature sensitivity of some vertebrate mutants (e.g. *mitfa* mutation in zebrafish and the *eyeless* rx3 mutant in medaka (Loosli *et al.*, 2001; Zeng *et al.*, 2015) depends on the generation of alternative splice forms at different temperatures.

2.2 Results

2.2.1 In the *yap^{nl13}* mutant, Yap transcriptional activity is reduced specifically in the eye.

A compensatory role of Taz for RPE development has been previously described in other zebrafish *yap* mutant alleles (Miesfeld et al., 2015). We thus asked whether the redundancy of Taz and its activity may be responsible for the reduced penetrance of the coloboma phenotype observed in *yap^{nl13}* mutant raised at 28°C. To evaluate the presence of an increase in *taz* transcription, suggesting a compensatory event in *yap^{nl13}* mutant, we performed qRT-PCR experiments. We furthermore evaluated the expression levels of *yap* to observe whether *yap^{nl13}* mutation is paired to an increase of *yap* transcription. We hypothesised that, in absence of functional Yap, an increase of *yap* transcription could take place to compensate for the lack of Yap transcriptional activity.

To assess the overall transcriptional activity of both *yap* and *taz* we used the transcription levels of *ctgfa* as a readout. *ctgfa* is a well characterised downstream effector of both Taz and Yap and its transcription is directly regulated by both Yap and Taz. For this reason, *ctgfa* expression levels are commonly used as a proxy for Yap and Taz transcriptional activity (Zhang, Smolen and Haber, 2008; Zhao, Tumaneng and Guan, 2011; Astone *et al.*, 2018). We performed the qRT-PCR experiments on both wild types and *yap^{nl13}* mutants raised at 28°C and 32°C, to compare the transcriptional levels of our gene-set in conditions of reduced and full penetrance of *yap^{nl13}* coloboma phenotype.

Our experiments showed that *yap* expression is significantly reduced in *yap^{nl13}* mutant embryos raised at both 28°C and 32°C when compared to the abundance of *yap* transcripts in wild type embryos (**Fig 2.0 A;** Yap 28°C ΔCt= 0.378±0.041, mean±SEM; Yap 32°C ΔCt= 0.394±0.032, mean±SEM; multiple t-tests: n.s. p>0.05; N=3 n=35). Conversely, while *taz* transcription is reduced in *yap^{nl13}* embryos raised at 28°C, in *yap^{nl13}* embryos raised at 32°C *taz* is significantly overexpressed (**Fig 2.0 A**; Taz 28°C ΔCt= 0.619±0.064, mean±SEM; Taz 32°C ΔCt= 1.137±0.073, mean± SEM; multiple t-tests: p<0.05; N=3 n=35). However,

ctgfa downregulation is not significantly different in *yap*^{nl13} mutant embryos raised either at 28°C and at 32°C (**Fig 2.0 A**; Ctgfa 28°C ∆Ct=0.578±0.159, mean±SEM; Ctgfa 32°C ∆Ct=0.742 ± 0.211 mean±SEM; multiple t-tests: n.s. p>0.05; N=3 n=35). This suggests that increased transcription of *taz* in *yap*^{nl13} does not result in a recovery of the pathway activation.

Our RT-qPCR experiments highlighted a downregulation of *ctfa* in the mutants at both 28°C and at 32°C, which suggests an overall reduction of the transcriptional activity of Yap. To confirm this result, and to furthermore assess whether the downregulation of Yap transcriptional activity is specific to the eye, we performed confocal live imaging on Yap reporter line (Tg(4xGTIIC:d2GFP)). The imaging revealed a significant decrease of 4xGTIIC:d2GFP expression in *yap*^{nl13} mutant embryos, indicating a downregulation of Yap transcriptional activity in the mutant (**Fig 2.0 B**, Gray Value Wild Type = 0.22974±0.008, mean±SEM; Gray Value *yap*^{nl13}= .1124±0.020, mean±SEM**;** t-Test: p<0.05). The downregulation of 4xGTIIC:d2GFP is restricted to the eye region: while the intensity of 4xGTIIC:d2GFP is significantly reduced in the eye of *yap*^{nl13} mutant embryos, the reported transcriptional activity of Yap in the rest of the embryo is not significantly different in *yap*^{nl13} mutants compared to wild type embryos (**Fig 2.0 C** and data not shown). This observation suggests that the eye specific phenotype in *yap*^{nl13} mutants is due to an eye-specific reduction of Yap transcriptional activity.

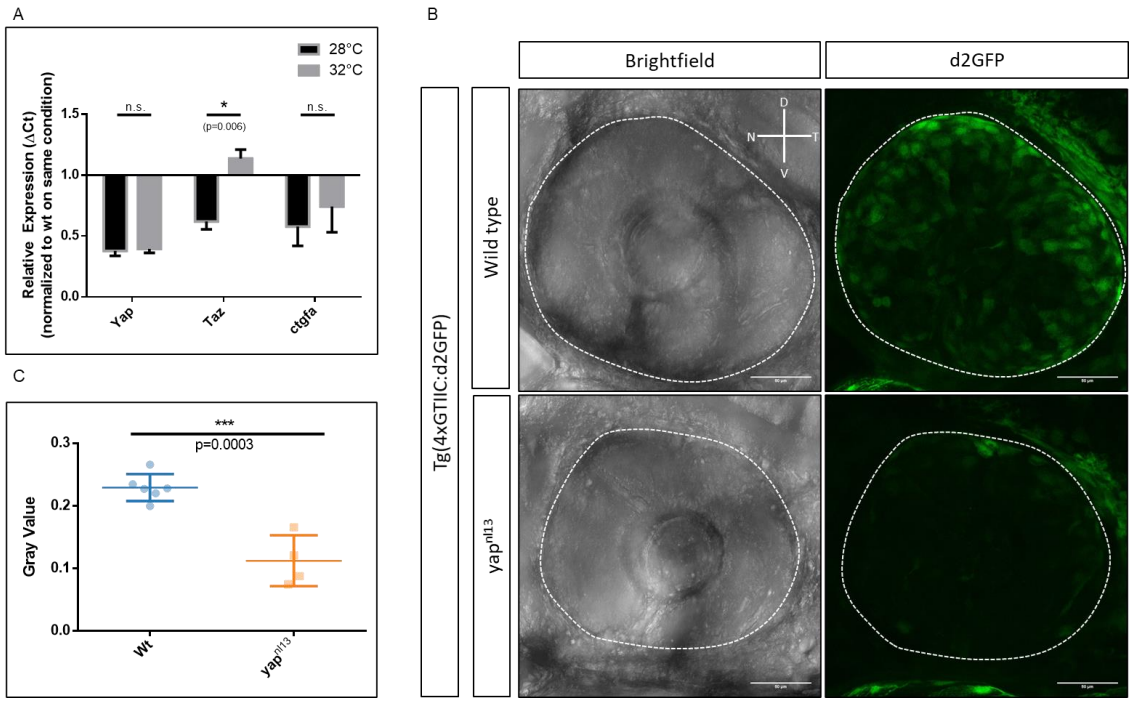

Figure 2.0| *taz* is not responsible for compensating mechanisms in *yap*^{nl13} mutant.
A| Relative expression levels (ΔCt) of *yap*, *taz* and *ctgfa* in *yap*^{nl13} mutant embryos raised at both 28°C and 32°C. Transcript abundances are normalised to expression levels of the gene set measured in wild type embryos raised at the same conditions (continuous line)**.** **B|** Imaging of Yap reporter line (Tg(4xGTIIC:d2GFP)) in both wild-type and *yap*^{nl13} mutants. Yap Dotted lines marking the position of the region of interested (ROI) used for measurements. N=nasal; T=temporal; D=dorsal; V=ventral; **C|** Measurement of the absolute gray value measured in the ROI on the green channel in figure B.

2.2.2 The eye specificity of the *yap*^{nl13} phenotype is not correlated with tissue specific *yap* isoforms.

As tissue specific regulation of *yap* transcriptional activity can result from tissue specific splicing events (Hoshino et al., 2006; Porazinski and Ladomery, 2018), we asked whether the specificity of the *yap*^{nl13} phenotype could be due to the presence of an altered composition of tissue specific *yap* isoforms. We thus first tested the existence of specific *yap* splice forms in the head of wild type embryos. We then tested whether the presence of such alternative transcripts is altered in *yap*^{n13} mutants. To do so we performed reverse transcription PCR (RT-PCR) on dissected heads and trunks from both wild types and *yap*^{nl13} mutants. Embryos were dissected at 48hpf, which is the earliest moment in which the phenotype in *yap*^{nl13} is identifiable, allowing us to screen for *yap*^{nl13} mutant embryos. To test for the occurrence of exon skipping events on each *yap*'s exon, we designed primers on the exons flanking the exon tested for exon skipping events **(Fig 2.1 A)**. This would generate shorter amplicons in the events of exon skipping, allowing us to identify the different *yap*'s splicing events. Our experiments recorded the occurrence of one splicing event in wild-type embryos in which exon 4 is skipped **(Fig 2.1 C.c)** which has been previously described in literature (Hu et al., 2013). We furthermore confirmed the presence of the three alternative splicing events in *yap*^{nl13} mutants previously described for this mutant (Miesfeld et al., 2015) **(Fig 2.1.C.d, e; D.d, e)**. However, from these RT-PCR experiments we could not detect splicing events occurring exclusively in the head or in the trunks of both wild type and *yap*^{nl13} mutant embryos **(Fig 2.1 C, D)**, suggesting the absence of eye specific *yap* splice forms.

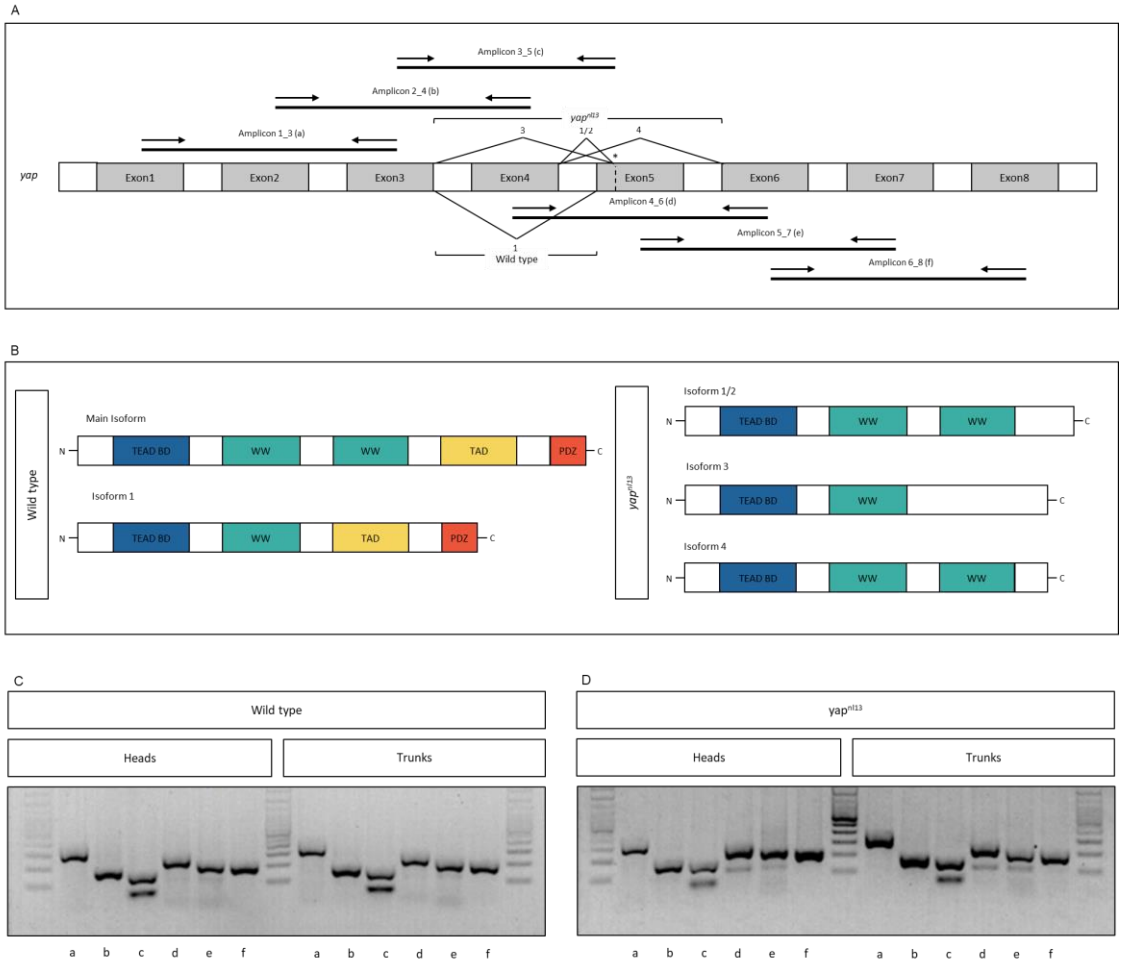

Figure 2.1| No *yap* specific isoforms are observed in the head region of both wild type and *yap*^{nl13} mutant embryos.
A| Schematic representation of *yap* cDNA reporting the primer design used for RT-PCR experiments and the splicing sites in both wild type and in *yap*^{nl13}. The asterisk and dashed line represent the site of *yap*^{nl13} mutation.
B| Schematics of Yap protein in wild types an *yap*^{nl13} (Jiang et al., 2009; Miesfeld et al., 2015)**. C,D|** Results of the RT-PCR performed on cDNA extracted from both heads and trunks of wild type embryos (C) and *yap*^{nl13} mutant embryos (D). The lettering refers to the primer set described above.

yap tissue-specific activity can be also regulated by the modulation of the relative abundance of the different *yap* isoforms (Finch-Edmondson *et al.*, 2016). We thus asked whether the population of *yap* isoforms is differently enriched in the head of the zebrafish embryo and whether this enrichment is altered in *yap*^{nl13} mutants. To answer this question, we sought to understand whether the exons undergoing alternative splicing events (i.e. exon 4 in the wild-type and exon 4 and exon 5 in *yap*^{nl13} mutants) are specifically enriched in the head of the zebrafish embryo and whether this enrichment is altered in *yap*^{nl13} mutants. To do so we performed quantitative RT-PCR (qRT-PCR) to evaluate the relative abundances of the exons subject to splicing events and compared them between heads and trunks in both wild type and *yap*^{nl13} mutant embryos**.** qPCR experiments have been thus performed using primers belonging to each exon we wanted to assess the abundance of **(Fig.2.2 A)**. Due to technical limitations forced by the design of primers suitable for qPCR, we could not generate forward and reverse primers belonging to the same exon in the case of exon 4. We thus designed two sets of primers, one covering exon 3 and 4, and the other covering exon 4 and 5 (Fig. 2.2 A). The levels of expression of the analysed exons were normalised on the expression levels of exon 1 in *yap*. Exon 1 is not affected by *yap*^{nl13} mutation nor by alternative splicing events and it is thus representative of the overall levels of *yap*^{nl13} transcription. From our experiments we could not detect any significant difference between the relative abundance of any of the analysed exons between heads and trunks in neither wild types nor *yap*^{n1l3} mutant embryos (**Fig. 2.2 B;** ΔCt values for wild types: Exon3_4 = 1.427±0.071; Exon 4_5= 1.252 ±0.158; Exon 5 = 1.304±0.110; ΔCt values for *yap*^{nl13} Exon 3_4= 0.910±0.025; Exon 4_5 ΔCt = 1.159±0.22; Exon 5 = 1.060±0.0173; Mean±SEM. Kruskall-Wallist test adjusted p-values: for wild types: exon 3_4/exon4_5 = 0.08842; exon 3_4/exon 5 = 0.9918; exon 4_5/exon5 >0.999; for wild *yap*^{nl13} mutants: exon 3_4/exon4_5 = 0.8903;exon 3_4/exon 5 **?**0.9999; exon 4_5/exon5 >0.999;)

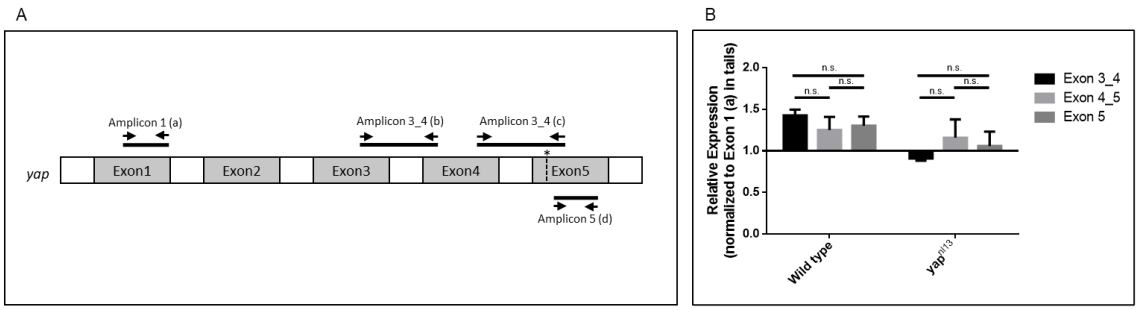

Figure 2.2| None of the detected *yap* splice forms is differentially expressed in embryos head when compared to trunks in both wild type and *yap*^{nl13} mutant.

A| Schematic representation of *yap* cDNA sequence and primers used for qRT-PCR experiments. The asterisk and the dashed line represent the site of *yap*^{nl13} mutation. **B|** Abundance of the tested exons normalised to the abundance of exon 1 in embryos' trunk (continuous line). The difference in the measured ΔCt is not significant (Kruskall-Wallist test)

2.3 Discussion

Our observations suggest that the role of *yap* in eye development is not regulated by tissue-specific modulation of alternative splicing events. Furthermore, it appears that the specificity of the *yap*^{nl13} phenotype is not a consequence of either alteration of eye-specific splice-forms, or of changes in the enrichment of any *yap* alternative transcripts specifically in the eye.

We did not detect the occurrence of splicing events specific for the head region that would suggest the existence of eye-specific *yap* isoforms in the wild type or in the *yap*^{nl13} mutant**.** We found the presence of one alternative splicing event in wild-type *yap* and three alternative transcripts in the *yap*^{nl13} mutant. These observations are in line with previous studies that reported the existence of a single *yap* splice variant in wild-type zebrafish (Hu et al., 2013) and three *yap* splice-forms in the *yap*^{nl13} mutant (Miesfeld et al., 2015). However, all the alternative transcripts that we observed were present in both the head and trunks of wild types and *yap*^{nl13} mutants of zebrafish embryos. These results suggest that none of transcripts observed is specific to one of these regions, and also challenge the existence of a *yap* isoform with activity specific to the eye.

Furthermore, our results did not show differences in the relative enrichment of any of the identified *yap* splice-forms in either the head and trunks of wild-types or *yap*^{nl13} mutants. Since different *yap* isoforms have different transcriptional potencies and transcriptional partners, the tissue-specific enrichment of the alternative transcripts can modulate Yap activity (Gaffney et al., 2012; Hoshino et al., 2006; Hu et al., 2013). However, our observations suggest that this is not the case for the regulation of Yap transcriptional activity in the eye. Also, all the alternative *yap* transcripts in the *yap*^{nl13} mutant have the same relative composition in both heads and trunks. This further suggests that the specificity of the *yap*^{nl13} mutant eye phenotype is not due to a change in Yap's isoforms composition.

While from our data it appears unlikely that alternative splicing events occurring specifically in the eye are responsible for the eye specific phenotype in *yap*^{nl13} mutants, we cannot completely exclude this possibility. In fact, our experimental

setup only discriminated between the expression profile of the whole head and trunks, possibly hiding expression profiles details exclusive to the eyes.

The observations on the Yap reporter line indicate that *yap*^{nl13} induces an eye-specific reduction of Yap transcriptional activity, which contributes to the hypothesis that the *yap*^{n1l3} phenotype is the result of a tissue-specific disruption in pathway activation. Different Yap isoforms can have variable protein-protein interactions depending on the cellular context (Gaffney *et al.*, 2012; Porazinski and Ladomery, 2018). Therefore, it is possible that new Yap isoforms, generated by the *yap*^{nl13} mutation, have reduced tissue-specific transcriptional activity without being expressed specifically in the eye. We could speculate that the *yap*^{nl13} mutation affects the stability of the complex between Yap and some eye-specific co-transcriptional factors while not affecting its interaction with other partners. The hypothesis of a reduced stability of the complex between Yap and its target could also provide an explanation for the temperature sensitivity of the *yap*^{nl13} mutant. In fact, it is possible that the altered stability of the complex between Yap and an eye-specific partner results in a sensitivity of the protein-protein to the incubation temperature.

Alternatively, it is possible that one of the splice forms identified in the *yap*^{nl13} mutant is responsible for reduction of Yap transcriptional activity in the eye: it could be hypothesised that the relative abundance of the different splice forms is modulated at different incubation temperature, causing the temperature sensitivity of *yap*^{nl13} penetrance. Typically, the temperature sensitivity of a mutation depends on the altered stability of the encoded protein, or on the altered stability of complex between the mutated protein and its partners (Lovato *et al.*, 2009; Tan *et al.*, 2009). Conversely, in vertebrates -where the occurrence of temperature sensitive mutations is much rarer- there are examples in which the temperature dependence of a mutation is due to alternative splicing events or altered transcription levels. One example of this mechanism is provided by the *mitfa*^{vc7} zebrafish mutant (Zeng *et al.*, 2015). This mutant lacks neural crest cell derived melanocytes when raised at restrictive temperature, while it shows no phenotype when raised at permissive temperature. The temperature dependence of *mitfa*^{vc7} is not linked to the instability of its gene product. Instead, the *mitfa*^{vc7}

mutation leads to the transcription of aberrant splice variants at restrictive temperature, which results in the production of proteins with reduced or null activity that interfere with the wild type product. We can hypothesize that, by a similar mechanism, one of the *yap* alternative spliceforms disrupting Yap transcriptional activity is enriched at high temperatures. It is possible that at 28°C the presence of such a *yap* isoform could be low enough that the system compensates for it, while at 32°C its abundance is increased enough that any compensatory mechanisms is ineffective.

The change in protein-protein interaction stability between Yap and one of its eye-specific partners, or the temperature-dependent enrichment of one specific *yap* spliceform could explain temperature-dependent changes in the yap^{nl13} activity. However, it is unlikely that the transcription of *yap* itself is directly modulated in a temperature-dependent manner. In fact, we observed a downregulation in *yap* expression in the yap^{nl13} mutant in both in embryos raised at 28°C and 32°C. This is different from what was observed in other temperature-dependent eye mutants like medaka *eyeless (el)* (Loosli et al., 2001; Winkler et al., 2000). This mutant carries an intronic mutation in the *Rx3* gene and when raised at restrictive temperature it completely lacks eyes. The phenotype of this mutant is linked to the temperature-dependent repression of the *Rx3* gene caused by the position of the *el* mutation (Loosli et al., 2001). While the exact mechanism of such transcriptional repression has not been resolved, it is suggested that the *eyeless* mutation alters accessibility of the *Rx3* locus to the transcriptional machinery. A temperature dependent and tissue specific regulation of *yap* transcription in the yap^{nl13} is an intriguing possibility considering that both the examples provided by the *eyeless* and the $mitfa^{vc7}$ mutants involve eye related genes.

Because of the structural homology between Yap and Taz, different studies have reported the compensatory role of *taz* in response to *yap* mutations (Gao *et al.*, 2014; Varelas, 2014; Plouffe *et al.*, 2018; Tang *et al.*, 2018). While *taz* is compensating for the lack of *yap* in the yap^{mw48} zebrafish, this is not the case in the yap^{nl13} mutation. The lack of upregulation of *taz* in yap^{nl13} embryos raised at 28°C, where the penetrance is reduced, suggests that enhanced *taz* activity is not responsible for the amelioration of the phenotype in this condition. This

hypothesis is corroborated by the increase of *taz* transcription that we observed in *yap*^{nl13} mutant embryos raised at 32°C where the mutation is, conversely, fully penetrant. The fact that *taz* does not compensate for the lack of *yap* is also supported by the fact that *ctgfa* transcription is consistently downregulated in *yap*^{nl13} embryos raised at both 28°C and 32°C, and is not affected by the upregulation of *taz* in *yap*^{nl13} embryos raised at 32°C. The reduced transcriptional activity of both Yap and Taz is also supported by the decreased expression of 4xGTIIC:d2GFP that was observed in *yap*^{nl13} mutants.

The increase of *taz* transcription in *yap*^{nl13} mutant embryos raised at 32°C could however be explained as a compensatory mechanism. It is possible that in a stress situation, the observed increase in *taz* transcription represents a compensation for the lack of Yap transcriptional activity. Such a compensatory mechanism appears however to be insufficient to restore the pathway downstream of Yap, as both *ctgfa* and 4xGTIIC:d2GFP are not restored to wild-type transcriptional levels. Indeed, it has been observed that overexpression of *vsx2*-driven *taz* in wild-type embryos can induce disorganization in the zebrafish retina (Miesfeld et al., 2015). Therefore, it is possible that while not compensating for the lack of functional Yap protein, the overexpression of *taz* could cause the exacerbation of the *yap*^{nl13} phenotype at high temperature.

Overall, we hypothesize that the *yap*^{nl13} mutation leads to the synthesis of a Yap protein unable to generate a stable complex with some eye-specific partner. This results in a reduction of Yap transcriptional activity specifically in the eye. The reduced transcriptional activity of Yap possibly triggers a compensatory mechanism leading to an increase in *taz* transcription in embryos under stressing conditions. However, this compensatory mechanism is not able to overcome the lack of Yap transcriptional activity, resulting in a reduced activation of the pathway downstream Yap which finally leads to the eye specific phenotype of *yap*^{nl13} mutant.

Chapter 3.

Cell differentiation and proliferation are not affected in the RPE of *yap*^{nl13} mutants.

3.1 Introduction

Misregulation of both cell proliferation and cell differentiation in the developing eye are possible causes underlying the coloboma phenotype in both mouse and zebrafish (Ozeki *et al.*, 2000; Morcillo *et al.*, 2006; Lee, Lee and Gross, 2013; Babcock *et al.*, 2014; Deml *et al.*, 2016). Regulation of cell death and proliferation is required for the initiation of choroid fissure formation (Morcillo et al., 2006). In mice, loss of dorsoventral patterning, following disruption of the *Bmp7* activity, leads to absence of choroid fissure formation due to reduced cell proliferation and apoptosis in the ventral region of the eye. Indeed previous studies in mice revealed that apoptosis is required for the maintenance of the choroid fissure during development (Ozeki *et al.*, 2000). In this study it was observed that while apoptosis was observable in the choroid fissure region of the eye throughout development, at the moment of choroid fissure fusion cell death was not detectable suggesting that the persistence of the choroid fissure opening is sustained by cell death.

Reduction in cell proliferation and increase of cell death in the developing neuroretina are reported as causing coloboma in the *mab21l2* zebrafish mutant (Deml *et al.*, 2015). The *MAB21l2* gene was first isolated in humans through pedigree studies of patients affected by microcornea, cataract and coloboma. Mutation of *mab21l2* in zebrafish also leads coloboma phenotype. Analyses of cell proliferation and apoptosis in this mutant revealed an increase of cell death and defects of proliferation across the whole optic cup and in the ventral retina. Similarly, it has been shown in zebrafish that knockdown of the gene *aldh7a1* leads to failure in choroid fissure closure due to loss of cell proliferation (Babcock et al., 2014). The ALDH gene family is critical for organ development as it contributes to the synthesis of the morphogen retinoic acid. In zebrafish, the gene *aldh7a1* has a strong localised expression in the eye, supporting a role in the morphogenesis of this organ. The study shows that reduction of *aldh7a1* expression leads to reduction of cell proliferation in the optic cup. This reduction in proliferation does not allow the apposition of the nasal and temporal margins of the choroid fissure, ultimately resulting in ocular coloboma.

Abnormal increase of apoptosis in the optic cup has been associated to coloboma phenotype also in the *bcl6a* zebrafish mutant (Lee et al., 2013). Similar to the *mab21l2*, the *bcl6a* gene has been identified through screening of human patients showing coloboma phenotype. The coloboma phenotype in the *bcl6a* zebrafish knockdown is associated with an increase in cell apoptosis across the whole retina as a consequence of loss of p53 repression. In this mutant, inhibition of p53 reduced cell death driven by the loss of *bcl6a* and rescued the coloboma phenotype.

Cell proliferation, specifically in the RPE, is one of the forces driving optic cup invagination (Carpenter *et al.*, 2015): it was proposed that the differential proliferation of the RPE and of the neuroretina in the optic cup leads to the formation of its curvature in a “bimetallic strip”-like system. As the RPE expands more than the underlying neuroretina, the difference in the extension between the two tissues forces the optic cup to bend to accommodate for the difference in cell number. This model was proposed by observation of the $Wls^{fl/fl}$ knock-out mouse. In this model, loss of the Wnt ligand *wntless* (*wls)* in the periocular ectoderm led to a reduction of Wnt-mediated RPE proliferation. The decreased proliferation induced by the *Wls* loss was specific to the RPE and did not affect the neuroretina: this ultimately resulted in loss of the differential expansion between the neuroretina and the RPE, leading to misfolding of the optic cup.

Impaired cell proliferation can thus lead to coloboma as a consequence of misshapen optic cup or disrupted eye patterning which impairs the apposition of the two margins of the choroid fissure. However, in zebrafish, cell proliferation and apoptosis are not required for choroid fissure fusion itself (Gestri *et al.*, 2018). In zebrafish, no apoptotic events were detected during choroid fissure fusion. It was furthermore observed that inhibiting cell proliferation once the optic cup patterning is complete does not impact this process.

The regulation of cell proliferation and apoptosis are thus required for choroid fissure closure in earlier developmental stages to ensure the correct morphogenesis and patterning of the optic cup. Once the morphogenesis and patterning of the optic cup are established, choroid fissure fusion likely occurs independently from cell proliferation and apoptosis. Impaired cell differentiation

can however lead to failure in choroid fissure closure without affecting optic cup morphogenesis. One example is provided by *Fgfr1/2* conditional knockout mice (Chen *et al.*, 2013). In this knockout, the dorsal-ventral polarity of the optic cup is unaffected, and eye morphogenesis occurs normally with the only exception of failure in choroid fissure fusion. This study showed that the failure in choroid fissure closure depends on misregulation of FGF-mediated differentiation of the cell population at the choroid fissure. It was demonstrated that FGF signalling is critical in regulating the timing of choroid fissure cells fate switch which allows their integration in the neuroretina and in the RPE at the moment of choroid fissure fusion. Disruption of FGF signalling led to extension of the *Mitf* expression domain in the inner layer of the choroid fissure, in place of the neuroretina domains, impairing the possibility of its two margins of to fuse. Impaired cell differentiation can thus lead to failure in choroid fissure closure in the latest stage of eye development.

Cell differentiation, cell proliferation and of apoptosis are all key processes through which organ growth is regulated during development and the transcriptional factor Yap has a critical role in their fine tuning. The activity of Yap is negatively regulated by the Hippo pathway, one of the first pathways recognized to be critical in the regulation and maintenance of organ size during development. The function of the Hippo pathway was first investigated in *Drosophila* through screening for mosaic mutants showing tissue overgrowth phenotype. These studies allowed the identification of some of the main effectors of the Hippo pathway and clarified its role in the control of tissue growth (Justice *et al.*, 1995; Xu *et al.*, 1995). More recent studies on the overgrowth phenotype of *hippo Drosophila* mutants revealed that the Hippo pathway regulates cell proliferation and cell apoptosis in developing tissues (Wu *et al.*, 2003). In particular, *Drosophila hippo* mutants show hyperproliferation of the imaginal discs and resistance to the pro-apoptotic signals that would normally counterbalance imaginal disc cell proliferation. Aside from the overgrowth phenotype however, the *hippo* mutants analysed showed no major disruption of tissue patterning: in these mutants, the overgrown imaginal discs developed into mature organs larger than the wild type, without any major defects. These observations corroborated the consideration of the Hippo pathway being a master regulator for organ size

during development. Interestingly, this study found that the *Drosophila* phenotype could be rescued by expression of a human homologue of *hippo* (*MST2*)**,** revealing that the Hippo pathway is evolutionarily conserved even across different subphyla (Wu *et al.*, 2003).

Following works identified *Yorkie* (*yki)* (the *Drosophila* ortholog of *yap*) as the final nuclear effector of the Hippo pathway. One study in *Drosophila* (Huang *et al.*, 2005) has shown that overexpression of *yki* induces overgrowth of the wing and eye imaginal discs in the pupal eye, recapitulating the phenotype of Hippo mutants. Similar to the previously described Hippo mutants, the *yki* overexpression overgrowth phenotype is also caused by increased proliferation rate and resistance to apoptosis. This study critically identified *yki/yap* as the terminal effector of the Hippo signalling cascade, directly regulating cell proliferation.

The role of the Hippo pathway and *yap* in the regulation of organ growth discovered in *Drosophila* is strongly conserved in vertebrates**.** In adult mouse, liver-specific induction of *YAP* expression resulted in severe organ overgrowth (up to 4-fold liver size increase) (Camargo et al., 2007; Pan, 2007). The liver overgrowth is accompanied by cells smaller than the wild type and highly proliferative, indicating that the increase of organ size is the consequence of increased cell proliferation. The increase of proliferation in *YAP* overexpressing mouse liver is also accompanied by resistance to apoptotic signals similarly to what is observed in *yki Drosophila* mutants (Camargo et al., 2007). Furthermore, the same study revealed the role of *YAP* in the maintenance and expansion of the pools of undifferentiated cells in the mouse intestine: *YAP* overexpression resulted in expansion of the pool of undifferentiated cells in the intestinal crypts, leading to an overall decrease of differentiated enterocytes. Overall, these studies show that the Hippo pathway, and *yap* in particular, have a critical role in the regulation of organ growth by controlling cell proliferation and apoptosis. They furthermore revealed the role of *yap* in the regulation of cell specification prior to organ and tissue proliferation and growth.

In zebrafish, mutations in *yap* and in its homologue *taz* have been previously associated with defects in the RPE (Miesfeld et al., 2015)**.** In particular, the

yap^{mw48} zebrafish mutant shows extensive loss of RPE cells in the larval eye while the underlying neural retina appears normal. Observations on RPE cell death and proliferation revealed that these processes were not altered by the *yap*^{mw48} mutation. The role of *yap* and *taz* in RPE differentiation was observed with transplants experiments. Clones of cells derived from a transplant from a *yap*$^{-/-}$; *taz*$^{-/-}$ donor embryo failed to differentiate into RPE when grafted into wild type hosts. This indicates that *yap* and *taz* are both required for the specification of RPE progenitor cells. In accordance with this, overexpression of wild-type *yap* in wild type embryos induced formation of ectopic RPE cells and, conversely, overexpression of a dominant negative *yap* allele results in loss of RPE cells. This study elucidated how *yap* and *taz* are critical signals for the specification of the RPE in zebrafish.

Differently from the *yap*^{mw48} mutant, the *yap*^{nl13} mutant zebrafish phenotype is characterised by coloboma and the RPE shows lack of continuity mainly limited to the choroid fissure region. Similarly to what is described in *yap*^{mw48} mutants, in *yap*^{nl13} mutant embryos the neuroretina is unaltered (Miesfeld et al., 2015). We thus asked whether the *yap*^{nl13} zebrafish mutant also shows defects in the specification and in the expansion of the RPE domain. The fact that *yap* is involved in RPE specification suggested that the phenotype of *yap*^{nl13} mutant could be the consequence of defects in this tissue. This hypothesis is also supported by the fact that in *yap*^{nl13} zebrafish mutants, the neuroretina is overall unaltered. Furthermore, overexpression of wild-type *yap* specifically in the RPE is sufficient to rescue the *yap*^{nl13} coloboma phenotype (Gaia Gestri, unpublished data). The results of these experiments suggest that the coloboma phenotype of *yap*^{nl13} zebrafish mutants is the consequence of defects in the development of the RPE.

Here, we investigated the effects of the *yap*^{nl13} mutation in the early phases of the RPE development. Critically, the earliest phases of the expansion of the RPE across the developing optic vesicle are strongly reliant on *de novo* specification which is followed only in later stages by an expansion mediated by cell-stretching (Cechmanek and McFarlane, 2017). We thus focused on understanding whether the *yap*^{nl13} mutation prevent RPE differentiation or affects RPE cell proliferation

during the early phases of RPE-genesis. We hypothesised that the coloboma phenotype could arise as a consequence of a depletion of the RPE domain at the time of RPE specification: a reduction in the pool of RPE cells could result in optic cup invagination defects leading to a coloboma phenotype. The reduction of the RPE domain could be the consequence of both a reduced initial pool of RPE cells or a reduced expansion rate of this tissue. Here, we used 4D confocal imaging to investigate the effects of the *yap*^{nl13} mutation in the early phases of the RPE development to understand whether *yap*^{nl13} mutation leads to reduction in RPE specification and/or in RPE cell proliferation.

3.2 Results

3.2.1 Specification and expansion of the RPE are not delayed in the *yap^{nl13}* zebrafish mutant.

Given that *yap^{nl13}* mediated coloboma is due to defects in the RPE we decide to test whether the specification and expansion of the RPE were reduced in *yap^{nl13}* mutant embryos. We performed time lapses on the Tg(*bhlhe40*:eGFP) reporter line embryos injected with H2B:RFP construct. These embryos show expression of GFP in the RPE domain and ubiquitous nuclear RFP (Cechmanek and McFarlane, 2017). The time-lapses were performed with an interval of 45 minutes between every frame on both wild type and *yap^{nl13}* mutant embryos raised at 32°C starting from 16hpf (for details on confocal imaging acquisition refer to Chapter 6: Material and Methods). We started the time-lapse experiments before the beginning of GFP expression in the RPE in order to visualize the early phases of RPE specification. The imaging was stopped at optic cup stage in order to track the expansion of the RPE.

Comparing the development of the RPE between wild type and *yap^{nl13}* mutant embryos, we observed that the earliest moment in which expression of *bhlhe40:eGFP* is detectable does not differ between wild-type and *yap$^{n1l3.}$*mutants. This suggests that *yap^{nl13}* mutation does not delay the onset of RPE specification (N = 12 wt; N= 6 *yap^{nl13}*; **Fig. 3.0**). Qualitatively, the expansion of *bhlhe40:eGFP* expression domain through time appears to be similar between wild type and *yap^{nl13}* mutant embryos **(Fig. 3.0)**. Even though in the *yap^{nl13}* the GFP signal appears to be less intense, both the dynamics of its increase and the extent of the RPE domain are not visibly reduced. This suggests that both the timing of RPE specification and the dynamics of its expansion are not altered by the *yap^{nl13}* mutation. This experiment furthermore highlights the integrity of the RPE during differentiation: the expression pattern of *bhlhe40:eGFP* appears to be continuous both in wild type and in *yap^{nl13}* zebrafish embryos. Furthermore, it does not reveal the presence of regions where GFP is not expressed which would indicate defects in the RPE specification prior to melanisation.

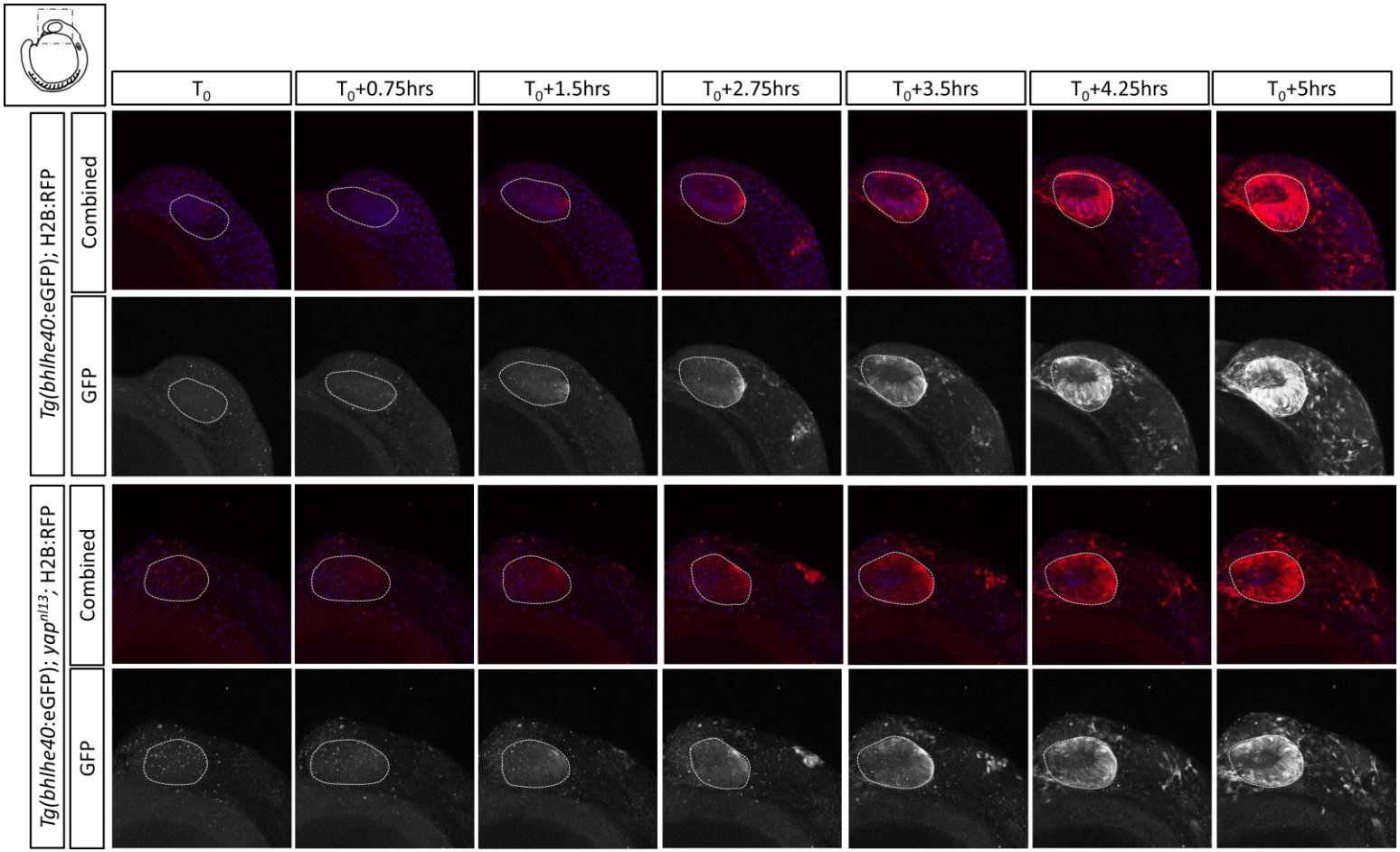

Figure 3.0| Expansion of the RPE on the optic vesicle is not affected in *yap*^{nl13} mutant embryos.
Maximum projection of individual frames from time lapse imaging of *Tg(bhlhe40:eGFP)* embryos raised at 32°C. The dashed line indicates the optic vesicle.

3.2.2 The specification and proliferation rate of the RPE are not affected in the *yap^{nl13}* zebrafish mutant.

To gain a deeper insight into how the *yap^{nl13}* mutation affects the specification of the RPE and its expansion, we performed quantitative analysis on the data obtained from the time-lapse imaging. We analysed the size of the RPE at the moment of its onset and its rate of growth. To assess the size of the RPE domain at the time of specification, we first observed the number of cell nuclei at the earliest moment in which we could detect RPE signal in both wild type and *yap^{n1l3}* mutant embryos (18 hpf). With the use of IMARIS software, we isolated the RPE volume and segmented individual RPE cell nuclei **(Fig. 3.1 A, B)**. This process was performed at the earliest frame we could detect signal from *Tg(bhlhe40:eGFP)* expression (T_{sp}). At this timepoint, the number of nuclei detected in the nascent RPE of *yap^{nl13}* mutant embryos was not significantly different from the number of nuclei detected in the nascent RPE of wild type larvae (**Fig. 3.1 C**; Cell Count T_{sp}: Wild Type = 22.35± 1.432; *yap^{nl13}*= 26.63±3.585; Mean±SEM; Non-parametric t-test for unpaired data = p>0.05).

We furthermore addressed the possibility that, although the cell number is unvaried in the RPE of *yap^{nl13}* mutant embryos, the size of RPE cells at early specification might be altered resulting in a different final RPE domain size. We thus compared the areas of the RPE surfaces obtained through segmentation. Similarly to the cell number results, we could not identify any statistically significant difference between the size of RPE cells in *yap^{nl13}* mutant embryos and in wild-types at 18 hpf (**Fig 3.1 D**; RPE Surface at T_{sp}: Wild Type = 5504±221.1; *yap^{nl13}* = 5525±301.4 ; Mean±SEM; Non-parametric t-test for unpaired data = p>0.05). Overall, these results indicate that the *yap^{nl13}* mutation does not affect the initial specification of the RPE as both the number of early RPE cells and their size remained unvaried in *yap^{nl13}* zebrafish mutant.

As we did not observe any alteration in the early specification of the RPE in the *yap^{nl13}* mutant, we asked whether its later expansion is affected by this mutation. To address this question, we calculated the increase of RPE cell number between the earliest moment of RPE specification (T_{sp}) and after 1.5 hours (T_{sp}+1.5hrs).

We thus extracted the data relative to the RPE nuclei numbers in the frames T_{sp}+1.5hrs following the same processing performed for T_{sp} data analysis. We then calculated the fold increase of RPE cells as the ratio of RPE nuclei counted in T_{sp}+1.5 and T_{sp} and compared the obtained values between wild types and *yap*^{nl13} mutant embryos. The calculated value is representative of the overall rate of the RPE expansion including cell proliferation, recruitment and de-novo differentiation. The fold increase values that we calculated are not significantly different between the wild type and the *yap*^{nl13} mutant embryos (**Fig. 3.1, E**; Cell Count Fold Increase: Wild Type = 3.847±0.2932; *yap*^{nl13} = 3.140±0.3138; Mean±SEM; Non-parametric t-test for unpaired data = p>0.05).

Some of the *yap*^{nl13} mutant eyes are smaller than the wild type eyes when analysed at 3dpf. Thus while the expansion of the RPE does not seem to be affected in the *yap*^{nl13} mutant, it is possible that the overall coverage of the eye is affected if *yap*^{nl13} mutant eyes are smaller at earlier stage. To assess whether this is the case we quantified the area of the eye at the moment of RPE specification by manual segmentation and calculated the ratio between the obtained value and the measure RPE surface. Our results show that at the moment of RPE specification the eye of wild types and *yap*^{nl13} mutants have no significant difference in overall surface (**Fig 3.2 A,B;** Eye Surface: Wild Type= 403.8 ± 24.40 N=10 *yap*^{nl13} = 400.2 ± 27.34 N=6 0.9253. Mean±SEM; Unpaired t-test for unpaired data = p=0.925). Similarly, the ratio between RPE surface and overall eye surface, representing the overall RPE coverage of the eye, is not significantly different between wild type and *yap*^{nl13} embryos (**Fig 3.2 C;** RPE Surface /Eye surface ratio: Wild Type= 0.1454 ± 0.01870 N=10 *yap*^{nl13} 0.1496 ± 0.01916 N=6 0.8843 Mean±SEM; Unpaired t-test for unpaired data p=0.884). These data suggest that the lack of difference in RPE size between wild type and *yap*^{nl13} mutant is also representative of unchanged coverage of the eye from the RPE in the *yap*^{nl13} mutants.

Consistently with our previous qualitative observation, these data confirm that the *yap*^{nl13} mutation does not affect the early stages of expansion of the RPE. Overall, our results indicate that the *yap*^{nl13} mutation does not affect early RPE-genesis

suggesting that the coloboma phenotype in *yap*^{nl13} zebrafish mutant may arise by misregulation of RPE growth in later stages of development.

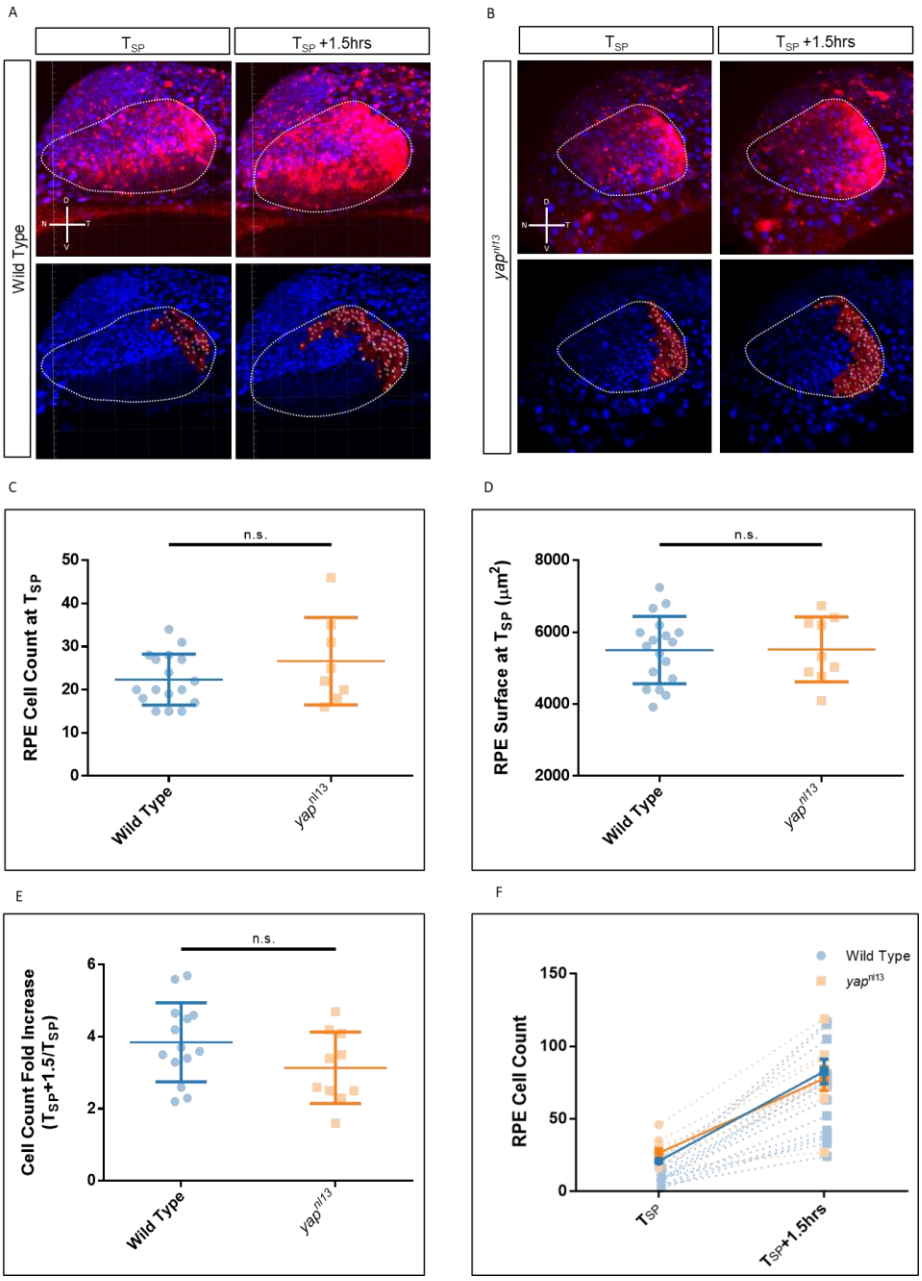

Figure 3.1| RPE specification and expansion are unaffected in the *yap*^{nl13} zebrafish mutant.
A-B| Representative view of two time-frames used for assessing the number of RPE cells at the moment of specification (T_{sp}) and 1.5hrs later (T_{sp}+1.5hrs). The bottom row shows an example of the segmented surface of the RPE and the measured nuclei. (D=dorsal; V=ventral; N=nasal; T = temporal) **C|** Cell count in the RPE at the moment of specification (shown in: A,B; T_{sp}) in wild type and *yap*^{nl13} mutant embryos. **D|** Measurement of RPE cell surface at the moment of specification (shown in: A,B; T_{sp}); **E|** Measurement of the cell number fold increase calculated as the ratio between T_{sp} and T_{sp}+1.5hrs shown in figure A. **F|** Comparison of individual cell counts in both wild type and *yap*^{nl13} mutant embryos at both the measured time points.

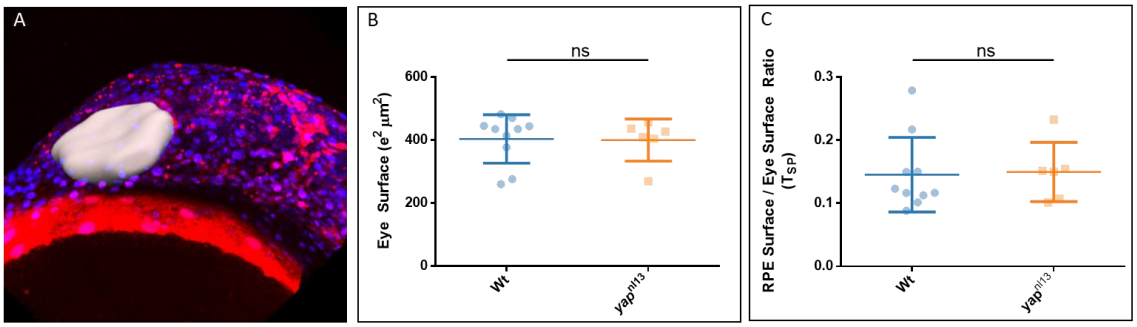

Figure 3.2| The size of the eye and the RPE coverage are not affected in the yapnl13 zebrafish mutant.

A| Representative view of the time frame used for segmentation of the eye volume and calculation of the eye surface. **B|** Quantification of the eye surface at the time of RPE specification (T_{SP}) in wild type and *yap*^{nl13} mutant embryos. **C|** Quantification of the ratio between the obtain RPE surface and the overall eye surface in wild type and *yap*^{nl13} mutant embryos

3.3 Discussion

Our results suggest that *yap*^{nl13} mutation does not affect the earliest stages of RPE-genesis: we observed that the onset of RPE specification is not delayed in the *yap*^{nl13} mutant and that the size of the RPE domain in this phase is not altered. We also observed that RPE expansion is not altered in the *yap*^{nl13} mutant and that RPE integrity is maintained as it covers the whole optic vesicle without points of discontinuities.

The data we collected showed that the initial specification of the RPE is not affected by the *yap*^{nl13} mutation: both the size of the early RPE and its cell number are not altered in the *yap*^{nl13} zebrafish mutant. Our observations differ from what was previously described for the *yap*^{mw48} zebrafish mutant where the disruption of Yap transcriptional activity resulted in the lack of RPE differentiation (Miesfeld et al., 2015). However, the *yap*^{mw48} phenotype is more severe than that of *yap*^{nl13} mutants. It is possible that the more dramatic phenotype of the *yap*^{mw48} zebrafish mutant is caused by the early truncation in the Yap protein caused by this mutation. As the WW domains are required for Yap interaction with other co-transcriptional factors, it is possible that the persistence of these domains in the *yap*^{nl13} mutant allows the recruitment of transcription activation complexes (Finch-Edmondson et al., 2016; Salah and Aqeilan, 2011). Thus, while the direct transcriptional activity of Yap is disrupted due to the loss of the transactivation domain, the formation of complexes with other co-transcriptional factors (such as Taz) could be sufficient to partly compensate for the protein truncation. While this compensation could be sufficient to induce RPE differentiation in the *yap*^{nl13} zebrafish mutant, it may be not sufficient to ensure the correct development of the RPE during later phases of eye morphogenesis.

Previous experiments performed in the lab suggested that in the *yap*^{nl13} zebrafish mutant, RPE proliferation is not affected (data not shown). Immunohistochemistry experiment labelling for the mitotic marker phospho-histon H3 (PH3), showed in fact no significant reduction in the number of proliferative cells in the RPE of *yap*^{nl13} mutant embryos at 24hpf and 48hpf compared to the wild types. However, while the immunohistochemistry experiments allowed to assess the mitotic state

of the RPE at specific time points, they do not provide dynamic information on the expansion of the RPE during eye. Our time-lapse experiments did not reveal changes in the rate of expansion of the RPE domain in the *yap*^{nl13} mutant. While these analyses do not directly account for changes in cell proliferation and mitotic rate, they indicate that the final number of RPE cells is not significantly affected by the *yap*^{nl13} mutation. Indeed, it has been recently showed that at these early stages the expansion of the RPE is mainly reliant on cell proliferation(Moreno-Mármol *et al.*, 2020). This is similar to what have been shown in the *yap*^{mw48} zebrafish mutant in which disruption in *yap* transcriptional activity does not alter cell proliferation or apoptosis in the RPE (Miesfeld et al., 2015). It is thus possible that, also in the *yap*^{nl13} mutant, the lack of alteration in the RPE expansion rate is the consequence of normal proliferation. Conversely, if RPE proliferation was indeed affected, our results could indicate the presence of compensatory mechanisms which regulate differentiation or recruitment to account for the reduction in cell proliferation. Altogether, our data from time-lapse analysis, combined with both the previous observation on phospho-histone H3 immunohistochemistry and with the observation reported on the *yap*^{wm48} zebrafish mutant, suggest a scenario in which the *yap*^{nl13} mutation does not affect the expansion of the RPE nor its proliferation.

While the role of *yap* in the control of the RPE specification has become evident by the observation of the *yap*^{mw48} zebrafish mutant, our results suggest that *yap* has a role in eye development beyond that in RPE specification. As early RPE-genesis is unaltered in *yap*^{nl13} zebrafish mutant, it is possible that this mutation affects later stages of eye development. Differently from the early phase of RPE-genesis, the later phase of RPE domain expansion mostly relies on cell stretching and on the regulation of tissue tension (Cechmanek and McFarlane, 2017). Thus, considering its role in mechanotransduction, it is reasonable to hypothesize that *yap* has a critical role in this phase of RPE-genesis. It is possible that, while the expansion of the RPE is not affected in the *yap*^{nl13} zebrafish mutant, a difference in RPE cell contractility might impair the bending of the optic cup providing an alternative mechanism for coloboma formation in the *yap*^{nl13} mutant. The observations performed in *yap*^{nl13} and *yap*^{wm48} mutants may thus highlight two complementary functions of *yap* in the development of the RPE: while in the early

phases *yap* is critical to regulate the specification of this tissue, in the later phases of eye development *yap* may regulate the stretching of the RPE over the optic vesicle.

Chapter 4.

Myosin-mediated cell contractility is critical for eye morphogenesis and is impaired in *yap*^{nl13} mutants.

4.1 Introduction

Whilst the molecular mechanisms driving eye development have been subject to scientific investigation since the onset of embryology as a research field, only in the past decades effort has been put in understanding the mechanobiology of the developing eye. During eye morphogenesis the neuroectoderm that gives origin to the eye undergoes dramatic movements and morphological remodelling. The entity of the mechanical forces driving the movements of eye morphogenesis has been object of a number of recent studies both *in vitro* and *in vivo*.

In the understanding of the biophysics of the developing eye, the extracellular matrix (ECM) is a strong morphogenetic force supporting the folding of the eye *in vivo*. The extracellular matrix is a complex glycoprotein-rich layer that surrounds the eye, the lens and that fills up the space between the optic vesicle and the lens during every step of eye morphogenesis (Kwan et al,2014). It is composed by a number of molecules, the most studied of which are the mesh-forming laminin, fibronectin and collagen IV. These components, shared by all vertebrates, are present in the ECM surrounding the eye, from the earliest stage of eye development (Parmigiani and McAvoy, 1984; Peterson *et al.*, 1993, 1995).

A study in chick (Oltean et al., 2016) showed that the stiffness of the tissues surrounding the optic vesicle is critical in providing the mechanical constriction driving the correct expansion of the optic vesicle and the subsequent optic cup invagination. Such stiffness is generated partly by the deposition of ECM from both the optic vesicle and the surface ectoderm. This study has shown that removal of the surface ectoderm at different developmental stages has very different outcomes on optic cup formation. Removing the surface ectoderm prior to optic placode formation, but not afterwards, inhibited optic cup formation. However, this did not remove the ECM surrounding the optic vesicle: to decouple the role of ECM and surface ectoderm, collagenase digestion has been performed to remove ECM at different developmental stages. The study revealed that collagenase treatments after surface ectoderm removal significantly increase the number of embryos failing to go through optic vesicle invagination, highlighting the role of ECM in the formation of the optic cup. These results

suggested that the ECM surrounding the optic vesicle generates a force opposing to its lateral expansion. This resisting force is critical to physically contain and constrain optic vesicle growth and to force its distal portion to an inward movement that generates the optic cup. Enzymatic removal of the ECM through collagenase during optic vesicle invagination lessens the mechanical force opposing its evagination leading to the formation of a convex optic cup **(Fig. 4.0 A)**.

Laminin is one of the main components of the ECM and its function has been mostly investigated *in vitro*: Laminin is a critical substrate for cell adhesion and it is an important signalling factor for cell survival and for establishment of cell polarity (Hamill *et al.*, 2009; Chaudhuri *et al.*, 2014). Different Laminin mutants in zebrafish showed that these proteins are required for optic cup morphogenesis. The zebrafish mutants *lamb1* and *lamc1* showed lens dysplasia and coloboma (Lee and Gross, 2007; Ivanovitch, Cavodeassi and Wilson, 2013; Bryan, Chien and Kwan, 2016). Furthermore, the zebrafish *laminin* mutant *lama1* shows several eye defects: optic vesicle invagination is impaired and the optic cup fails to properly enwrap the lens, which is, in turn, ovoidal rather than spherical (Bryan, Chien and Kwan, 2016). Furthermore, the retina in *lama1* mutant embryos is strongly disorganised. In particular, the absence of laminin resulted in disruption in cell polarity: in the retina of *lama1* mutants, staining for apical and basal markers revealed the presence of ectopic apical and basal domains. Loss of Laminin furthermore resulted in increased level of apoptosis which could not be rescued by knock-down of p53. The fact that loss of Laminin induced p53-indipendent apoptosis suggested that the high level of cell death could be due to anoikis: programmed cell death in consequence of loss of matrix attachment(Bryan, Chien and Kwan, 2016).

The critical role of laminins in eye development is furthermore evident in humans. One example is given by the phenotype in Pierson syndrome which arises from an autosomal recessive mutation in the Lamininβ2 gene (*LAMB2*) (Bredrup *et al.*, 2008). Pierson syndrome is a congenital nephrotic syndrome, leading to important and life-threatening kidney disorders. Together with the kidney defects, Pierson syndrome is accompanied by eye abnormalities, which can be, in the

earliest phases of the syndrome, the only visible phenotype. *LAMB2* mutation leads to a wide range of eye defects including lenticonus, iris hypoplasia, retinal detachment, glaucoma and misshapen lens.

Fibronectin (*fn*) is another main component of the extracellular matrix. The role of this protein in eye development has been explored in the *hirame* medaka mutant (Porazinski et al., 2015). In this mutant, loss of *yap* results in loss of actomyosin tension generation which leads to impairment in the deposition of Fibronectine and of its assembly. One of the phenotypes of the *hirame* mutant is the dislocation of the lens and loss of the filopodia between the lens and the neuroretina. To observe the specific effect of Fibronectine assembly independently from the loss of cytoskeletal tension, this study analysed the phenotype of *fibronectin* overexpression, which also results in aggregation of Fn fibres and disruption of its deposition. Indeed, the overexpression of *fibronectine* resulted on lens dislocation and loss of cellular processes connecting it to the neuroretina. The role of Fibronectine in the positioning of the lens was furthermore confirmed by the observation of the medaka Fn1 mutant *fukawarai* (*fku*) which also shows lens dislocation. These results indicated that Fibronectine is required in the eye for the correct alignment of ocular tissues and in the positioning of the lens (Porazinski *et al.*, 2015).

Overall, the extracellular matrix plays a central role the development of the eye and is required for the regulation of a variety of mechanisms. Firstly, ECM provides critical signalling for cell survival and differentiation. The ECM furthermore provides a mechanical substrate for the developing eye and allows the transmission of mechanical forces generated at a cellular level to the tissue level. Together with the mechanical properties of the tissues surrounding the eye, it has emerged that a difference in tissue stiffness between the presumptive neuroretina and the presumptive RPE (pRPE) is required for the correct invagination of the optic cup (Carpenter et al., 2015; Eiraku et al., 2012, 2011). A study performed *in vitro* revealed that a differential accumulation of phosphorylated myosin in the RPE and in the neuroretina leads to differences in the stiffness in these two tissues (Eiraku et al., 2011). The study has shown that the RPE has a higher level of phospho-myosin when compared to the

neuroretina. Measuring the stiffness of the two tissues with atomic force microscopy showed that the increase of phosphorylated myosin in the RPE makes this tissue significantly more rigid than the neuroretina. To confirm that the measured difference in tissue rigidity is dependent on the different accumulation of phosphorylated myosin, myosin contractility has been chemically inhibited. Inhibiting of myosin contractility resulted in loss of rigidity in the RPE, which acquired a stiffness more similar to the one measured in the neuroretina (Eiraku *et al.*, 2011).

The differential stiffness of the RPE and of the neuroretina is critical for the invagination of the optic cup (Eiraku et al., 2012). During the evagination of the optic vesicle, phosphorylated myosin is evenly distributed in the expanding neuroepithelium. As the most distal region of the neuroepithelium (the presumptive neural retina pNR) reduces its cell contractility and becomes less rigid, it begins to invaginate. In this phase the difference of stiffness between the neuroretina and RPE becomes critical. The study showed in fact that inhibition of myosin phosphorylation during the evagination of the neuroectoderm -while the differential stiffness of the RPE and neuroretina becomes established- leads to failure in forming the optic cup. Conversely, inhibition of actomyosin contractility once the optic vesicle is completely evaginated and the RPE is already more rigid than the neuroretina, has no effects on the following invagination. From these data it has been proposed the “relaxation-expansion” model for self-folding of the optic cup. In this model as the neuroretina proliferates, the pRPE acts as a stiff shell surrounding it. The rigid retina pigment epithelium mechanically resists to the proliferation of the softer neuroretina, containing its circumferential expansion and driving its inward folding (Moreno-Marmol, Cavodeassi and Bovolenta, 2018) **(Fig. 4.0 B)**.

While the “relaxation-expansion” model mostly focuses on the difference in contractility between the neuroretina and the RPE, indeed the morphogenesis of the eye *in vitro* only occurred in the presence of Matrigel (Eiraku et al., 2012). Matrigel is a common culture substrate containing a number of structural proteins (e.g. laminin, nidogen, collagen) providing an ECM-like environment. The fact that *in vitro* optic cup formation requires Matrigel highlights that the ECM is critical

for eye morphogenesis. It can thus by hypothesised that, *in vivo* the stiffness of the RPE relies on a combination of factors: while the internal regulation of actomyosin contractility is critical in the generation of intrinsic forces within the RPE, the ECM is reasonably another factor increasing the rigidity of this tissue. A recent study in zebrafish furthermore indicated that impairment of the deposition of ECM surrounding the RPE leads to aberrant invagination of the optic cup (Bryan *et al.*, 2020). This study provides a further correlation between RPE stiffness and ECM.

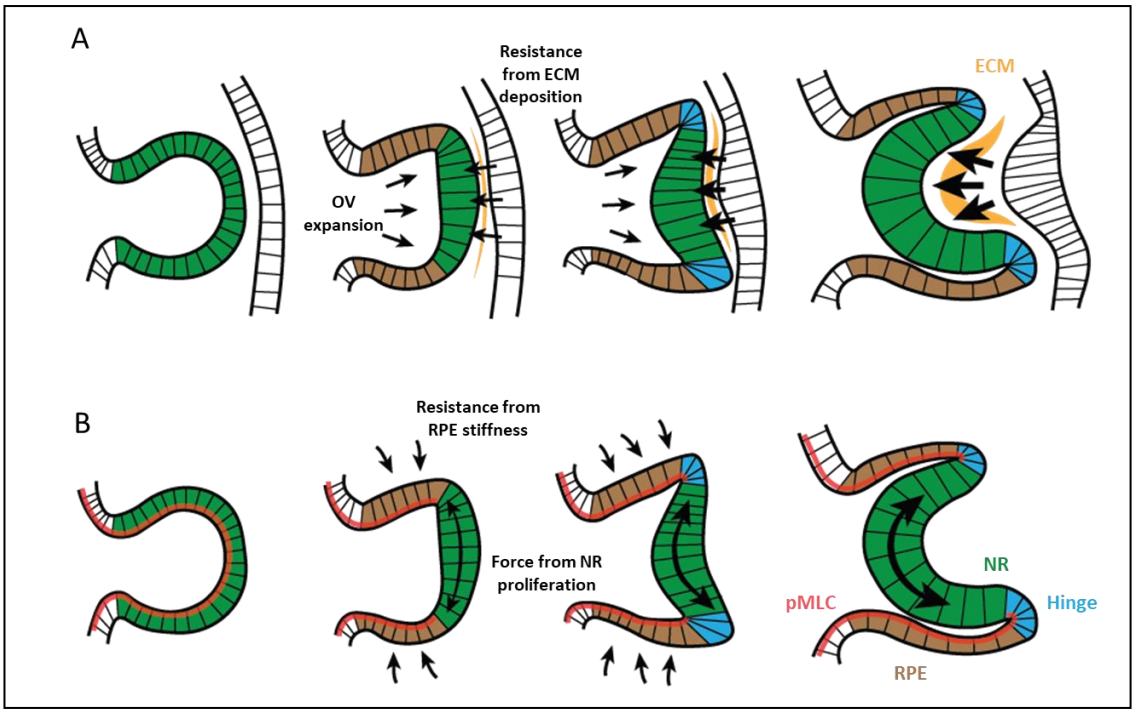

Figure 4.0| Models for optic vesicle invagination
A| The expansion of the optic vesicle (OV) is resisted by the extracellular matrix (ECM) secreted from the retina pigment epithelium (RPE) and the surface ectoderm (SE). The resistance from the ECM firstly leads flattening of the presumptive NR and then leads to the inward movements of the NR and to the formation of the optic cup (OC). **B|** Relaxation-Expansion model for OV invagination. After OV evagination, the levels of pMLC in the presumptive NR decrease. The proliferation of the softer NR generates a tangential force which is opposed by the stiffer RPE, forcing the invagination of the NR (Adapted from: Eiraku *et al.*, 2011)

While at a tissue level, the RPE needs to be rigid, individual RPE cells need to be sufficiently plastic to conform to the involution movements of the optic cup and to accommodate the growth of the NR. Consequently, the expansion of the RPE involves dramatic changes in cell shape. While it is specified as a pseudostratified epithelium, the RPE is stretched, its nuclei align, and it becomes a cuboidal epithelium (Graw, 2010; Moreno-Marmol, Cavodeassi and Bovolenta, 2018). In teleosts, this change in shape is furthermore continued and the mature RPE finally becomes a squamous epithelium (Li et al., 2000). The flattening of RPE cells is the main mechanism for RPE expansion over the NR as cell division is, conversely, dispensable (Cechmanek and McFarlane, 2017). Indeed, immunostaining experiments against phospho-histon H3 (pHH3), a mitotic marker, revealed low rates of proliferation, suggesting that cell division is not the main mechanism for RPE expansion**.** It was in fact observed in zebrafish that treating embryos with a strong inhibitor of cell proliferation (aphidilcolin) at optic cup stage does not result in loss of RPE (Cechmanek and McFarlane, 2017). These results suggested that cell stretching rather cell proliferation is the main force driving the expansion of the RPE domain after *de novo* specification. Although cell stretching appears to be critical in the expansion of the RPE, the mechanisms underlying the change in RPE cell morphology are not yet fully understood. It is still unclear whether this change in shape is cell-autonomous (i.e. driven by the active cellular regulation of the cytoskeleton) or whether it is the consequence of passive stretching driven by the involution of the neuroretina (Moreno-Marmol, Cavodeassi and Bovolenta, 2018).

Integration of tissues' mechanical information and fine tuning of cellular response to mechanical stimuli seem to be a critical element in eye development. We thus sought to investigate whether the coloboma phenotype in *yap*^{nl13} mutant could be explained by an impaired regulation of RPE cellular contractility and to an overall dysregulation of mechano-homeostasis. Mechanical homeostasis (as most of the homeostatic cellular systems) relies on two elements: on the one hand, the detection and translation of extracellular mechanical cues, and on the other hand, the mechanisms regulating the cellular response to such cues, responsible to balance the extracellular forces through regulation of the actomyosin cytoskeleton (intracellular forces) (Butcher et al., 2009). Yap has been identified

as one of the main elements in the control of mechanotransduction and mechano-homeostasis as it is involved both in the integration of extracellular mechanical information (mechanosensation) and in the cellular mechanical response to it (Aragona et al., 2013; Asaoka and Furutani-Seiki, 2017; Calvo et al., 2013; Dupont et al., 2011).

Yap's role in mechanosensation depends on its nuclearization and thus in its function as transcriptional activator. At a cellular level, Yap nuclearization, and thus its activity, is regulated by substrate rigidity, cell geometry and by strain forces (Dupont et al., 2011; Halder et al., 2012; Totaro et al., 2018). In particular *in vitro* experiments (Dupont et al., 2011) revealed that increase of the stiffness of culture medium is sufficient to induce Yap nuclearization. Cell plated on stiff fibronectin-coated hydrogel showed a higher transcriptional level of Yap's effectors (e.g. *CTGFA)* and an increase in the luciferase activity in a luciferase Yap reporter line (4xCTIIC-lux). The increase of transcriptional activation was paired with an increase in Yap nuclearization. The same study showed how Yap transcriptional activity is regulated by changes in cell shape. By constraining individual cells onto micro-patterned surfaces is possible to drive Yap nuclearization solely by the entity of cell confinement. In cells restricted on small surfaces, which show round or bulky shapes, Yap has been found to be mostly cytoplasmic. Conversely, in cells plated onto larger surfaces, showing a cell profile more similar to the one possessed by cells on an epithelium, Yap appears to be strongly nuclearized. A second study from the same group showed how Yap transcriptional activity can be induced by an increase of cell stretching (Aragona *et al.*, 2013). In this study it has been shown that in cells which have been mechanically stretched to increase their surface, the nuclearization of Yap increases. A more recent study in *Drosophila* (Fletcher et al., 2018) revealed that Yorkie (Yki, Yap ortholog in *Drosophila*) is nuclearized in epithelia subject to mechanical strain. In stretched cells, which acquire a flattened morphology, Yki is nuclearized and the expression of Yki target genes is consequently increased.

Changes in substrate stiffness, cell shape and mechanical strain are transduced intracellularly to Yap by changes in composition and in contractility of the actomyosin cytoskeleton. It has been shown that if actomyosin contractility is

inhibited with Blebbistatin treatments, increasing the stiffness of the culture medium does not increase Yap nuclearization and the consequent transcriptional activity (Dupont et al., 2011). Inhibition of actomyosin contractility furthermore stops Yap transcriptional activation in response to changes in cell shape. Differently from untreated cells, when cells treated with Blebbistatin are stretched and forced into a spread morphology, Yap is not nuclearized and consequently no increase in Yap's target transcription has been measured (Dupont et al., 2011).

The downstream targets of Yap close a feedback loop mechanism coupling mechanosensation and changes in mechanical responses of the cell. In particular, it is emerging that Yap transcriptional activity regulates the remodelling and the regulation of the actomyosin cytoskeleton. A clear example of this feedback loop is provided by the *hirame* (*hir*) medaka mutant, which carries a mutation in the *yap* gene (Porazinski et al., 2015). The *hir* mutant displays body flattening as a consequence of impaired generation of actomyosin contractile forces. It was observed that tissues in *hir* mutant are not able to generate the tension necessary to resist gravity resulting in a disrupted body axis. This study has furthermore identified ARHGAP18 (Rho GTPase-Activating Protein 18) as one Yap effector directly regulating actomyosin contractility. ARHGAP18, together with other members of the ARHGAP family, is known to regulate actomyosin contractility and cell shape through the regulation of proteins of the Rho family. Yap regulation of actomyosin contractility through activation if ARHGAP proteins has been furthermore reported in later studies on mammalian cell culture. All of these studies highlight the function of Yap in controlling myosin-mediated cell contractility clarifying the presence of a closed feedback loop in Yap-mediated mechanotransduction (Bai et al., 2016; Morikawa et al., 2015; Qiao et al., 2017; Xin et al., 2013)**.**

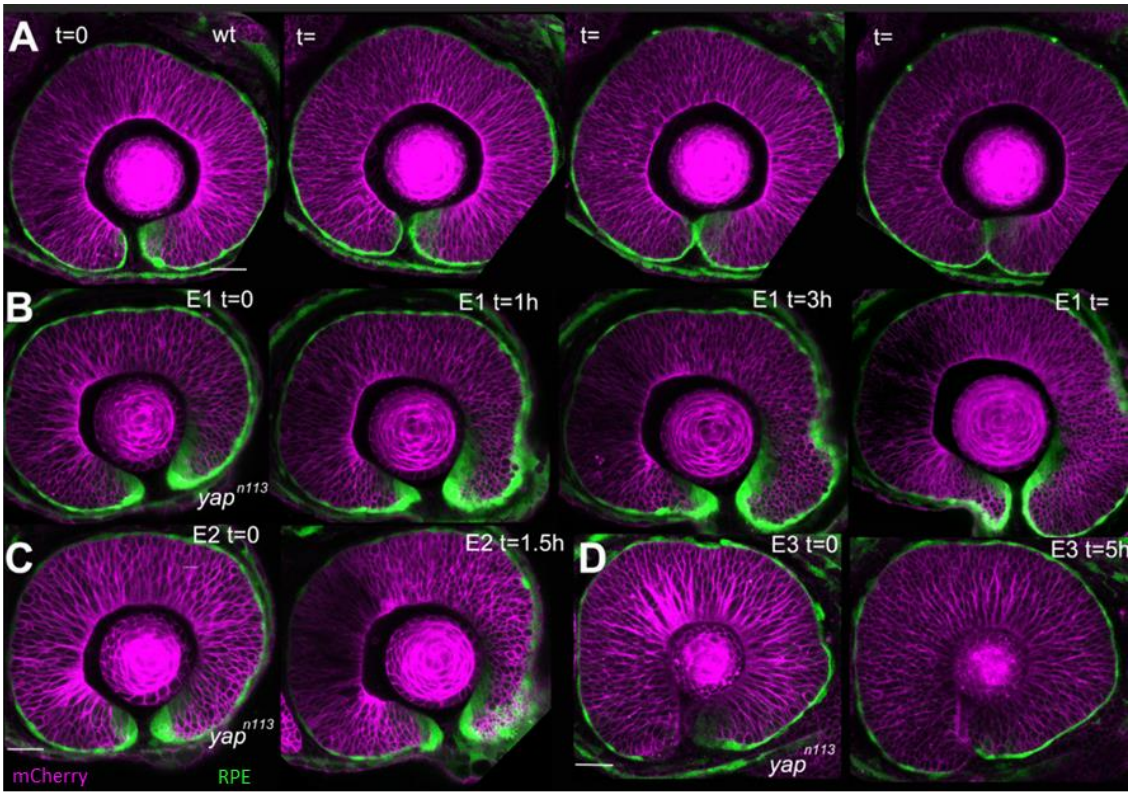

Figure. 4.6 |Time-lapse imaging of choroid fissure closure in wild type and yapnl13 zebrafish embryos
A| Choroid fissure closure in wild type embryos**. B, C|** The two sides of the RPE fail to come in contact in the yap^{nl13} mutant. **D|** Example of yap^{nl13} mutant embryos in which the two sides of the choroid fissure come in contact while the RPE loses continuity (Credit: Gaia Gestri).

It has to be noted that previous time-lapse experiments performed in the lab (Fig 4.6) showed the occurrence of two separate mechanisms for coloboma formation in the *yap^{nl13}* zebrafish mutant. In the majority of observed cases, the two margins of the choroid fissure do not come in contact and the expansion of the neuroretina generates a ventral protrusion (Fig.4.6 B, C). More rarely it has been observed that the two margins of the choroid fissure do come in contact, followed by a rupture of the RPE adjacent to the point of fusion which leaves the underlying neuroretina exposed (Fig 4.6 D). The two observed dynamics for coloboma formation in the *yap^{nl13}* zebrafish mutant might be representative of two consequences of a lack of regulation in cell tension across the RPE On the one hand reduction of stiffness in the RPE could result in disruption in the overall eye invagination process, impairing the capability of the two sides of the choroid fissure to come in contact. On the other hand, the observed rupture of the RPE

might represent an impairment of this tissue to actively accommodate to the tension generated by the invagination of the NR.

We thus investigated how the *yap*^{nl13} mutation affects the mechanical properties in the developing zebrafish eye, and we asked whether such alterations could be causative for the coloboma phenotype of the *yap*^{nl13} zebrafish. To assess the tensile state of the RPE we used phospho-myosin as a direct readout for cell contractility. Non-Muscle Myosin (NMM) is one of the main cytoskeletal motor proteins: it binds actin and it generates mechanical force upon phosphorylation (Houdusse and Sweeney, 2016). At a cellular level, myosin and actin form a network at the cell cortex: the cortical ring. In the cortical ring, myosin cross-links with antiparallel actin filaments and when phosphorylated generates a mechanical pull contracting the cortical actomyosin. The contractility of the cortical ring is responsible for the generation of the intracellular mechanical forces balancing the cell's hydrostatic pressure and mediating cell shape (Chugh and Paluch, 2018; Khalilgharibi et al., 2019). Myosin is also responsible for changes in shape and tensions at a tissue scale. As previously mentioned in the case of the RPE, increase of myosin phosphorylation at a cellular level can result in increased stiffness at a tissue level consequently driving the optic cup invagination. However, many of the morphogenetic events occurring in development are driven by myosin contractility as most of the tissue folding events in development are driven by actomyosin-mediated changes in cell shape (Heer and Martin, 2017).

Cell shape can be used as a different proxy to infer the tensile integrity of a tissue as it is directly dependent on actomyosin contractility and its interaction with external forces. In an epithelium cell shape is the result of the equilibrium of both intracellular (i.e. actomyosin contractility) and extracellular forces, generated and transmitted at tissue level. Overall, in a tissue, intracellular forces generated by the actomyosin ring balance at the cell-cell interface with the forces generated by adhesion molecules and mechanical stresses affecting the whole tissue (Heisenberg and Bellaïche, 2013). External stresses can elastically deform an epithelium: to accommodate changes in the tension distributed across the tissue while preserving its integrity, the cellular cortical actomyosin can change its

contractile state. Changes in cell shape are thus representative of the balance between cortical contractility and tissue mechanical force (Guillot and Lecuit, 2013).

In a healthy epithelium, the correct balance of intra and extracellular forces generally results in the generation of regular cell pattern**.** Cells distribute in fact across the epithelium subdividing its surface in order to optimize the balance between the internal cell osmotic pressure, cell crowding, and the tension generated at the membrane level by the cortical actomyosin. The achievement of such balance results in an epithelium in which each individual cell is predominantly polygonal. Conversely, imbalances in cell tension across an epithelium can result in altered cell packing pattern and in the generation of irregular cell shapes (Sánchez-Gutiérrez et al., 2016).

The mature RPE is indeed a cell monolayer composed by tightly packed, highly regular polygonal cells (Georgiadis *et al.*, 2010; Graw, 2010; Díaz-Coránguez, Ramos and Antonetti, 2017). It is located between the retina and the choroid and composes the outer blood-retina barrier (BRB). The integrity of RPE is critical for its function: the RPE maintains the immune privilege of the eye, supports the stability of the underlying photoreceptors and regulates the solutes diffusion between the subretinal space and the choroid blood supply (Georgiadis *et al.*, 2010; Graw, 2010; Díaz-Coránguez, Ramos and Antonetti, 2017). The strong cell-cell adhesion required by the RPE is reliant on three main junction types: tight, gap and adherens junctions. These three junctions serve the different roles in the RPE: adherens junctions are critical in maintaining the mechanical adhesion of the epithelium, tight junctions regulate the paracellular diffusion across the RPE and gap junctions allow cell-cell communication across the tissue. Zonula occludens-1 (ZO1-) is a scaffolding protein common between all of the three cellular junctions present in the RPE. It has been identified as a main determinant for of the RPE as it is critical in the determination of RPE cell morphology and differentiation *in vivo* (Georgiadis *et al.*, 2010).

4.2 Results

4.2.1 Actomyosin contractility is reduced in *yap*^{nl13} mutants' RPE cells.

To assess the effects of *yap*^{nl13} mutation on RPE tensile integrity, we firstly performed immunostaining experiments to check for changes in RPE cell shape and in the levels of myosin phosphorylation, which reflects tissue tension, in *yap*^{nl13} mutant. To visualize the RPE cell shape we furthermore used antibodies against zonula occludens-1 (ZO-1) that stain the apical pole of RPE cells allowing us to identify individual RPE cells. The immunostaining was performed on eyes dissected from embryos at 48hpf raised at 32°C.

From our immunohistochemistry (IHC) experiments we could observe that RPE cells in *yap*^{nl13} mutants appear more irregular compared with the wild types. Furthermore, in the eye regions where this difference is more accentuated, a reduction in the abundance of cortical phosphorylated myosin is visible in mutants **(Fig 4.1 A)**. To obtain a quantitative evaluation for the cell irregularity observed in *yap*^{nl13} mutant RPE, we analysed cell membrane tortuosity and compared it between wild-types and *yap*^{nl13} mutants. Cells were manually segmented using the ZO-1 staining. The level of tortuosity was calculated using the tortuosity index as P/Ptr. P is defined as the sum of the perimeters of each cell obtained by manual segmentation. Ptr is defined as the sum the perimeter of the polygon having its vertices at the tricellular junction of each individual cell **(Fig 4.1 B, C)**. The measured tortuosity index was significantly reduced in wild types when compared with *yap*^{nl13} mutants (n=6, n=7; Tortuosity Index Wt: 1.035 ± 0.002975 SEM; Tortuosity Index Mut: 1.094 ± 0.009459 SEM; P value = 0.0004 Unpaired t- test). These results suggest a reduction in the regulation of RPE cell tension in *yap*^{n113} mutants.

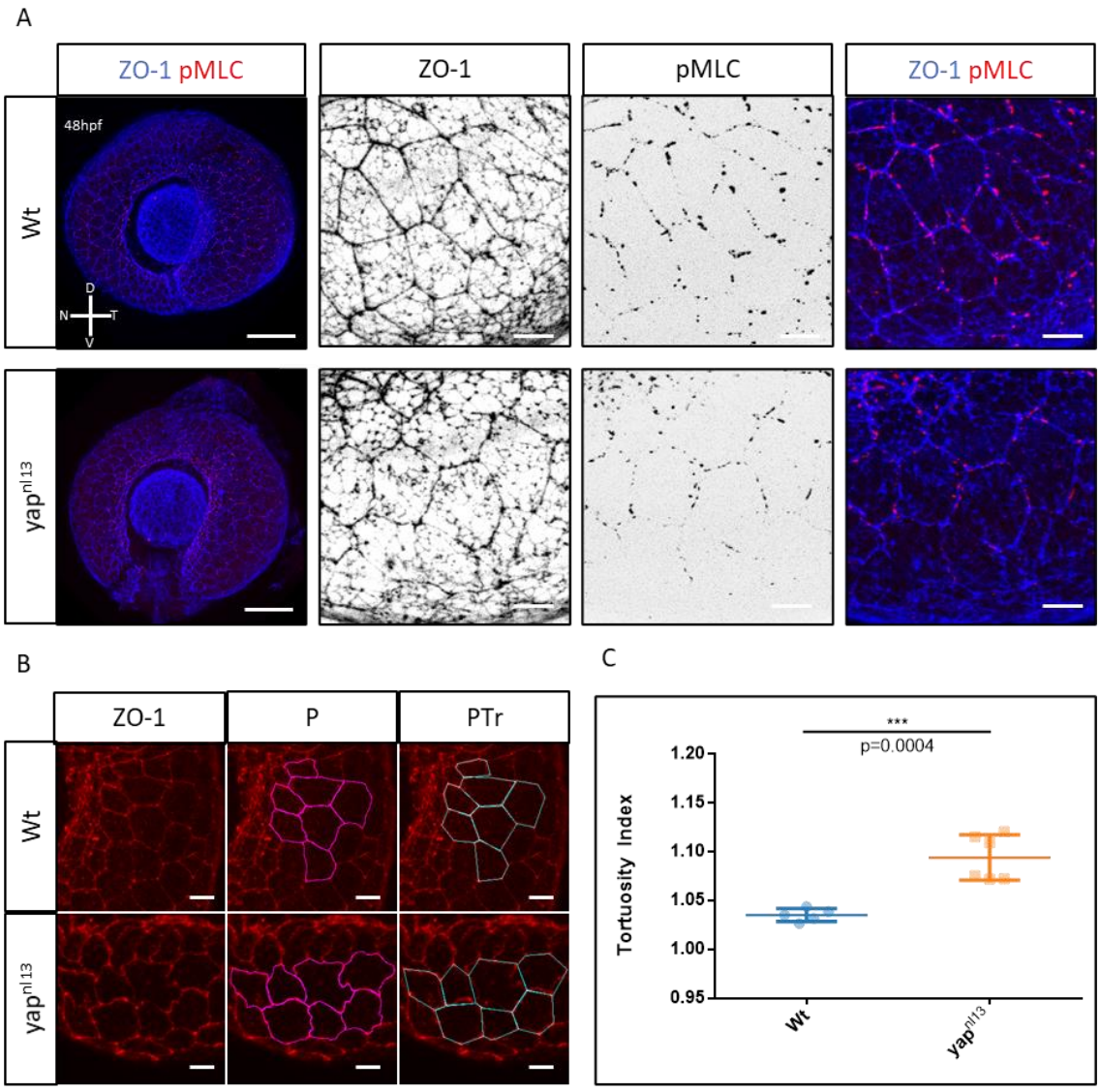

Figure 4.1| Reduction in myosin phosphorylation and irregular cell shape in *yap^{nl13}* mutants RPE cells.
A| Immunostaining on dissected eyes against Zonula Occludens 1 (ZO1) and phosphorylated myosin (pMLC) (scale bar = 50µm and 10 µm; N= nasal, T=temporal, D=dorsal, V=ventral). **B|** Example of the measures taken for the calculation of the tortuosity index (P: manually segmented perimeter; PTr: perimeter of the polygon having as vertices the tricellular junctions of each cell; scale bar = 10µm) **C|** Quantification of tortuosity index (P/PTr) for wild-type and *yap^{nl13}* mutants.

To assess whether the mutation in *yap* gene leads to an impairment of the RPE at a tissue level, the cellular organization of the retinal pigment epithelium was analysed. To do so we performed immunohistochemistry (IHC) experiments on dissected eyes expressing a Yap reporter in *yap*^{nl13} background (Tg(4xGTIIC:d2GFP)^{nl13}). We used myosin phosphorylation antibodies (pMLC) to visualize the levels of RPE actomyosin contractility, anti-GFP to visualise the transcriptional activity of Yap and ZO1 antibodies to label and manually segment RPE cells. We then quantified the intensity of pMLC and Yap signal by directly measuring the gray value after the imaging and obtained the values of individual cells surface areas by manual segmentation using ZO1 staining to identify individual RPE cells. To visualize the spatial distribution of the measured Yap activity, myosin phosphorylation and RPE cell surface, polar heatmaps have been used. To build the polar heatmap, each measured value has been mapped on the plot using the angular distance from the choroid fissure and the radial distance from the centre of the eye as coordinates **(Fig. 4.2 A)**.

In the wild-types, the analysis on the distribution of cell surface area (CSA) shows that CSA is increased in the temporal and nasal region of the RPE whilst is reduced in the ventral region, in proximity of the choroid fissure, and in the RPE region directly surrounding the lens **(Fig. 4.2 A3)**. The distribution of myosin phosphorylation levels across the RPE **(Fig. 4.2 A2)** appears to be spatially inversely correlated with the distribution of CSA. Furthermore, strong signal from myosin phosphorylation appears in the central zone of the eye, corresponding to the hinge region of the optic cup. Conversely, Yap transcriptional activity is very low in the central region of the RPE **(Fig. 4.2 A1)**. Even if Yap transcriptional activity in the central region of the RPE is low, its pattern does not fully complement the distribution of pMLC: Yap transcriptional activity is higher in the peripheral region of the RPE where myosin phosphorylation is not strongly reduced.

To assess whether the reduction of Yap activity correlates with an impaired cell contractility across the RPE and an abnormal distribution of CSA, Yap activity, myosin phosphorylation and CSA were analysed in *yap*^{nl13} embryos. Consistent with our previous observations, the levels of GFP reporting Yap activity are

strongly reduced in *yap*^{nl13} mutants **(Fig. 4.2 A1')**. In the eyes of *yap*^{nl13} mutant embryos pMLC staining is also strongly reduced **(Fig. 4.2 A2')**. This reduction is more obvious in the peripheral regions of the RPE, in areas where Yap transcriptional activity is strong in the wild type embryos. Similar to what is observed in wild-type, *yap*^{nl13} mutant RPE cells in the nasal and temporal region of the eye have a larger CSA than the region in the choroid fissure and in the dorsal region of the eye **(Fig. 3.2 A3')**. In *yap*^{nl13} mutant embryos however the distribution of the CSA appears to be less uniform compared to what observed in the wild type. In the eye of *yap*^{nl13} mutant embryos, there is an accumulation of cells with a higher CSA in the nasal and temporal region of the RPE.

We proceeded comparing the CSA of RPE cells between *yap*^{nl13} mutants and wild types. We observed that in *yap*^{nl13} mutant, the cells with a larger CSA seem to distribute more specifically in the nasal and temporal regions of the RPE while in the wild type the distribution across the RPE is more uniform. We thus extracted the CSA relative to the cell in the temporal and nasal region of the RPE and we compared them between wild type and *yap*^{nl13} mutants. To do so, we selected cells that were comprised between 45° and 135°, and between 225° and 315°C being these the nasal and temporal region of the RPE respectively. While the mean CSA value of RPE cells in wild-type is not significantly different from the *yap*^{nl13} mutants, the statistical distributions of CSA in wild-types and *yap*^{nl13} mutants are significantly different, as revealed by comparison of the cumulative distribution (Kolmogorov-Smirnov D = 0.168;) **(Fig 4.2 B,C)**. The CSA probability distribution confirms the qualitative observations on the CSA heatmaps **(Fig 4.2 D, E,F)**: the CSA distribution in temporal and nasal RPE cells in *yap*^{nl13} appears much broader, extending over the distribution of the CSA measured in the wild type.

These results suggest that loss of Yap activity results in downregulation of cell contractility across the RPE: at a tissue level, *yap*^{nl13} results in an overall relaxation of the RPE which is more passive to the tissue stretching that occurs during optic cup invagination. This results in misregulation of cell shape across the RPE that lead to an increase of the maximum CSA size, in the region of the RPE subject to high tensile strain. As RPE stiffness is a critical factor leading

optic cup invagination, loss of myosin-mediated contractility could be the cause underlying the coloboma phenotype of *yap*^{nl13} zebrafish mutant.

A

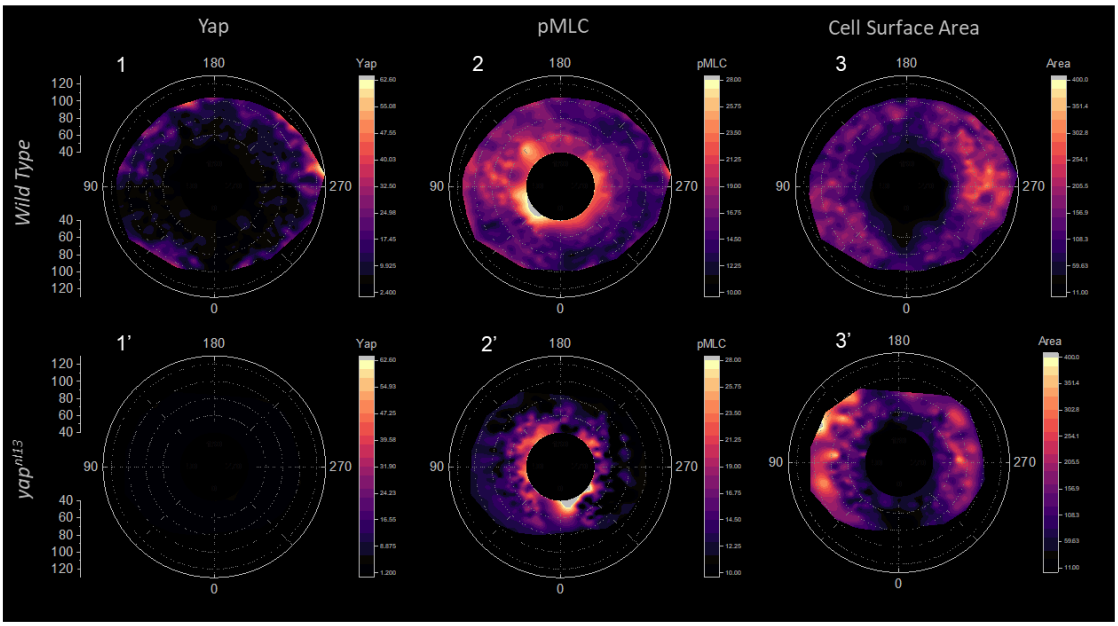
Yap
pMLC
Cell Surface Area
Wild Type
yap^nl13
1
2
3
1'
2'
3'
180
90
270
0
Yap
pMLC
Area

B

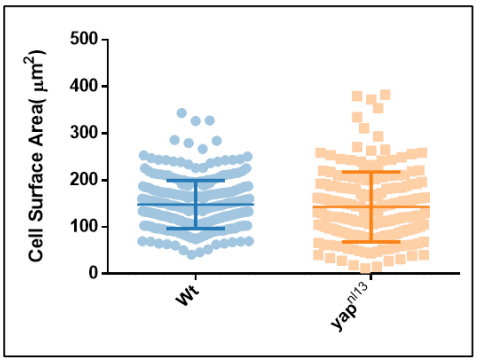
Cell Surface Area(μm²)
500
400
300
200
100
0
Wt
yap^nl13

C

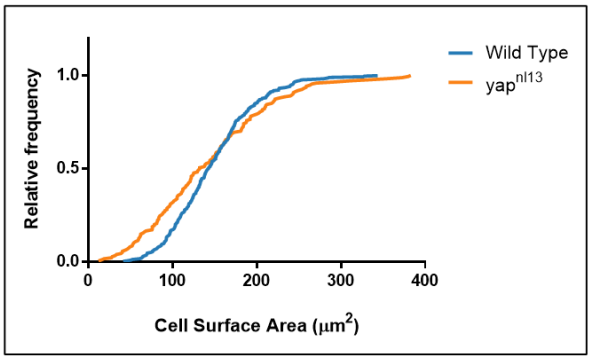
Relative frequency
1.0
0.5
0.0
0
100
200
300
400
Cell Surface Area (μm²)
Wild Type
yap^nl13

D

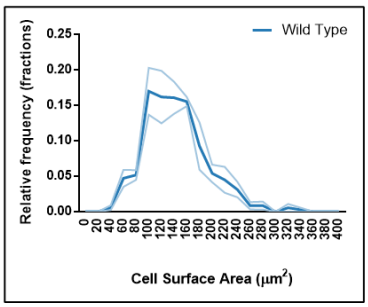
Relative frequency (fractions)
Wild Type
Cell Surface Area (μm²)

E

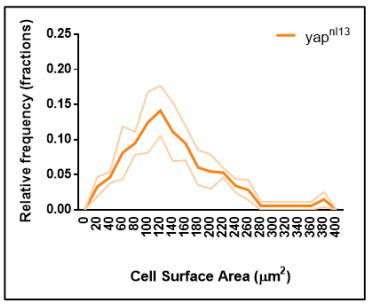
Relative frequency (fractions)
yap^nl13
Cell Surface Area (μm²)

F

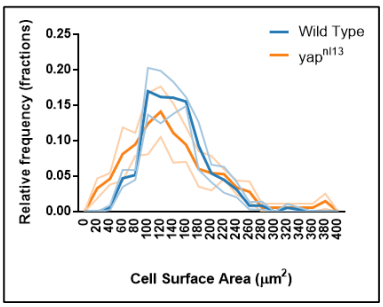
Relative frequency (fractions)
Wild Type
yap^nl13
Cell Surface Area (μm²)

Figure 4.2| Cell Surface Area (CSA) and myosin phosphorylation are differently distributed across the RPE in wild-type and *yap*^{nl13} mutant.
A| Polar-heatmaps showing the gray values obtained from immunohistochemistry of GFP; pMLC and ZO1 in Tg(4xGTIIC:d2GFP)^{nl13} embryos. The data plotted represent the intensity of GFP in both wild-types and *yap*^{nl13} mutants (A1, A1'), the intensity of pMLC in both wild-types and *yap*^{nl13} (A2, A2' *yap*^{nl13}) and CSA in both wild-types and *yap*^{nl13} (A3, A3'). 0° represents the choroid fissure position (ventral region of the eye), 180° represents the dorsal region of the eye and 90° and 270° represent the nasal and temporal regions respectively. **B|** CSA values measured in wild-type embryos and *yap*^{nl13} mutants RPE in the nasal and temporal region of the RPE. **C|** Cumulative probability distribution of CSA of wild-type and *yap*^{nl13} mutants in the nasal and temporal region of the RPE. **D,E|** Probability distribution of CSA in wild-type (D) and *yap*^{nl13} mutants (D) in the nasal and temporal region of the RPE. **F|** Comparison of the probability distribution of CSA measured in wild-types and *yap*^{nl13} mutants RPE.

4.2.2 Chemical inhibition of actomyosin contractility leads to full penetrance of coloboma in *yap*^{nl13} mutants

The reduction of pMLC indicates a decrease in tensile properties of the RPE in *yap*^{nl13} mutants at 2/3 dpf. We thus wanted to test whether the reduction in actomyosin contractility is the cause or the consequence of the coloboma phenotype in *yap*^{nl13} mutant. Since *yap*^{nl13} mutants shows incomplete penetrance in embryos raised at 28°C, we argued that in this condition the reduction in actomyosin contractility is not sufficient to cause consistent failure in choroid fissure closure. However, we hypothesised that, if a misregulation of cell contractility in the RPE of *yap*^{nl13} mutants is the cause of the coloboma phenotype, *yap*^{nl13} embryos raised at 28°C would be more sensitive to an additional reduction of myosin phosphorylation than wild-type embryos. We thus tested this hypothesis by chemically reducing myosin phosphorylation both in wild-types and in *yap*^{nl13} embryos. To do so, we exposed developing embryos to Para-Nitro-Blebbistatin. Blebbistatin is a well characterised specific inhibitor of myosin phosphorylation which has been successfully used *in vivo* in the zebrafish model system (Képiró et al., 2014; Voltes et al., 2018).

We performed titration experiments to identify the highest subcritical concentration of Blebbistatin which led to lack of developmental defects in wild-

type embryos. Wild-type embryos raised from 5hpf to 48hpf in continuous exposure to 2µM Para-Nitro-Blebbistatin show no overt developmental defects **(Fig 4.3 D, D')**. To assess the cellular effect of Blebbistatin in absence of overt defect, we observed whether Yap activity was altered in wild-type treated embryos. As changes in actomyosin contractility regulate Yap nuclearization and activity, we considered that a decrease of Yap activity would be indicative of the inhibitory activity of Blebbistatin (Halder et al., 2012; Panciera et al., 2017; Voltes et al., 2018) .We thus performed immunostaining experiments on Yap reporter line embryos (Tg(4xGTIIC:d2GFP)) after Blebbistatin treatment to assess for a decrease in Yap transcriptional activity **(Fig 4.3 A)**. Our results showed that incubation of Para-Nitro-Blebbistatin 2µM, although not inducing any obvious phenotype, induces a significant reduction in Yap transcriptional activity in wild-type embryos. Conversely, the same experiment performed on (Tg(4xGTIIC:d2GFP)^{nl13} embryos revealed that 2µM Blebbistatin treatments has no effects on Yap activity in *yap*$^{nl13.}$ mutants (**Fig 4.3 B**; One-way ANOVA(95% CI of dif) test N=6; Wild Type DMSO vs Wild Type Blebbistatin: Mean diff: 12.88; significant(*); *yap*^{nl13} DMSO vs *yap*^{nl13} Blebbistatin: Mean diff: -1.736 (n.s.)).

While 2µM Blebbistatin treatments have no effect on eye development in wild-type embryos, exposure of *yap*^{nl13} mutant embryos from 5hpf until 24hpf to Blebbistatin leads to full penetrance of a coloboma phenotype in embryos raised at 28°C (Phenotype occurrence in control(%)= 5.000±1.340; Treated(%): 20.71±1.679 Mean±SEM; Mann-Whitney test p-value = 0.0002; not shown) and exacerbates the severity of coloboma phenotype **(Fig 4.3 D)**.

Myosin contractility is critical for optic cup development during optic vesicle evagination. However, once the optic cup starts to invaginate it becames insensitive to myosin phosphorylation inhibition (Eiraku et al., 2012, 2011). We thus hypothesised that the reduction in actomyosin contractility in *yap*^{nl13} mutant would result in a sensitivity to Blebbistatin specifically during optic vesicle evagination whilst the following phases of eye morphogenesis would be more resilient to Blebbistatin exposure. To test this hypothesis, we exposed *yap*^{nl13} mutant embryos to Para-Nitro-Blebbistatin 2µM to cover the whole period of optic vesicle evagination (5hpf-19hpf) and from optic vesicle invagination onward

(19hpf-24hpf). While *yap*^{nl13} embryos treated from 5hpf to 19hpf led to full penetrance of *yap*^{nl13} coloboma phenotype, the penetrance in mutant embryos treated from 19hpf showed no significant increase when compared to control embryos (**Fig 4.3 E**; One-way ANOVA Turkey's multiple comparisons test N=4 n=40 to 80; Ctr vs 5hpf-19hpf: Mean Diff. = -0.5918; 95% CI: -0.8833 to -0.3003; significant (**); Ctr vs 19hpf-24hpf: Mean Diff. = -0.1959; 95% CI: -0.5107 to -0.1190; Not Significant; 5hpf-24hpf vs 19-24hpf; Mean Diff.=0.3959; 95% CI: 0.08106 to 0.7108; significant (*)).

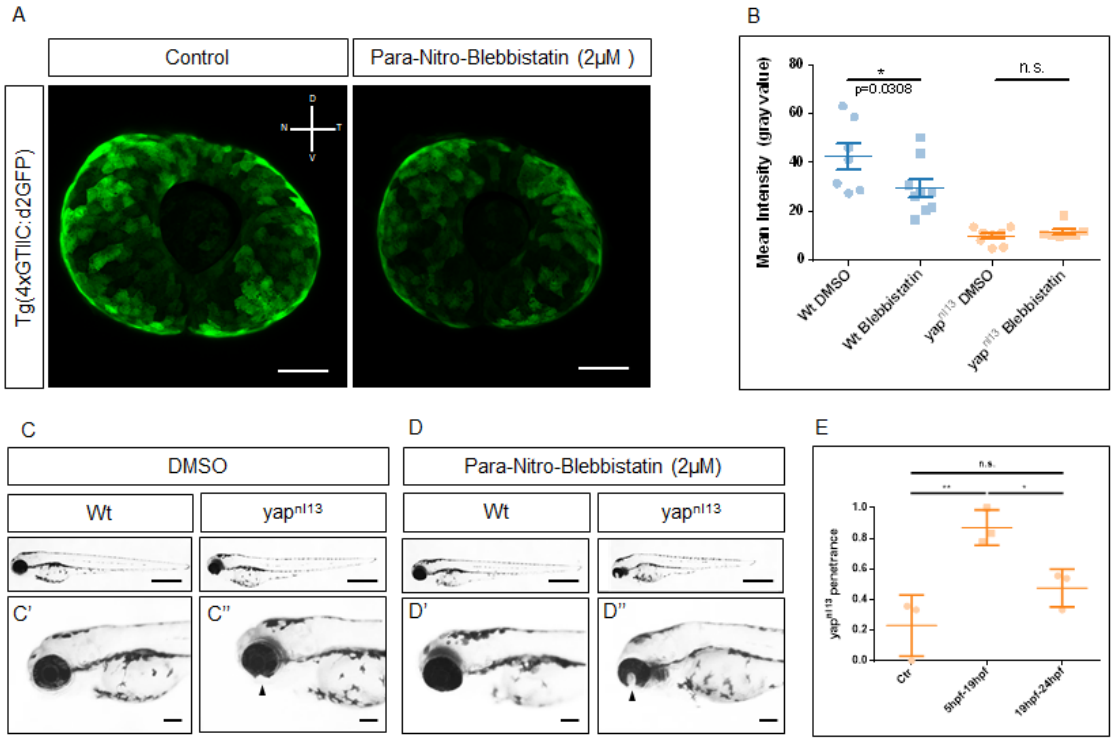

Figure 4.3| Actomyosin contractility inhibition through para-nitro-blebbistatin exacerbates *yap*^{nl13} mutant coloboma phenotype.
A| Immunostaining against GFP in Tg(4xGTIIC:d2GFP) Yap reporter line. **B|** Intensity of Yap transcriptional activity reported by GFP staining (scale bar = 50µm) **C|** Lateral view of wild-type embryos untreated (C') and exposed to 2µM Para-Nitro-Blebbistatin (C'') The arrowhead is pointing at the unclosed choroid fissure. **D|** Lateral view of *yap*^{nl13} mutant embryos untreated(D') and exposed to 2µM Para-Nitro-Blebbistatin (D''). The arrowhead is pointing at the unclosed choroid fissure. **E|** Percentage of *yap*^{nl13} mutant embryos showing coloboma phenotype in untreated conditions and when exposed to Blebbistatin between 5hpf and 19hpf (5hpf-19hpf) and between 19hpf and 24hpf (19hpf-14hpf).

4.2.3 Inhibition of endogenous myosin phosphorylation in the eye leads to coloboma in *yap*^{nl13} mutants.

The results from the Blebbistatin treatment showed that downregulation of myosin phosphorylation restores full phenotypic penetrance in *yap*^{nl13} mutants raised at 28°C. The fact that Blebbistatin-mediated inhibition of myosin phosphorylation has effect only during the optic vesicle evagination, which is strongly myosin dependent, highlighted the specificity of this effect. However, the manipulation of myosin phosphorylation through chemical inhibition, although molecularly specific, is not tissue specific. To explore whether inhibition of actomyosin contractility specifically in the eye is sufficient to aggravate the frequency and/or the penetrance of the coloboma phenotype in *yap*^{nl13} mutant, we induced overexpression of myosin phosphatase under an eye specific promoter (*rx3*) through injection of UAS:mypt-mCherry plasmid in *tg(rx3:Gal4-VP16)*^{vu271}; *yap*^{nl13} embryos (Weiss et al., 2012).

Embryos raised at 28°C were screened for mCherry positive cells at 24hpf **(Fig 3.4 A)**, and assessed for coloboma phenotype at 3dpf. Our results showed that eye-specific overexpression of myosin phosphatase has no effect on wild-type embryos **(Fig 3.4 B,B')** while it leads to full penetrance of the coloboma phenotype in *yap*^{nl13} embryos raised at 28°C (Fig 3.4 C; N=4; n= 100 to 200; Ctr: mean=14.25; SEM 2.955; UAS:*mypt:* mean = 25.00 SEM = 4.062; Paired t-test: p-value = 0.033). Together with an increase in penetrance of the phenotype, *yap*^{nl13} mutant embryos overexpressing *mypt* showed an increase in the severity of the coloboma phenotype **(Fig 3.4 D, D')**. These results confirmed an increased sensitivity to myosin phosphorylation reduction in the eye of *yap*^{nl13} mutants.

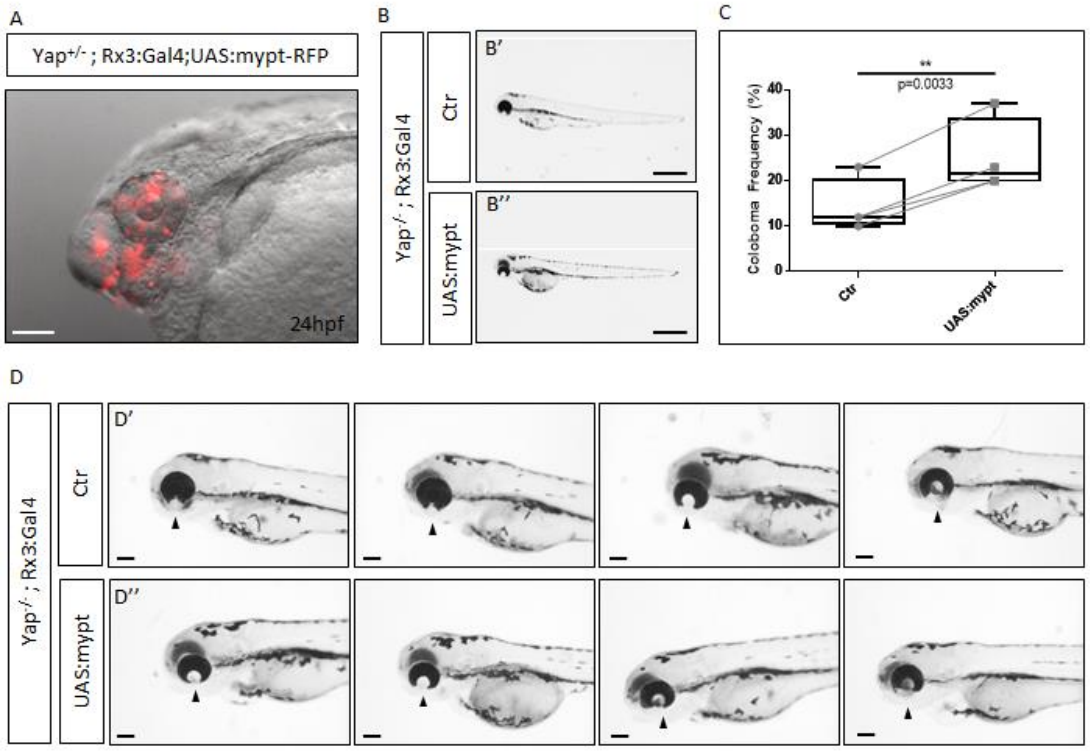

Figure 4.4| Overexpression of *mypt* exacerbates *yap*^{nl13} mutant coloboma phenotype.
A| Representative embryo positive for expression of UAS:mypt-RPF construct. (scale bar = 100µm) **B|** Lateral view of uninjected (B') and UAS:mypt-RPF positive (B'') *yap*^{nl13} mutant embryos (scale bar = 500µm). **C|** Frequency of embryos showing coloboma in the progeny of a *yap*$^{nl13/+}$ incross, positive for UAS:mypt-RPF and uninjected. **D|** Lateral view of *yap*^{nl13} mutants uninjected (D') and positive for UAS:mypt-RPF (D''). The arrowheads are pointing at the opened choroid fissure (scale bar = 100µm). The embryos have been screen for phenotype at 4dpf.

4.2.4 Downregulation of myosin phosphatase rescues coloboma in the yap nl13 mutant.

We hypothesised that, if indeed a reduction in myosin phosphorylation is responsible for the coloboma in the *yap*^{nl13} zebrafish mutant, an increase of the levels of cellular phosphorylated myosin would conversely rescue the coloboma phenotype. To test this hypothesis, we used morpholino injection to downregulate myosin phosphatase (*mypt1*). Downregulation of *mypt1* reduces the turnover of myosin dephosphorylation leading to an accumulation of the active form of myosin and a consequent increase in cell contractility (Ito *et al.*, 2004). Injection of MOmypt1 leads to a statistical significant decrease in the occurrence of coloboma in the progeny of a *yap*$^{+/nl13}$ heterozygous incross (Frequency of Coloboma(%): Control = 17.00±3.764; mypt1 MO = 2.875±1.125; Mean±SEM; Mann Whitney test: p=0.0286). Together with a decreased occurrence in the phenotype, downregulation of *mypt1* also shows amelioration of the coloboma: in the injected group, the coloboma appears to be less severe than the control group. Even if in MOmypt1 injected embryos we observed a rescue of the coloboma phenotype in *yap*^{nl13} mutants, the MOmypt1 injected embryos have smaller eyes when compared with uninjected embryos (Frequency of small eye(%): Control = 0; mypt1 MO = 14.250±7.284; Mean±SEM). These results support the hypothesis that the *yap*^{nl13} mutation is responsible for a decrease in cell stiffness which leads to the coloboma phenotype in *yap*^{nl13} mutant embryos.

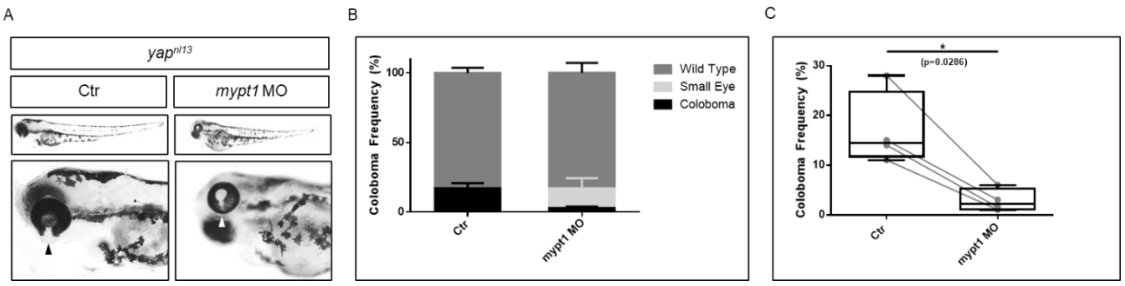

Figure 4.5| Knock-down of *mypt* rescues *yap*^{nl13} mutant coloboma phenotype.
A| Example of *yap*^{nl13} mutant embryos showing coloboma both in the morphants and in the control group. The coloboma phenotype in the morphant is ameliorated (Arrowheads pointing at the choroid fissure). **B|** Incidence of coloboma and small eye phenotype in the progeny of a *yap*$^{nl13/+}$ incross in the *mypt1* morphant and control groups. **C|** Incidence of coloboma phenotype in the progeny of a *yap*$^{nl13/+}$ incross in the *mypt1* morphant and control groups. The embryos have been screen for phenotype at 4dpf.

4.3 Discussion

Yap is one of the main effectors in cellular mechanotransduction. Our results showed that *yap*-mediated mechanotransduction is required in the development of the eye. We observed that in the *yap*^{nl13} zebrafish mutant, the generation of myosin mediated cell contractility is impaired and that loss of myosin contractility results in mechanically more passive behaviour of the RPE. While reduction of myosin phosphorylation increases the penetrance of the *yap*^{nl13} mutant, promoting the phosphorylation of myosin is sufficient to rescue the coloboma phenotype. These results indicate that, in the *yap*^{nl13} mutant, loss of myosin-mediated cell contractility in the RPE is causative for the coloboma phenotype.

4.3.1 Yap regulates RPE stiffness in zebrafish.

Our results indicate that the coloboma phenotype in *yap*^{nl13} zebrafish mutant is due to a reduction of tissue tension in the RPE. This result is consistent with previous results in the medaka *hirame* (*hir*) mutant (Porazinski et al., 2015). The *hirame* mutant phenotype is characterised by overall flattening of the body axis due to a lack of tissue tension generation. In this mutant the overall amount of phosphorylated myosin is significantly reduced and the tissues' capability to generate tension is disrupted. Direct assessment of tissue stiffness in *hir* confirmed that loss of phosphorylated myosin led to loss of tissue tension generation: both the recoil of tissues after laser micro-ablations and the degree of deformation of tissue under pipetting suction indicated a reduction of tissues' elasticity. While in the zebrafish *yap*^{nl13} mutant the reduction of tissue tension is restricted to the eye, possibly to the RPE, in the medaka *hir* mutant, phosphorylated myosin is reduced in several organs resulting in strong malformations of the heart, eye, brain and somites (Porazinski et al., 2015). Despite the phenotypic discrepancies observed, due probably to the presence of different paralogs between species (Javier Vázquez-Marín 2019), here we reported that the mechanism of action of Yap is conserved between medaka and zebrafish.

The *hirame* mutant also shows an eye phenotype: it exhibits protrusion of the lens and overall flattening of the eye. The lens protrusion phenotype of the *hirame* mutant has been attributed to disruption of the ECM: immunostaining against fibronectin (Fn) revealed that deposition of this protein is strongly altered. Blockage of Fn1 assembly in wild type embryos phenocopied the lens protrusion phenotype in the *hir* mutant. Conversely, disruption of fibronectin deposition did not induce flattening of the optic cup. This suggested that, while Fn is critical for Yap-mediated organ alignment, it is not required for the role of Yap in the overall regulation of organ shape which is mostly reliant on actomyosin contractility. Differently from the *hirame* mutant, the *yap*^{nl13} zebrafish mutant does not show lens protrusion nor flattening of the eye. This difference may be correlated to the fact that, in the *yap*^{nl13} mutant, the overall body axis is not disrupted, and the phenotype is restricted to the eye. Given that an interplay between Yap and the ECM has been found in different contexts (Calvo et al., 2013, 2013; Chaudhuri et al., 2014; Dupont, 2016; Dupont et al., 2011), it will be important to understand the effects of perturbing ECM deposition on the *yap*^{nl13} mutant. In particular, the *yap*^{nl13} mutant can be used as a sensitised background providing a tool to dissect the function of the specific ECM components during eye morphogenesis.

Our data indicate that the reduction in tissue tension that we observed in the RPE is the consequence of loss in actomyosin contractility. The requirement for high contractility in the RPE for the correct development of the eye is in agreement with the relaxation-expansion model for the self-driven optic cup invagination (Eiraku et al., 2012). In this model, the main factor driving the invagination of the optic cup is the higher stiffness of the RPE compared to the neuroretina. Atomic force microscopy confirmed that the accumulation of phosphorylated myosin in the RPE increases its stiffness, while the neuroretina remains softer (Eiraku et al., 2012, 2011). The role of myosin-mediated contractility in the RPE as a driving force in optic cup morphogenesis has been observed also in the mouse model (Carpenter *et al.*, 2015) .In mouse, disruption of Wnt signalling in the eye results in reduced myosin phosphorylation in the RPE which leads to the generation of a misfolded optic cup and coloboma.

Our results show that the RPE is composed by cells of different size. In particular, we observed that cells in the nasal and temporal retina are bigger than the cells in the rest of the eye**.** Epithelia have different strategies to adopt to their mechanical environment: tissues can change either their proliferation/cell death rate or they can change cell shape or cell position. We hypothesize that the enlargements of the RPE cells could depend on a compensatory cell relaxation to accommodate the involution movements while maintaining the RPE integrity. Indeed, we observed an inverse correlation between the distribution of phosphorylated myosin and of the distribution of cell surface area-CSA, indicating that larger cells are also the ones with decrease actomyosin contractility. Consistently, the increase in RPE CSA in the most nasal and temporal region of the eye corresponds to the regions of the eye undergoing to the more dramatic involution movements (Kwan et al., 2012).

The CSA distribution pattern across the RPE is also maintained in the *yap*^{nl13} mutant eye. The fact that this pattern arises also in the absence of functional Yap indicates that the RPE cells enlargement in the nasal and temporal region is a passive response to external mechanical cues. However, in the *yap*^{nl13} mutant RPE, the difference between CSA in the most nasal and temporal region and the rest of the eye appear magnified. This suggests that, in absence of functional Yap, cells in the nasal and temporal region of the RPE present less resistance to the stretching tissue. In the *yap*^{nl13} zebrafish mutant, where the integration of the tissue mechanical cues is impaired, cells behave completely passively to the strain which the RPE is subject to: not generating any resisting force, the RPE cells subject to higher strain, stretch to an higher extent to what observed in the wild-type counterpart. Loss of active response of the RPE to the mechanical strain across the tissue could also explain the incurrence of rupture of the RPE at the side of choroid fissure: it is possible that in some of the mutants, the tension in the RPE might be sufficient to allow the proper morphogenesis of the optic cup but not to maintain tissue integrity. It is possible that in the final stages of the eye morphogenesis, the lack in the RPE mechanical compensation for the generated tension results in disruption of the RPE continuity

The more passive cellular behaviour suggested by the CSA distribution in the *yap*^{nl13} mutant is strongly supported by the overall reduction in myosin phosphorylation in the RPE that we observed from our immunostaining experiments. Our experiments of inhibition of myosin-mediated contractility furthermore confirm that a loss of cell contractility is occurring in the eye of *yap*^{nl13} zebrafish mutant: the fact that inhibition of myosin phosphorylation leads to coloboma phenotype in the *yap*^{nl13} mutants and not in the wild types indicates deficiencies in the overall contractility caused by the mutation. While we hypothesize that reduction of contractility is occurring mainly in the RPE, our experiments of inhibition of myosin-mediated contractility have been performed on the whole eye: we thus cannot directly distinguish whether the increased penetrance of the *yap*^{nl13} mutation we observed is due to reduction of cell tension specifically in the RPE or in the whole optic structure. Nonetheless the coloboma phenotype as a consequence of myosin phosphorylation inhibition arises only in combination of the *yap*^{nl13} mutation. Since *yap* in the eye is mainly expressed in the RPE, we hypothesize that failure in choroid fissure closure depends by pre-existent loss of phosphorylated myosin in this tissue.

While our experiments suggest a reduction in the rigidity of the RPE, we do not have direct measurement of the stiffness of this tissue. A number of techniques have been developed to directly probe the mechanical properties of a tissue (Sugimura et al., 2016). A first approach to test the mechanical properties at a cellular level could rely on laser ablations. Multiphoton laser ablations have been previously used to assess the elastic properties of both tissues and cells (Liang et al., 2016). Similar to the experiments performed on the *hirame* medaka mutants, tissue-level information regarding the stiffness of the RPE can be obtaining by performing laser micro-incisions in the RPE and observing the following recoil of the tissue. These experiments would provide a direct measurement on the stiffness of the RPE in the *yap*^{nl13} zebrafish mutant allowing to confirm that loss of myosin phosphorylation correlates with loss of stiffness in the RPE.

Together with actomyosin contractility, the deposition of ECM is a critical factor in the regulation of the stiffness of a tissue. We do not have direct information

regarding disruption of the ECM in the *yap*^{nl13} zebrafish mutant. It is however possible that, similarly to what presented in the *hir* medaka mutant, deposition of the ECM is altered in *yap*^{nl13} fish. Altered properties of the ECM could explain the temperature sensitivity of the *yap*^{nl13} zebrafish mutant. Changes of the stiffness of ECM network depending on the incubation temperature are reported in vitro: the Matrigel network softens at temperatures above 37°C (Soofi et al., 2009). Similarly, collagen network changes its properties in a temperature-dependent manner (Jones et al., 2014; Licup et al., 2015). It is thus a possibility to be investigated whether, in the *yap*^{nl13}, alteration of ECM deposition makes its more susceptible to the temperature changes. If this was the case, it could be hypothesised that, at higher temperature, the ECM in the *yap*^{nl13} zebrafish mutant softens over a critical value leading to failure in optic cup closure.

4.3.2 Choroid fissure closure requires myosin-mediated contractility in zebrafish.

While the choroid fissure closure is impaired in the *yap*^{nl13} zebrafish mutant, the earlier phases of eye morphogenesis do not appear to be affected by this mutation. From time-lapse imaging (**Fig 4.6**) it is furthermore observable that in the majority of the cases, the two margins of the choroid fissure fail to come in contact as the neuroretina appears to drive them apart at the expected moment of choroid fissure closure. The fact that early invagination is not affected in the *yap*^{nl13} zebrafish mutant is open to two possible interpretations. On the one hand it is possible that, differently from what suggested by the *in vitro* “relaxation-expansion” model, *in vivo* the stiffness of the RPE is not the main factor driving optic cup invagination. Indeed *in vivo* there is a redundancy of mechanisms driving eye morphogenesis which can be in place to contribute to the robustness of the eye morphogenesis. This interpretation would restrict the role of RPE stiffness in driving eye morphogenesis to the final stages of optic cup invagination. It is possible that the stiffness of the RPE is critical to drive the inward movement of the neuroretina once the overall mechanical forces generated in the optic cup are above a certain threshold. The RPE would thus ensure that the folding of the neuroretina pushes the two margins of the choroid fissure in contact allowing its fusion.

On the other hand, it is possible that RPE stiffness is indeed required during the whole development of optic cup, but the role of *yap* is restricted in time. It is possible that *yap* regulates RPE stiffness only late in development while different signalling pathways are responsible for the regulation of actomyosin contractility earlier in development. We can hypothesize that during early optic cup morphogenesis the increase of RPE stiffness is due to some Yap-independent regulation of actomyosin contractility. Conversely, Yap transcriptional activity could be critical only in the later phases of optic cup invagination, when the RPE needs to integrate and balance two different mechanical properties: the maintenance of the intrinsic tension and stiffness of the RPE, and the strain and stretching derived from the final stages of the inward movements of the neuroretina which needs to be compensated for.

Our data furthermore reveal that the *yap*^{nl13} zebrafish mutant is sensitive to blebbistatin-mediated reduction in myosin contractility very early in development. Indeed, regulation of contractility in the presumptive RPE is critical for the proper folding of the optic cup during development. The early sensitivity of the embryos to blebbistatin could be explained by the fact that, early in development, *yap* is required for mechanisms other than the regulation of cell tension across the RPE. Inhibition of myosin phosphorylation would thus act cumulatively in earlier developmental stages: as mechanotransduction is already impaired at later stages in the *yap*^{nl13} zebrafish mutant, blebbistatin treatment would result only in marginal reduction of the inhibition of myosin phosphorylation. Conversely, early blebbistatin treatments would reduce the generation of cell tension in a developmental stage which is not affected by the *yap*^{nl13} mutation, thus having an effect additive to the one of the mutations.

To understand whether *yap* regulates cell contractility only in later stages of development, it is key to obtain data on the levels of phosphorylation of the RPE at earlier stages. Immunostaining against pMLC performed at earlier stages of optic cup invagination will elucidate when actomyosin contractility is reduced in the RPE of *yap*^{nl13} zebrafish mutant. Reduction of myosin phosphorylation in the *yap*^{nl13} mutant from the beginning of optic cup invagination would suggest that RPE stiffness is less critical for the earliest phases of eye invagination.

Conversely, reduction in actomyosin contractility in the later phases would indicate that *yap*-mediated contractility is mostly crucial for the final stages of optic cup invagination and choroid fissure closure.

The possibility that the contractility of the RPE is regulated by multiple pathways is furthermore suggested by the fact that in the *yap*^{nl13} zebrafish mutant, myosin phosphorylation in the hinge region of the RPE is not reduced. It is possible that the control of myosin phosphorylation in hinge cells does not relies on yap signalling and is thus not affected by *yap*^{nl13} mutation. Wnt pathway is an interesting candidate as an alternative pathway collaborating with Yap in the regulation of the RPE mechanical properties. Indeed, Wnt is involved in eye development from early patterning to morphogenesis (Cavodeassi *et al.*, 2005; Fuhrmann, 2008; Fujimura, 2016). Wnt signalling is furthermore involved in mechanotransduction both integrating mechanical information and regulating the cytoskeleton (Lai, Chien and Moon, 2009; Morgan, Murphy and Russell, 2013; Cha *et al.*, 2016). A role of Wnt-mediated mechanotransduction in optic cup morphogenesis is provided by a study in the mouse model. It has been shown that Wnt can regulate actomyosin contractility within the RPE (Carpenter et al., 2015): the Wnt ligand mutant *wntless* (*Wls*) shows a decrease of myosin phosphorylation in the whole RPE and failure of choroid fissure fusion. Furthermore, the crosstalk between Wnt and Yap has been reported in different contexts (Imajo *et al.*, 2012; Morgan, Murphy and Russell, 2013; Azzolin *et al.*, 2014; Piccolo, Dupont and Cordenonsi, 2014; Agarwala *et al.*, 2019): it is an intriguing possibility that regulation of the RPE stiffness is mediated by the interplay of these two pathways in different moments of development.

The increase both in the penetrance and expressivity of the coloboma phenotype upon inhibition of actomyosin contractility indicates that in the RPE, Yap transcriptional activity is dependent on myosin contractility: *yap* works in a regulatory feedback loop in which the mechanical cues from the environment are integrated and this integration acts on cell tension leading, in turn, to changes in the tissues' mechanical properties (Asaoka and Furutani-Seiki, 2017; Porazinski et al., 2015). Consistently, we observed that, in wild type Yap reporter line embryos (Tg(4xGTIIC:d2GFP)), inhibition of myosin contractility through

Blebbistatin resulted in downregulation of Yap transcriptional activity. This suggests that, while mutation on the *yap* gene downregulates myosin-mediated contractility, in turn, downregulation of cell contractility results in a decrease of Yap transcriptional activity. The existence of such feedback loop provides a possible trigger initiating the Yap-mediated regulation of transcriptional activity.

Chapter 5.

General Discussion

Coloboma, a condition derived from failure of choroid fissure closure during eye development, is one of the main causes of visual impairments in humans (Gregory-Evans *et al.*, 2004; Williamson *et al.*, 2014; Reis and Semina, 2015). While many of the processes of eye development have been investigated in depth, the mechanisms underlying choroid fissure closure remain poorly understood. In particular, little is known about the role of the RPE in choroid fissure fusion.

Yap is one of the genes required for choroid fissure fusion, both in humans and in zebrafish (Williamson *et al.*, 2014; Miesfeld *et al.*, 2015; Holt *et al.*, 2017). Studies on the zebrafish model system have identified two *yap* mutant alleles showing eye development defects: the *yap*^{mw48} shows loss in RPE specification and *yap*^{nl13} shows a coloboma phenotype, with temperature dependent penetrance, without any obvious RPE phenotype. Transgenic approaches to restore normal Yap function in discrete domains in which *yap* is normally expressed, such as neural retina, RPE or periocular mesenchyme (POM) show that providing wild-type Yap within the RPE is sufficient to rescue optic fissure closure in *yap*^{nl13} mutant embryos (Gestri G, unpublished results).

We show that, differently from the *yap*^{mw48} null allele, in *yap*^{nl13}, RPE specification occurs normally but RPE rigidity is compromised. The loss of RPE stiffness likely causes eye morphogenetic defects, revealing a fundamental role for the RPE in eye morphogenesis and optic fissure closure. Our results are consistent with a hypothesised role for RPE in forming a rigid shell around a softer neural retina thereby promoting shaping of the eye cup (Carpenter et al., 2015; Eiraku et al., 2012, 2011).

5.1 Myosin-mediated cell contractility is critical for eye morphogenesis and is impaired in yap^{nl13} mutant.

Our experiments reveal that Yap transcriptional activity is required for the maintenance of actomyosin contractility in the RPE and that loss of myosin contractility likely contributes to failure in choroid fissure closure in the *yap^{nl13}*. In particular, our results suggest that Yap is critical in detecting the strain exerted by the involution of the neuroretina upon the RPE and in regulating the contractile response of the cells subjected to such tensile stress. It thus appears that the involution of the neuroretina triggers Yap-mediated change of cell shape which is controlled through actomyosin contractility (See chapter 4). Our evidences are in line with the biomechanical models proposed for eye morphogenesis indicating that the stretching of the RPE is an active process which is required for the accurate morphogenesis of the eye (Eiraku, Adachi and Sasai, 2012; Carpenter *et al.*, 2015). The morphogenesis of the eye strongly relies on the mechanical properties of its constituent tissues (Carpenter et al., 2015; Eiraku et al., 2012; Sidhaye and Norden, 2017). In particular, the tensile properties of the RPE need to be finely tuned to accommodate the growth of the whole optic cup and to allow its invagination. In vertebrates, the RPE undergoes morphological changes, shifting from a pseudostratified to a cubical epithelium. In teleosts, these changes are even more dramatic as the mature RPE is composed by squamous cells. It is still debated whether such morphological changes are a passive behaviour, in which the neuroretina “stretches” the RPE, or an active behaviour, in which the RPE cells actively control and changes their morphology (Moreno-Marmol, Cavodeassi and Bovolenta, 2018). Yap has been identified as one of the critical proteins required for the regulation of mechanotransduction during development and was proposed as a potential candidate for the regulation of the RPE cell shape changes (Asaoka and Furutani-Seiki, 2017; Dupont et al., 2011; Moreno-Marmol et al., 2018). Our results are in line with this line of evidence and provide a possible mechanism by which *yap* can exert its role in the regulation of mechanotransduction in the development of the eye.

5.2 Cell differentiation and expansion are not affected in the RPE of the yap^{nl13} mutant.

Our analyses indicate that both the early specification of the RPE and its expansion are not affected by the loss of Yap transcriptional activity in the *yap^{nl13}* zebrafish mutant (See chapter 3). Previous studies identified the role of Yap in eye development and highlighted its role in both the maturation of the neuroretina and in the specification of the RPE (Jiang et al., 2009; Kim et al., 2016; Miesfeld et al., 2015). The study previously performed on the *yap^{mw48}* zebrafish mutant revealed that *yap* is required for the specification of the RPE, and loss of its transcriptional activity results in loss of RPE specification. This is an important difference with what we observe in the *yap^{nl13}* mutant, supporting the hypothesis that Yap has distinct functions during RPE development. It is possible that the differences in the products of *yap^{wm48}* and of *yap^{nl13}* mutants are responsible for the different phenotypes of these two mutants. Indeed, the transcripts of *yap^{mw48}* encode a Yap protein with a very early truncation which only contains part of the N-terminal TEAD binding domain thus acting as a null allele (Miesfeld *et al.*, 2015). Conversely, all the products of *yap^{nl13}* contain at least one of the two WW protein-protein domains and they all contain an intact Tead binding domain. It is thus possible that the *yap^{nl13}* hypomorphic mutation allows compensatory mechanisms to take place, resulting in correct specification of the RPE while not being able to regulate the mechanotransduction in later phases of eye development.

5.3 The RPE specificity of yap^{nl13} mutant phenotype is not correlated with tissue specific yap splice forms.

yap is broadly expressed across the zebrafish embryo (Hu *et al.*, 2013; Miesfeld *et al.*, 2015). However, while in the *hirame yap* medaka mutant, loss of *yap*-mediated contractility affects the whole embryo, the phenotype of the *yap^{nl13}* is restricted to the eye (Miesfeld *et al.*, 2015). Two other zebrafish alleles have been reported, *yap^{ncv101}* and *yap^{mw48}*: the former allele results in a Yap protein completely lacking of the TEAD-binding domain, while the second mutation leads to a stop codon truncating the TEAD-binging domain (Miesfeld *et al.*, 2015;

Nakajima *et al.*, 2017; Grimm *et al.*, 2019). The early truncation of the TEAD-binding domain, or its loss, results in a predicted loss of activity in the Yap protein generated in both the *yap*^{ncv101} and *yap*^{mw48} mutants making these functionally null alleles. Differently from *yap*^{nl13}, both the *yap*^{ncv101} and *yap*^{mw48} phenotypes are not exclusively restricted to the eye but involve also the vasculature and the lymphatic system.

In chapter 2, we investigate possible causes for the tissue specificity of the *yap*^{nl13} zebrafish mutant phenotype. While the *yap*^{nl13} mutation leads to the generation of three alternative transcripts, our results suggest that differently to what has been reported in other contexts, the specificity of *yap*^{nl13} mutant phenotype is not due the presence of a tissue-specific splicing event (Finch-Edmondson *et al.*, 2016; Porazinski and Ladomery, 2018; Srivastava *et al.*, 2019). However, before a conclusion can be drawn, further analyses are required: qPCR experiments will need to be performed on isolated eye tissue instead of whole dissected heads at multiple developmental stages to confirm these hypotheses.

The Yap paralogue Taz may also have a role in the phenotypic variability shown by the different *yap* mutant alleles compensating for the disruption of Yap activity. From our observations, we consider unlikely that Taz has a compensatory role ameliorating the *yap*^{nl13}. Indeed, while Taz is able to compensate for the loss of Yap transcriptional activity in a number of systems, such as for *yap*^{mw48} eye phenotype, there are reported examples in which Taz is not sufficient to rescue the loss of Yap, as in the case of the lymphatic system in *yap*^{ncv101} allele (Zhao, Li, Tumaneng, *et al.*, 2010; Dobrokhotov *et al.*, 2018; Lu, Finegold and Johnson, 2018; Vázquez-Marín *et al.*, 2019). This suggests that Taz and Yap can both have non-overlapping expression and function. In the case of the RPE, the *yap*^{mw48} zebrafish mutant revealed that Taz can compensate for the loss of Yap transcriptional activity mitigating the loss of RPE specification in the *yap*^{mw48} mutant (Miesfeld *et al.*, 2015). The fact that the latter cannot be rescued by Taz suggests that these two processes are regulated by Yap in two different and possibly independent mechanisms mediated by different partners. Indeed, while the Hippo pathway is a well-known regulator of Yap activity, Yap is also regulated by protein-protein interactions, mainly through its WW domains (Zhu, Li and

Zhao, 2015). For example, in other context Yap has been implicated in the modulation of Smad7 and β-catenin, both required for correct eye morphogenesis and CF fusion (Azzolin et al., 2014, 2014; Deng et al., 2018; Ferrigno et al., 2002; Fujimura, 2016).

We can thus hypotheses that in the eye, *yap* is regulated by the presence of eye specific transcription factors that require the presence of WW domains. Our data favour the possibility that the *yap*^{nl13} mutation reduces the stability of the complex between Yap and some eye-specific co-transcriptional factors, leading to an eye specific downregulation of Yap activity. Alternatively, the truncated *yap* proteins present in *yap*^{nl13} mutant may form a complex with an eye-specific partner, specifically involved in mechanotransduction, and sequester it. These hypotheses could explain both the tissue specificity of the *yap*^{nl13} phenotype and the difference with other *yap* mutant alleles.

5.4 Concluding remarks

This work contributes to the evidence highlighting the critical role of the tissue's physical properties during the development of the eye, providing a possible molecular mechanism for the regulation of the RPE stiffness. Overall, we observed a role of *yap* in eye development complementary to its function in the regulation of RPE specification. We propose that *yap* is critical in the maintenance of RPE tensile properties during late optic cup morphogenesis in order to allow the apposition of the two margins of the choroid fissure and, consequently, its fusion. An active control of cell morphology is required from the RPE to accommodate the inward movements of the neuroretina without losing its rigidity, which is in turn needed to contain the neuroretina expansion and to push its inward movement. In the *yap*^{nl13} zebrafish mutant, loss of actomyosin-mediated contractility results in a mechanically passive RPE which stretches upon the strain generated by the neuroretina and is not rigid enough to maintain the inward movement of this tissue.

Our observations suggest that the choroid fissure fusion in the *yap*^{nl13} zebrafish mutant is a bistable process: while the penetrance of the phenotype in the *yap*^{nl13} mutant is incomplete, we did not observe a gradient of phenotypic severity but, rather, the complete presence or absence of coloboma. When the system is perturbed (by raising the developmental temperature or by manipulation of cytoskeletal activity) and the system has been perturbed over a recovery point, *yap*^{nl13} becomes fully penetrant, increasing the occurrence of coloboma without significantly affecting its severity.

The interpretation of eye development as a bistable process is not uniquely based on our observation of the *yap*^{nl13} zebrafish mutant. The development of the eye is a very resilient process and it is able to compensate for a number of insults. However, when the entity of such insults exceeds a critical threshold, the development is bound to catastrophic failure without intermediate states. The data obtained from human screenings on microphthalmia, anophthalmia and coloboma (MAC) phenotypes also support this interpretation. While a variety of genes can cause eye defects, the same identified mutation can often give rise to different phenotypes in different individuals. MAC phenotypes furthermore often occur syndromically and in association with other developmental defects. These observations suggest that the eye phenotypes arise from the coexistence of identified mutations and a sensitised background, provided by other cryptic mutations or by environmental factors. While such sensitised background alone would not lead to eye phenotypes, the presence of a second mutation would be sufficient to push the system to developmental failure and, thus, to an abnormal eye phenotype. Indeed, the identification of sensitizing backgrounds (as the *yap*^{nl13} zebrafish mutant) provides a useful tool to identity eye-related genes which show no phenotype in isolation allowing to understand their role in eye development.

5.5 Future directions

The phenotype of the *yap*^{nl13} is specific to the eye and the loss of Yap transcriptional activity that we observed is specific to this tissue. To confirm the absence of tissue specific *yap*^{nl13} transcripts that we suggest from the observations discussed in chapter 2, the same analyses that we performed on whole embryos heads could be performed on isolated eyes. This would exclude the possibility of samples from the rest of the head region are covering the absence of a particular splice form in the eye.

The observations discussed in chapter 4 indicated a reduction in myosin mediated cell tension in the RPE. Myosin-mediated cell contractility is required for the invagination of the optic cup (Carpenter et al., 2015; Eiraku et al., 2012; Nicolás-Pérez et al., 2016). However, this process is not altered in the *yap*^{nl13} zebrafish mutant. We hypothesised that the regulation of the mechanical properties of the RPE during optic cup invagination is controlled by different and independent processes. It is possible that *yap* is critical in the maintenance of the RPE mechanical properties in the later phases of optic cup invagination while the regulation of RPE contractility in earlier phases is *yap* independent. To confirm this, it will be important assess the levels of myosin phosphorylation across the RPE at early developmental stages.

From the morphological analysis of RPE cells, we inferred a reduction of cell tension and a more passive behaviour of this tissue. However, it will be important to directly assess the mechanical properties of the RPE to confirm that the reduction in cell contractility leads to an increased relaxation of the RPE and a reduction of its stiffness. Different approaches can be used to assess the mechanical properties of a biological tissue (Serwane et al., 2016; Sugimura et al., 2016). As mentioned in chapter 4, information regarding the tensile state of the RPE could be obtained through the observation of the recoil behaviour of the RPE upon laser ablations. While this approach would provide information on the RPE mechanical properties at the time of the ablation, it could not provide dynamic information regarding the changes of RPE tension through development. An intriguing possibility is provided by the existence of molecular

tension sensors (Borghi et al., 2012; Cai et al., 2014; Sugimura et al., 2016). Molecular tools based on FRET have been developed to infer the tensile forces at cell-cell adhesion: these tools are based on conformational changes of adhesion molecules (e.g. Vinculin and cadherin) which alter the position of two fluorophores integrated in the proteins allowing FRET to occur only in absence of cell-cell tension. The use of such molecular tools could provide insights on both spatial and temporal changes on the RPE tensile state occurring in the *yap*^{nl13} zebrafish mutant.

Together with the regulation of mechanotransduction through the actomyosin cytoskeleton, *yap* is critical in the detection of the ECM stiffness and, in turn, it regulates its deposition (Das et al., 2016; Dupont et al., 2011; Sun et al., 2016). Indeed, the ECM has a critical role in the maintenance of the RPE, in the regulation of its stiffness and in the control of optic cup invagination (Bryan et al., 2016; Kwan, 2014). Furthermore, ECM has a critical role in the transmission of the forces generated during the invagination of the optic cup (Carpenter et al., 2015; Kwan, 2014; Martinez-Morales et al., 2009; Oltean et al., 2016) (See chapter 4). The *yap*^{nl13} zebrafish mutant provides a tool to investigate the role of individual ECM components in the morphogenesis of the eye. As mentioned in chapter 4, the *yap*^{nl13} mutants can be used as a sensitised background to assess the effects of mutations of different ECM components in eye development.

5.6 Conclusions.

This work aimed to understand the role of *yap*-mediated choroid fissure closure in zebrafish. The following points were addressed:

1. Through RT-PCR and qPCR we excluded the existence of head-specific *yap* transcripts responsible for the specificity of yap^{nl13} coloboma. We furthermore observed that differently from other *yap* zebrafish mutant, in the yap^{nl13} mutant, *taz* is unlikely to be compensating for the loss of *yap* transcriptional activity.
2. Through 4D confocal imaging we have been able to observe that early RPE-genesis is not affected by yap^{nl13} mutation as both the RPE specification and its expansion are not reduced in this mutant.
3. Our analysis of the RPE in yap^{nl13} mutant allowed us to identify a key role for *yap* in the mechanotransduction of the RPE and for the RPE in the morphogenesis of the optic vesicle. We observed that loss of myosin-mediated contractility is one of the mechanisms underlying failure in choroid fissure fusion in the yap^{nl13} zebrafish mutant and that induction of myosin phosphorylation is sufficient to rescue the coloboma phenotype in this mutant.

Chapter 6.

Methods

6.1 Embryos and fish lines

Zebrafish embryos were obtained from natural spawning. Unless differently stated, embryos were raised at 28°C in E3-medium (5 mM NaCl, 0.18 mM KCl, 0.33 mM $CaCl_2$, 0.33 mM $MgSO_4$). For embryos used in imaging experiments, 0.003% 1-phenyl-2-2-thiourea (PTU) was added to the E3 medium to avoid embryos pigmentation. The fish lines used in this study were previously established: *yap*^{nl13} ; Tg(4XGTIIC:d2GFP) ; Tg(tfec:GAL4, mCherry); Tg(bhlhe40: GFP); *Tg{rx3::Gal4-VP16}*^{vu271Tg} ; TL(wild-type) (Lister *et al.*, 2011; Weiss *et al.*, 2012; Miesfeld and Link, 2014; Miesfeld *et al.*, 2015).

6.2 Whole-mount Immunohistochemistry (IHC)

Embryos (48 hpf) were fixed in 4%PFA + 4% sucrose in PBS at room temperature for 1 hour and rinsed 3x 5 minutes in PBTr (PBS with 0.8% Triton X-100, Sigma Cat# X100). Individual eyes were dissected and collected in single PCR tubes. Dissected eyes were permeabilised with one rinse in 0.02 mg*m proteinase (PK, sigma,Cat# 03115887001), post fixed with 4% PFA +4% sucrose in PBS for 20 minutes, rinsed in 3x5 minutes in PBTr and blocked for one hour at room temperature in IB Solution (10% heat inactivated normal goat serum (Sigma Cat# G9023), 1% dimethyl-sulfoxide (DMSO, Sigma, Cat# 276855), 0.8% Triton-X100 (Sigma Cat# X100 in PBS). Primary antibody incubations were performed at 4°C overnight in block solution using the following antibodies: rabbit anti-P-Myosin Light-Chain 2 (dilution 1:100, Cell Signaling, Cat# 3671P), mouse Zonula Occludens 1 (dilution 1:200 Thermo Fisher Cat# 33910), mouse phospho-histone H3(Ser10) (Dilution 1:1000 Millipore Cat# 05-806), chicken anti-GFP (Dilution 1:500 Abcam Cat# ab13970). After the staining embryos were washed over day (minimum 6x 30 minutes) and incubated in secondary antibodies overnight at 4°C using Alexa Fluor 488-conjugated, 568-conjugated and 633-conjugated secondary antibodies (1:200, Molecular Probes). Samples were finally washed over day (minimum 6x 30 minutes and mounted for confocal imaging.

6.3 Chemical Treatments

Para-nitro-blebbistatin (Optopharma, Cat# has been suspended in 100% DMSO to a final concentration of 5 mM.Treated embryos have been exposed to para-nitro-blebbistatin (Cat# DRN111 Optopharma,Malnasi-Csizmadia 2014) diluted from stock in E3 medium to the desired concentration.

6.4 Image acquisition and analysis

Live confocal imaging was performed on a Leica TCS SP8 microscope with a 10x/0.30 NA HC APO LU-V-I Water dipping objective (Leica). For live imaging, embryos were included in 0.5% Low melting point agarose (Sigma, Cat# 16520050) and kept at 2°C. Imaging was performed by bidirectional scanning at a speed of 600Hz with an image resolution of 1024px x 1024px. For imaging of immunostaining samples, a Leica TCS SP8 microscope has been used, with a 25x/0.95 NA PL IRAPO water immersion objective (Leica). Immunostaining samples were mounted using 1% low melting point agarose using plastic rings mounted by silicon grease on a thickness No.1 coverslip. Imaging was performed by bidirectional scanning at a speed of 600Hz with an image resolution of 1024px x 1024px, line averaging 3x. Z-stack projections were created using Fiji (Imagej) software. For CSA quantification, individual cells were manually segmented using Fiji Polygon tool. Microsoft Excel, GraphPad Prism 6 and Origin Pro have been used for statistical analyses and data presentation.

6.5 Genomic DNA extraction

Genomic DNA is extracted from fin-clips or whole embryos using HotSHOT protocol (Trede NS, 2007). The samples were incubated in alkaline solution (25 mM KOH, 0.2 mM EDTA, pH 12) using volumes of 50µL for fin clip samples or 25µLfor single embryos extraction. The incubations were performed at 95°C for 30 minutes. After incubation, the solutions were neutralised with the same reaction volume of neutralization solution (40 mM Tris-HCl, pH5).

6.6 Digestion Genotyping

Genotyping of *yap*^{nl13}. mutants has been performed through PCR (forward primer: 5'-ACCTCAATGTACTTTTTGTGCCA-3'; reverse primer: 5'-AGTCGGATGGGGTTGTTTCC-3') followed by enzymatic digestion to assess for the presence of BbvCI restriction site, abolished in *yap*^{nl13} mutant.

For each digestion reaction 5µL of the PCR product were added to 5 µL of reaction mix (reaction mix: 1 µL 10x Cutsmart Buffer (NEB, Cat# B7204S); 0.2 µL BbvCI restriction enzyme (NEB, Cat# R0601L, 3.8 µL water) and incubated at 37°C overnight.

6.7 RNA extraction and cDNA library preparation

Total RNA was extracted from 30 whole zebrafish embryos in 1.0 mL of Trizol Reagent (Invitrogen, Cat#15596026). Tissues were homogenised with the use of a micropestle and incubated at room temperature for 5 minutes. 200 µL of Chloroform were added, the samples were incubated for 3 minutes at room temperature and centrifuged at 12000 g for 15 minutes at 4C. Approximately 400 µL of the aqueous phase were transferred to a clean tube and RNA was precipitated by adding 500 µL of ice-cold isopropanol. The samples were mixed and incubated at room temperature for 10 minutes. RNA was then precipitated by 10 minutes centrifugation at 12000 g at 4°C. Supernatant was discarded, and the pellet washed with ice-cold 75% Ethanol, dried and resuspended in 22 µL of RNAse-free water and stored at - 20°C. cDNA synthesis was performed with the use of SuperScript II Reverse Transcriptase Kit (Invitrogen, Cat# 48190011). A final reaction volume of 20 µL was prepared using 200 ng of random primers (Invitrogen, Cat# 48190011), 10 mM dNTP mix (Promega, Cat# U1511) and 500 ng of total RNA. The solution was heated to 65°C for 5 minutes and moved on ice. To the mixture were added: 4 µL of 5x First-Strand Buffer (SS II RT kit), 2 µL of 0.1M DTT (SS II RT kit) and 1µL of RNaseOut (Invitrogen, Cat# 10777019). The solution was incubated at 25°C for 2 minutes and 1 µL of SuperScript II Reverse Transcriptase was added. cDNA synthesis was performed in a thermocycler programmed as follow: 25°C for 10 minutes, 42°C for 50 minutes, 70°C for 15 minutes. 4°C until stopped.

6.8 Quantitative RT-PCR

Quantitative PCR was performed in triplicates for each primer pair, using 100 ng of cDNA sample. Promega GoTaq qPCR Master Mix was used (Cat# A6001) and the amplifications were performed as follow: 64°C or 2 minutes of denaturation, followed by 40 cycles of amplification (94°C for 15 seconds, 60°C for 30 seconds, 70°C for 30 seconds), and melt curve analysis heating from 60°C to 90C at 0.5°C step. The mean threshold cycle (Ct) values were normalised to the housekeeping gene ef1a. The result was calculated as a fold increase between the tested condition and control condition (2 ΔCt). The primers used for qPCR experiments were the following:

Primer Name	Sequence	Amplification Efficiency*
yap Forward	CCAGACAAGCCAGTACAGAT	93.7%
yap Reverse	GAAGTATCTCTGTCCCGAAGG	
ef1a Forward	TCTCTCAATCTTGAAACTTATCAATCA	90%
ef1a Reverse	AACACCCAGGCGTACTTGAA	
taz Forward	GCATCCAGATGGAGAGAGAG	97.5%
taz Reverse	GCTGTTATTGGGCATGTTTC	
fn1b Forward	CAGTACTGTACAGTCAGGGGAAGC	97.5%
fn1b Reverse	CACGACCGTTGTCATTACAGCC	
ctgfa Forward	CTGCACAGCCAGAGATG	96.6%
ctgfa Reverse	CACTTCCCAGGCACTTT	

*Efficiency was calculated as follows: E(%)=(10-1/slope -1)*100. To obtain the slope value, validation runs have been performed using dilution series of template DNA for each primers pair in order to generate a standard curve plotting Ct values to the log of template DNA concentration.

6.9 RT-PCR

For the RT-PCR experiments each reaction was prepared following GoTaq G2 Flexi PCR kit by Promega. Each reaction was prepared as follow: 1.25µL10X Go Taq reaction buffer (Cat# M792A), 0.375µL 50mM MgCl2, 0.25µL dNTp mix 0.2mM (each dNTP) (Cat# C1141, C1145), 0.125µL GoTaq DNA polymerase, up to 1µL template DNA (varying according to concentration). The reaction volume was upped to 12.5µL final volume with nuclease free water. The PCR reactions were performed using a thermocycler (Eppendorf MasterCyclerPro) using the following protocol: 95°C for 5 minutes, 95°C for 30seconds, 55°C-60°C (depending on primer composition) for 30 seconds, 72°C for 30seconds. The PCR cycled was repeated for 35 cycles followed by final 5 minutes at 72°C.

The primers used were the following:

Primer Name	Sequence
Yap Exon1_3 Forward	ATGTTCTGTTGCTGCACAGG
Yap Exon 1_3 Reverse	TGAGAAAGCTGCCAGACTCA
Yap Exon 2_4 Forward	AGATGGCCAAGACCCCTTC
Yap Exon 2_4 Reverse	GAGGTAATAGCTTGTTCCCACC
Yap Exon3_5 Forward	CCTGTGCAGCAACAGAACAT
Yap Exon3_5 Reverse	GGAAATTCGCTGCTGGTTCA
Yap Exon 4_6Forward	TCAATCACAAGAACAAAACCACC
Yap Exon 4_6 Reverse	CACAGGGTTTTGGGTGCC
Yap Exon 5_7 Forward	CTGAGGATCAAACAAGAGCTCC
Yap Exon 5_7 Reverse	AGGGACGCTGTAACTGCTC
Yap Exon 6_8 Forward	CAAGACGCCCGTAACATGAC
Yap Exon 6_8 Reverse	GCGTCTAGGTAATCGGGGAA
Yap Exon 1 Forward	AGACCGATCTGGAGGCTCTT
Yap Exon 1 Reverse	AGACCGATCTGGAGGCTCTT
Yap Exon 3_4 Forward	CCTGTGCAGCAACAGAACATC
Yap Exon 3_4 Reverse	AAACGCGGGTCAAGTCGT
Yap Exon 5 Forward	AGCCCACAGAGTGGAGTGA

Primer Name	Sequence
Yap Exon 5 Reverse	GCGAAGGAGCTCTTGTTTGA
Yap Exon 4_5 Forward	AACCACCTCTTGGCTGGAC
Yap Exon 4_5 Reverse	GCAACTGGGAACCTTGCTTT

6.10 Statistical analysis.

For the comparison between expression levels of *yap, taz* and *ctgfa* between wild type and *yap*^{nl13} embryos (Fig. 2.0 A), the normality of data has been excluded through Kolmogorov-Smirnov (KS) test for normality. The KS test has been followed by multiple t-test using Holm-Sidak method to test for significant difference across the detected expression levels in wild type and *yap*^{nl13} mutants.

The data relative the difference between gray value in the eye region in the Yap reporter line in wild type and *yap*^{nl13} mutant (Fig. 2.0 B) have been tested for normality using KS test. As the normality cannot be confirmed, the data have been compared by nonparametric Mann Whitney test for non paired data.

For the analysis of exon 3_4, 4_5 and exon 5 abundance level between head and trunks in wild type and *yap*^{nl13} (Fig. 2.2B) the ΔCt values obtained from our qPCR were compared by Kruskal-Wallis one-way ANOVA for non-parametric data (from the size of our dataset we could not assume normality) to assess for significance. All the data relative to the RPE cell count and overall RPE surface obtained from our time-lapse experiments have been tested for normality through KS test. The difference between RPE cell counts, RPE surface and RPE Fold increase in wild type and *yap*^{nl13} mutant embryos (Fig. 3.2 C, D, E) have been then thus compared through parametric t-test for unpaired data.

The values on overall eye surface at the moment of RPE specification, and the ratio between eye surface and RPE surface, have been tested for normality through KS test. The difference between the means of the differences gathered in the wild type and in the *yap*^{nl13} mutant has thus been assessed through Mann-Whitney test for non-parametric unpaired data.

To test for significance in the difference in tortuosity index in between wild type and *yap*^{nl13}-mutant (Fig 4.1) we performed a parametric t-test for unpaired data after having confirmed the normality of the data through KS test.

The significance of the difference between the means of CSA values of wild type and *yap*^{nl13} mutants (Fig. 4.2) has been tested through Mann Whitney non parametric test for unpaired data (normality of the data could not be assumed after KS test). The significance of the difference in distribution of the CSA values between wild type and *yap*^{nl13} has been tested through Kruskall Wallis test.

The significance of the difference in mean gray value intensity in the eye of wild type and *yap*^{nl13} zebrafish embryos, treated with blebbistatin and untreated (Fig 4.3 A) has been tested through parametric unpaired t-test (assumption of normality confirmed by KS test).

The difference in percentage of *yap*^{nl13} embryos showing coloboma in untreated condition, treated with blebbistatin between 5 and 19hpf and between 10 and 24hpf (Fig. 4.3) has been assessed through Kruskall Walliss non-parametric one way ANOVA for unpaired data (we could not assume normality of the data since the reduced number of the datapoints).

The significance in the reduction of coloboma frequency observed in *yap*^{nl13} zebrafish embryos injected with myosin phosphatase morpholino has been tested through nonparametric Mann Whitney test for unpaired data (normality of the data could not be assume due to the number of datapoints).

Chapter 7.**References**

Acampora, D. *et al.* (1995) 'Forebrain and midbrain regions are deleted in Otx2−/− mutants due to a defective anterior neuroectoderm specification during gastrulation', *Development*, 121(10), pp. 3279–3290.

Adler, R. and Belecky-Adams, T. L. (2002) 'The role of bone morphogenetic proteins in the differentiation of the ventral optic cup', *Development*, 129(13), pp. 3161–3171.

Agarwala, S. *et al.* (2019) 'Amotl2a interacts with the Hippo effector Yap1 and the Wnt/β-catenin effector Lef1 to control tissue size in zebrafish', *eLife*, 4. doi: 10.7554/eLife.08201.

Altunay, H. (2000) ‘Fine Structure of the Retinal Pigment Epithelium, Bruch’s Membrane and Choriocapillaris in the Horse’, *Anatomia, Histologia, Embryologia*, 29(3), pp. 135–139. doi: 10.1046/j.1439-0264.2000.00241.x.

Aragona, M. *et al.* (2013) ‘A Mechanical Checkpoint Controls Multicellular Growth through YAP / TAZ Regulation by Actin-Processing Factors Mechanical Regulation of Cell Proliferation through’, *Cell*, 154(5), pp. 1047–1059. doi: 10.1016/j.cell.2013.07.042.

Asaoka, Y. *et al.* (2014) ‘The Hippo Pathway Controls a Switch between Retinal Progenitor Cell Proliferation and Photoreceptor Cell Differentiation in Zebrafish’, *PLoS ONE*, 9(5). doi: 10.1371/journal.pone.0097365.

Asaoka, Y. and Furutani-Seiki, M. (2017) ‘YAP mediated mechano-homeostasis — conditioning 3D animal body shape’, *Current Opinion in Cell Biology*, 49, pp. 64–70. doi: 10.1016/J.CEB.2017.11.013.

Astone, M. *et al.* (2018) ‘Zebrafish mutants and TEAD reporters reveal essential functions for Yap and Taz in posterior cardinal vein development’, *Scientific Reports*, 8(1), p. 10189. doi: 10.1038/s41598-018-27657-x.

Azzolin, L. *et al.* (2014a) ‘YAP/TAZ Incorporation in the β-Catenin Destruction Complex Orchestrates the Wnt Response’, *Cell*, 158(1), pp. 157–170. doi: 10.1016/j.cell.2014.06.013.

Azzolin, L. *et al.* (2014b) ‘YAP/TAZ Incorporation in the β-Catenin Destruction Complex Orchestrates the Wnt Response’, *Cell*, 158(1), pp. 157–170. doi: 10.1016/j.cell.2014.06.013.

Babcock, H. E. *et al.* (2014) ‘aldh7a1 Regulates Eye and Limb Development in Zebrafish’, *PLOS ONE*, 9(7), p. e101782. doi: 10.1371/journal.pone.0101782.

Bailey, T. J. *et al.* (2004) ‘Regulation of vertebrate eye development by Rx genes’, *The International Journal of Developmental Biology*, 48(8–9), pp. 761–770. doi: 10.1387/ijdb.041878tb.

Barbieri, A. M. *et al.* (1999) ‘A homeobox gene, vax2, controls the patterning of the eye dorsoventral axis’, *Proceedings of the National Academy of Sciences of the United States of America*, 96(19), pp. 10729–10734.

Bazin-Lopez, N. *et al.* (2015) ‘Watching eyes take shape’, *Current Opinion in Genetics & Development*, 32, pp. 73–79. doi: 10.1016/j.gde.2015.02.004.

Bernier, G. *et al.* (2000) ‘Expanded retina territory by midbrain transformation upon overexpression of Six6 (Optx2) in Xenopus embryos’, *Mechanisms of Development*, 93(1), pp. 59–69. doi: 10.1016/S0925-4773(00)00271-9.

Bernstein, C. S. *et al.* (2018) ‘The cellular bases of choroid fissure formation and closure’, *Developmental Biology*, 440(2), pp. 137–151. doi: 10.1016/J.YDBIO.2018.05.010.

Berry, F. B. *et al.* (2008) 'FOXC1 is required for cell viability and resistance to oxidative stress in the eye through the transcriptional regulation of FOXO1A', *Human Molecular Genetics*, 17(4), pp. 490–505. doi: 10.1093/hmg/ddm326.

Bielen, H. and Houart, C. (2012) 'BMP signaling protects telencephalic fate by repressing eye identity and its Cxcr4-dependent morphogenesis', *Developmental Cell*, 23(4), pp. 812–822. doi: 10.1016/j.devcel.2012.09.006.

Borghi, N. *et al.* (2012) 'E-cadherin is under constitutive actomyosin-generated tension that is increased at cell-cell contacts upon externally applied stretch.', *Proceedings of the National Academy of Sciences of the United States of America*, 109(31), pp. 12568–73. doi: 10.1073/pnas.1204390109.

Boulton, M. and Dayhaw-Barker, P. (2001) 'The role of the retinal pigment epithelium: Topographical variation and ageing changes', *Eye*, 15(3), pp. 384–389. doi: 10.1038/eye.2001.141.

Bredrup, C. *et al.* (2008) 'Ophthalmological Aspects of Pierson Syndrome', *American Journal of Ophthalmology*, 146(4), pp. 602-611.e1. doi: 10.1016/j.ajo.2008.05.039.

Bryan, C. D. *et al.* (2020) 'Optic cup morphogenesis requires neural crest-mediated basement membrane assembly', *Development*, 147(4). doi: 10.1242/dev.181420.

Bryan, C. D., Chien, C.-B. and Kwan, K. M. (2016) 'Loss of laminin alpha 1 results in multiple structural defects and divergent effects on adhesion during vertebrate optic cup morphogenesis', *Developmental Biology*, 416(2), pp. 324–337. doi: 10.1016/j.ydbio.2016.06.025.

Bumsted, K. M. and Barnstable, C. J. (2000) 'Dorsal retinal pigment epithelium differentiates as neural retina in the microphthalmia (mi/mi) mouse', *Investigative Ophthalmology & Visual Science*, 41(3), pp. 903–908.

Bumsted, K. M., Rizzolo, L. J. and Barnstable, C. J. (2001) 'Defects in the MITF(mi/mi) apical surface are associated with a failure of outer segment elongation', *Experimental Eye Research*, 73(3), pp. 383–392. doi: 10.1006/exer.2001.1048.

Cabochette, P. *et al.* (2015) 'YAP controls retinal stem cell DNA replication timing and genomic stability', *eLife*. Edited by H. McNeill, 4, p. e08488. doi: 10.7554/eLife.08488.

Calvo, F. *et al.* (2013) 'Mechanotransduction and YAP-dependent matrix remodelling is required for the generation and maintenance of cancer-associated fibroblasts', *Nature Cell Biology*, 15(6), pp. 637–646. doi: 10.1038/ncb2756.

Camargo, F. D. *et al.* (2007a) 'YAP1 Increases Organ Size and Expands Undifferentiated Progenitor Cells', *Current Biology*, 17(23), pp. 2054–2060. doi: 10.1016/j.cub.2007.10.039.

Camargo, F. D. *et al.* (2007b) 'YAP1 Increases Organ Size and Expands Undifferentiated Progenitor Cells', *Current Biology*, 17(23), pp. 2054–2060. doi: 10.1016/j.cub.2007.10.039.

Carpenter, A. C. *et al.* (2015) 'Wnt ligands from the embryonic surface ectoderm regulate "bimetallic strip" optic cup morphogenesis in mouse', *Development (Cambridge, England)*, 142(5), pp. 972–982. doi: 10.1242/dev.120022.

Cavodeassi, F. *et al.* (2005a) 'Early Stages of Zebrafish Eye Formation Require the Coordinated Activity of Wnt11, Fz5, and the Wnt/β-Catenin Pathway', *Neuron*, 47(1), pp. 43–56. doi: 10.1016/j.neuron.2005.05.026.

Cavodeassi, F. *et al.* (2005b) 'Early Stages of Zebrafish Eye Formation Require the Coordinated Activity of Wnt11, Fz5, and the Wnt/β-Catenin Pathway', *Neuron*, 47(1), pp. 43–56. doi: 10.1016/j.neuron.2005.05.026.

Cavodeassi, F., Ivanovitch, K. and Wilson, S. W. (2013) 'Eph/Ephrin signalling maintains eye field segregation from adjacent neural plate territories during forebrain morphogenesis', *Development*, 140(20), pp. 4193–4202. doi: 10.1242/dev.097048.

Cechmanek, P. B. and McFarlane, S. (2017a) 'Retinal pigment epithelium expansion around the neural retina occurs in two separate phases with distinct mechanisms', *Developmental Dynamics*, 246(8), pp. 598–609. doi: 10.1002/dvdy.24525.

Cechmanek, P. B. and McFarlane, S. (2017b) 'Retinal pigment epithelium expansion around the neural retina occurs in two separate phases with distinct mechanisms', *Developmental Dynamics*, 246(8), pp. 598–609. doi: 10.1002/dvdy.24525.

Cha, B. *et al.* (2016) 'Mechanotransduction activates canonical Wnt/β-catenin signaling to promote lymphatic vascular patterning and the development of lymphatic and lymphovenous valves', *Genes & Development*, 30(12), pp. 1454–1469. doi: 10.1101/gad.282400.116.

Chan, S. W. *et al.* (2011) 'Hippo Pathway-independent Restriction of TAZ and YAP by Angiomotin', *The Journal of Biological Chemistry*, 286(9), pp. 7018–7026. doi: 10.1074/jbc.C110.212621.

Chaudhuri, O. *et al.* (2014) 'Extracellular matrix stiffness and composition jointly regulate the induction of malignant phenotypes in mammary epithelium', *Nature Materials*, 13(10), pp. 970–978. doi: 10.1038/nmat4009.

Chen, Q. *et al.* (2014) 'A temporal requirement for Hippo signaling in mammary gland differentiation, growth, and tumorigenesis', *Genes & Development*, 28(5), pp. 432–437. doi: 10.1101/gad.233676.113.

Chen, S. *et al.* (2013) 'Defective FGF signaling causes coloboma formation and disrupts retinal neurogenesis', *Cell Research*, 23(2), pp. 254–273. doi: 10.1038/cr.2012.150.

Chen, Y.-A. *et al.* (2019) 'WW Domain-Containing Proteins YAP and TAZ in the Hippo Pathway as Key Regulators in Stemness Maintenance, Tissue Homeostasis, and Tumorigenesis', *Frontiers in Oncology*, 9. doi: 10.3389/fonc.2019.00060.

Chiang, C. *et al.* (1996) 'Cyclopia and defective axial patterning in mice lacking Sonic hedgehog gene function', *Nature*, 383(6599), pp. 407–413. doi: 10.1038/383407a0.

Chow, R. L. *et al.* (1999) 'Pax6 induces ectopic eyes in a vertebrate', *Development (Cambridge, England)*, 126(19), pp. 4213–4222.

Chow, R. L. and Lang, R. A. (2001) 'Early eye development in vertebrates', *Annual Review of Cell and Developmental Biology*, 17, pp. 255–296. doi: 10.1146/annurev.cellbio.17.1.255.

Chuang, J. C. and Raymond, P. A. (2002) 'Embryonic origin of the eyes in teleost fish', *BioEssays*, 24(6), pp. 519–529. doi: 10.1002/bies.10097.

Davis, J. R. and Tapon, N. (2019) 'Hippo signalling during development', *Development (Cambridge, England)*, 146(18). doi: 10.1242/dev.167106.

Deml, B. *et al.* (2015) 'Mutations in MAB21L2 Result in Ocular Coloboma, Microcornea and Cataracts', *PLoS Genetics*, 11(2). doi: 10.1371/journal.pgen.1005002.

Deml, B. *et al.* (2016) 'Novel mutations in PAX6, OTX2 and NDP in anophthalmia, microphthalmia and coloboma', *European Journal of Human Genetics*, 24(4), pp. 535–541. doi: 10.1038/ejhg.2015.155.

Deng, F. *et al.* (2018) 'YAP triggers the Wnt/β-catenin signalling pathway and promotes enterocyte self-renewal, regeneration and tumorigenesis after DSS-induced injury', *Cell Death & Disease*, 9(2), pp. 1–16. doi: 10.1038/s41419-017-0244-8.

Díaz-Coránguez, M., Ramos, C. and Antonetti, D. A. (2017a) 'The inner blood-retinal barrier: Cellular basis and development', *Vision Research*, 139, pp. 123–137. doi: 10.1016/j.visres.2017.05.009.

Díaz-Coránguez, M., Ramos, C. and Antonetti, D. A. (2017b) 'The inner blood-retinal barrier: Cellular basis and development', *Vision Research*, 139, pp. 123–137. doi: 10.1016/j.visres.2017.05.009.

Dobrokhotov, O. *et al.* (2018) 'Mechanoregulation and pathology of YAP/TAZ via Hippo and non-Hippo mechanisms', *Clinical and Translational Medicine*, 7(1), p. 23. doi: 10.1186/s40169-018-0202-9.

Dupont, S. *et al.* (2011a) 'Role of YAP/TAZ in mechanotransduction', *Nature*, 474(7350), pp. 179–183. doi: 10.1038/nature10137.

Dupont, S. *et al.* (2011b) 'Role of YAP/TAZ in mechanotransduction.', *Nature*, 474(7350), pp. 179–183. doi: 10.1038/nature10137.

Dupont, S. (2016) 'Role of YAP/TAZ in cell-matrix adhesion-mediated signalling and mechanotransduction', *Experimental Cell Research*, 343(1), pp. 42–53. doi: 10.1016/j.yexcr.2015.10.034.

Dutta, S. *et al.* (2018) 'TRIP6 inhibits Hippo signaling in response to tension at adherens junctions', *EMBO reports*, 19(2), pp. 337–350. doi: 10.15252/embr.201744777.

Eckert, P. *et al.* (2017) 'Optic fissure margin morphogenesis sets the stage for consecutive optic fissure fusion, pioneered by a distinct subset of margin cells using a hyaloid vessel as scaffold', *bioRxiv*, p. 141275. doi: 10.1101/141275.

Eiraku, M. *et al.* (2011a) 'Self-organizing optic-cup morphogenesis in three-dimensional culture', *Nature*, 472(7341), pp. 51–56. doi: 10.1038/nature09941.

Eiraku, M. *et al.* (2011b) 'Self-organizing optic-cup morphogenesis in three-dimensional culture', *Nature*, 472(7341), pp. 51–56. doi: 10.1038/nature09941.

Eiraku, M., Adachi, T. and Sasai, Y. (2012a) 'Relaxation-expansion model for self-driven retinal morphogenesis: a hypothesis from the perspective of biosystems dynamics at the multi-cellular level.', *BioEssays : news and reviews in molecular, cellular and developmental biology*, 34(1), pp. 17–25. doi: 10.1002/bies.201100070.

Eiraku, M., Adachi, T. and Sasai, Y. (2012b) 'Relaxation-expansion model for self-driven retinal morphogenesis: a hypothesis from the perspective of biosystems dynamics at the multi-cellular level.', *BioEssays : news and reviews in molecular, cellular and developmental biology*, 34(1), pp. 17–25. doi: 10.1002/bies.201100070.

Ekker, S. C. *et al.* (1995) 'Patterning activities of vertebrate hedgehog proteins in the developing eye and brain', *Current biology: CB*, 5(8), pp. 944–955. doi: 10.1016/s0960-9822(95)00185-0.

Evans, A. L. and Gage, P. J. (2005) 'Expression of the homeobox gene Pitx2 in neural crest is required for optic stalk and ocular anterior segment development', *Human Molecular Genetics*, 14(22), pp. 3347–3359. doi: 10.1093/hmg/ddi365.

Ferrigno, O. *et al.* (2002) 'Yes-associated protein (YAP65) interacts with Smad7 and potentiates its inhibitory activity against TGF-beta/Smad signaling', *Oncogene*, 21(32), pp. 4879–4884. doi: 10.1038/sj.onc.1205623.

Fillatre, J. *et al.* (2019) 'TEADs, Yap, Taz, Vgll4s transcription factors control the establishment of Left-Right asymmetry in zebrafish', *eLife*. Edited by J. Vermot and D. Y. Stainier, 8, p. e45241. doi: 10.7554/eLife.45241.

Finch-Edmondson, M. L. *et al.* (2016a) 'Splice variant insertions in the C-terminus impairs YAP's transactivation domain', *Biochemistry and Biophysics Reports*, 6, pp. 24–31. doi: 10.1016/j.bbrep.2016.02.015.

Finch-Edmondson, M. L. *et al.* (2016b) 'Splice variant insertions in the C-terminus impairs YAP's transactivation domain', *Biochemistry and Biophysics Reports*, 6, pp. 24–31. doi: 10.1016/j.bbrep.2016.02.015.

Fish, M. B. *et al.* (2014) 'Xenopus mutant reveals necessity of rax for specifying the eye field which otherwise forms tissue with telencephalic and diencephalic character', *Developmental biology*, 395(2), pp. 317–330. doi: 10.1016/j.ydbio.2014.09.004.

Fitamant, J. *et al.* (2015) 'YAP Inhibition Restores Hepatocyte Differentiation in Advanced HCC, Leading to Tumor Regression', *Cell Reports*, 10(10), pp. 1692–1707. doi: 10.1016/j.celrep.2015.02.027.

Fuhrmann, S. (2008) 'Wnt signaling in eye organogenesis.', *Organogenesis*, 4(2), pp. 60–7.

Fuhrmann, S. (2010) 'Eye morphogenesis and patterning of the optic vesicle', *Current Topics in Developmental Biology*, 93, pp. 61–84. doi: 10.1016/B978-0-12-385044-7.00003-5.

Fuhrmann, S., Levine, E. M. and Reh, T. A. (2000) 'Extraocular mesenchyme patterns the optic vesicle during early eye development in the embryonic chick', *Development*, 127(21), pp. 4599–4609.

Fujimura, N. (2016a) 'WNT/β-Catenin Signaling in Vertebrate Eye Development.', *Frontiers in cell and developmental biology*, 4, p. 138. doi: 10.3389/fcell.2016.00138.

Fujimura, N. (2016b) 'WNT/β-Catenin Signaling in Vertebrate Eye Development.', *Frontiers in cell and developmental biology*, 4, p. 138. doi: 10.3389/fcell.2016.00138.

Fulford, A., Tapon, N. and Ribeiro, P. S. (2018) 'Upstairs, downstairs: spatial regulation of Hippo signalling', *Current Opinion in Cell Biology*, 51, pp. 22–32. doi: 10.1016/j.ceb.2017.10.006.

Gaffney, C. J. *et al.* (2012) 'Identification, basic characterization and evolutionary analysis of differentially spliced mRNA isoforms of human YAP1 gene', *Gene*, 509(2), pp. 215–222. doi: 10.1016/j.gene.2012.08.025.

Gage, P. J. *et al.* (2005) 'Fate Maps of Neural Crest and Mesoderm in the Mammalian Eye', *Investigative Ophthalmology & Visual Science*, 46(11), pp. 4200–4208. doi: 10.1167/iovs.05-0691.

Gao, Y. *et al.* (2014) 'YAP inhibits squamous transdifferentiation of Lkb1-deficient lung adenocarcinoma through ZEB2-dependent DNp63 repression', *Nature Communications*, 5(1), p. 4629. doi: 10.1038/ncomms5629.

Genevet, A. and Tapon, N. (2011) 'The Hippo pathway and apico-basal cell polarity', *The Biochemical Journal*, 436(2), pp. 213–224. doi: 10.1042/BJ20110217.

Georgiadis, A. *et al.* (2010) 'The Tight Junction Associated Signalling Proteins ZO-1 and ZONAB Regulate Retinal Pigment Epithelium Homeostasis in Mice', *PLoS ONE*, 5(12). doi: 10.1371/journal.pone.0015730.

Gestri, G. *et al.* (2018a) 'Cell Behaviors during Closure of the Choroid Fissure in the Developing Eye.', *Frontiers in cellular neuroscience*, 12, p. 42. doi: 10.3389/fncel.2018.00042.

Gestri, G. *et al.* (2018b) 'Cell Behaviors during Closure of the Choroid Fissure in the Developing Eye.', *Frontiers in cellular neuroscience*, 12, p. 42. doi: 10.3389/fncel.2018.00042.

Gestri, G., Link, B. A. and Neuhauss, S. C. F. (2012) 'The visual system of zebrafish and its use to model human ocular diseases.', *Developmental neurobiology*, 72(3), pp. 302–27. doi: 10.1002/dneu.20919.

Graw, J. (2010) 'Eye development', *Current Topics in Developmental Biology*, 90, pp. 343–386. doi: 10.1016/S0070-2153(10)90010-0.

Gregory-Evans, C. Y. *et al.* (2004) 'Ocular coloboma: a reassessment in the age of molecular neuroscience', *J Med Genet*, 41, pp. 881–891. doi: 10.1136/jmg.2004.025494.

Grimm, L. *et al.* (2019) 'Yap1 promotes sprouting and proliferation of lymphatic progenitors downstream of Vegfc in the zebrafish trunk', *eLife*, 8, p. e42881. doi: 10.7554/eLife.42881.

Guo, X. and Zhao, B. (2013) 'Integration of mechanical and chemical signals by YAP and TAZ transcription coactivators.', *Cell & bioscience*, 3(1), p. 33. doi: 10.1186/2045-3701-3-33.

Halder, G., Dupont, S. and Piccolo, S. (2012) 'Transduction of mechanical and cytoskeletal cues by YAP and TAZ', *Nature Reviews Molecular Cell Biology*, 13(9), pp. 591–600. doi: 10.1038/nrm3416.

Hamill, K. J. *et al.* (2009) 'Laminin deposition in the extracellular matrix: a complex picture emerges', *Journal of Cell Science*, 122(24), pp. 4409–4417. doi: 10.1242/jcs.041095.

Hansen, C. G., Moroishi, T. and Guan, K.-L. (2015) 'YAP and TAZ: a nexus for Hippo signaling and beyond', *Trends in Cell Biology*, 25(9), pp. 499–513. doi: 10.1016/j.tcb.2015.05.002.

Harding, P. and Moosajee, M. (2019) 'The Molecular Basis of Human Anophthalmia and Microphthalmia', *Journal of Developmental Biology*, 7(3). doi: 10.3390/jdb7030016.

Hartsock, A. *et al.* (2014) 'In Vivo Analysis of Hyaloid Vasculature Morphogenesis in Zebrafish: A role for the lens in maturation and maintenance of the hyaloid', *Developmental biology*, 394(2), pp. 327–339. doi: 10.1016/j.ydbio.2014.07.024.

Hasegawa, E., Truman, J. W. and Nose, A. (2016) 'Identification of excitatory premotor interneurons which regulate local muscle contraction during Drosophila larval locomotion', *Scientific Reports*, 6(1), p. 30806. doi: 10.1038/srep30806.

Heer, N. C. and Martin, A. C. (2017) 'Tension, contraction and tissue morphogenesis', *Development*, 144(23), pp. 4249–4260. doi: 10.1242/dev.151282.

Heermann, S. *et al.* (2015) 'Eye morphogenesis driven by epithelial flow into the optic cup facilitated by modulation of bone morphogenetic protein', *eLife*. Edited by T. T. Whitfield, 4, p. e05216. doi: 10.7554/eLife.05216.

Heisenberg, C.-P. *et al.* (2001) 'A mutation in the Gsk3–binding domain of zebrafish Masterblind/Axin1 leads to a fate transformation of telencephalon and eyes to diencephalon', *Genes & Development*, 15(11), pp. 1427–1434. doi: 10.1101/gad.194301.

Hernández-Bejarano, M. *et al.* (2015) 'Opposing Shh and Fgf signals initiate nasotemporal patterning of the zebrafish retina', *Development*, 142(22), pp. 3933–3942. doi: 10.1242/dev.125120.

Hirata, H., Samsonov, M. and Sokabe, M. (2017) 'Actomyosin contractility provokes contact inhibition in E-cadherin-ligated keratinocytes', *Scientific Reports*, 7, p. 46326. doi: 10.1038/srep46326.

Hodgkinson, C. A. *et al.* (1993) 'Mutations at the mouse microphthalmia locus are associated with defects in a gene encoding a novel basic-helix-loop-helix-zipper protein', *Cell*, 74(2), pp. 395–404. doi: 10.1016/0092-8674(93)90429-t.

Holt, R. *et al.* (2017) 'New variant and expression studies provide further insight into the genotype-phenotype correlation in YAP1 -related developmental eye disorders', *Scientific Reports*, 7(1), p. 7975. doi: 10.1038/s41598-017-08397-w.

Hornby, S. J., Ward, S. J. and Gilbert, C. E. (2003) 'Eye birth defects in humans may be caused by a recessively-inherited genetic predisposition to the effects of maternal vitamin A deficiency during pregnancy', *Medical Science Monitor: International Medical Journal of Experimental and Clinical Research*, 9(11), pp. HY23-26.

Horsford, D. J. *et al.* (2005) 'Chx10 repression of Mitf is required for the maintenance of mammalian neuroretinal identity', *Development*, 132(1), pp. 177–187. doi: 10.1242/dev.01571.

Hoshino, M. *et al.* (2006a) 'Transcriptional repression induces a slowly progressive atypical neuronal death associated with changes of YAP isoforms and p73', *The Journal of Cell Biology*, 172(4), pp. 589–604. doi: 10.1083/jcb.200509132.

Hoshino, M. *et al.* (2006b) 'Transcriptional repression induces a slowly progressive atypical neuronal death associated with changes of YAP isoforms and p73', *The Journal of Cell Biology*, 172(4), pp. 589–604. doi: 10.1083/jcb.200509132.

Houart, C. *et al.* (2002) 'Establishment of the Telencephalon during Gastrulation by Local Antagonism of Wnt Signaling', *Neuron*, 35(2), pp. 255–265. doi: 10.1016/S0896-6273(02)00751-1.

Houdusse, A. and Sweeney, H. L. (2016) 'How myosin generates force on actin filaments', *Trends in biochemical sciences*, 41(12), pp. 989–997. doi: 10.1016/j.tibs.2016.09.006.

Hu, J. *et al.* (2013a) 'Yes-Associated Protein (Yap) Is Required for Early Embryonic Development in Zebrafish (Danio Rerio)', *International Journal of Biological Sciences*, 9(3), pp. 267–278. doi: 10.7150/ijbs.4887.

Hu, J. *et al.* (2013b) 'Yes-Associated Protein (Yap) Is Required for Early Embryonic Development in Zebrafish (Danio Rerio)', *International Journal of Biological Sciences*, 9(3), pp. 267–278. doi: 10.7150/ijbs.4887.

Huang, J. *et al.* (2005) 'The Hippo signaling pathway coordinately regulates cell proliferation and apoptosis by inactivating Yorkie, the Drosophila Homolog of YAP', *Cell*, 122(3), pp. 421–434. doi: 10.1016/j.cell.2005.06.007.

Hyer, J., Mima, T. and Mikawa, T. (1998) 'FGF1 patterns the optic vesicle by directing the placement of the neural retina domain', *Development*, 125(5), pp. 869–877.

Ibar, C. *et al.* (2018) 'Tension-dependent regulation of mammalian Hippo signaling through LIMD1', *Journal of Cell Science*, 131(5). doi: 10.1242/jcs.214700.

Iglesias-Bexiga, M. *et al.* (2015) 'WW domains of the yes-kinase-associated-protein (YAP) transcriptional regulator behave as independent units with different binding preferences for PPxY motif-containing ligands.', *PloS one*, 10(1), p. e0113828. doi: 10.1371/journal.pone.0113828.

Imajo, M. *et al.* (2012) 'A molecular mechanism that links Hippo signalling to the inhibition of Wnt/β-catenin signalling', *The EMBO Journal*, 31(5), pp. 1109–1122. doi: 10.1038/emboj.2011.487.

Ito, M. *et al.* (2004) 'Myosin phosphatase: structure, regulation and function', *Molecular and Cellular Biochemistry*, 259(1–2), pp. 197–209. doi: 10.1023/b:mcbi.0000021373.14288.00.

Ivanovitch, K., Cavodeassi, F. and Wilson, S. W. (2013a) 'Precocious Acquisition of Neuroepithelial Character in the Eye Field Underlies the Onset of Eye Morphogenesis', *Developmental Cell*, 27(3), pp. 293–305. doi: 10.1016/j.devcel.2013.09.023.

Ivanovitch, K., Cavodeassi, F. and Wilson, S. W. (2013b) 'Precocious Acquisition of Neuroepithelial Character in the Eye Field Underlies the Onset of Eye Morphogenesis', *Developmental Cell*, 27(3), pp. 293–305. doi: 10.1016/j.devcel.2013.09.023.

James, A. *et al.* (2016) 'The hyaloid vasculature facilitates basement membrane breakdown during choroid fissure closure in the zebrafish eye', *Developmental Biology*, 419(2), pp. 262–272. doi: 10.1016/j.ydbio.2016.09.008.

Jiang, Q. *et al.* (2009) 'yap is required for the development of brain, eyes, and neural crest in zebrafish', *Biochemical and Biophysical Research Communications*, 384(1), pp. 114–119. doi: 10.1016/j.bbrc.2009.04.070.

Justice, R. W. *et al.* (1995) 'The Drosophila tumor suppressor gene warts encodes a homolog of human myotonic dystrophy kinase and is required for the control of cell shape and proliferation', *Genes & Development*, 9(5), pp. 534–546. doi: 10.1101/gad.9.5.534.

Kanai, F. *et al.* (2000) 'TAZ: a novel transcriptional co-activator regulated by interactions with 14-3-3 and PDZ domain proteins', *The EMBO journal*, 19(24), pp. 6778–6791. doi: 10.1093/emboj/19.24.6778.

Khan, Z. *et al.* (2014) 'Quantitative 4D analyses of epithelial folding during Drosophila gastrulation', *Development*, 141(14), pp. 2895–2900. doi: 10.1242/dev.107730.

Kim, J. W. and Lemke, G. (2006) 'Hedgehog-regulated localization of Vax2 controls eye development', *Genes & Development*, 20(20), pp. 2833–2847. doi: 10.1101/gad.1462706.

Kim, J. Y. *et al.* (2016) 'Yap is essential for retinal progenitor cell cycle progression and RPE cell fate acquisition in the developing mouse eye', *Developmental Biology*, pp. 1–12. doi: 10.1016/j.ydbio.2016.09.001.

Klapholz, B. and Brown, N. H. (2017) 'Talin – the master of integrin adhesions', *Journal of Cell Science*, 130(15), pp. 2435–2446. doi: 10.1242/jcs.190991.

Ko, C. S., Kalakuntla, P. and Martin, A. C. (2020) 'Apical Constriction Reversal upon Mitotic Entry Underlies Different Morphogenetic Outcomes of Cell Division', *Molecular Biology of the Cell*, 31(16), pp. 1663–1674. doi: 10.1091/mbc.E19-12-0673.

Krueger, D. *et al.* (2018) 'Downregulation of basal myosin-II is required for cell shape changes and tissue invagination', *The EMBO Journal*, 37(23). doi: 10.15252/embj.2018100170.

Kwan, K. M. *et al.* (2012) 'A complex choreography of cell movements shapes the vertebrate eye', *Development*, 139(2), pp. 359–372. doi: 10.1242/dev.071407.

Lai, S.-L., Chien, A. J. and Moon, R. T. (2009) 'Wnt/Fz signaling and the cytoskeleton: potential roles in tumorigenesis', *Cell Research*, 19(5), pp. 532–545. doi: 10.1038/cr.2009.41.

Lange, A. W. *et al.* (2015) 'Hippo/Yap signaling controls epithelial progenitor cell proliferation and differentiation in the embryonic and adult lung', *Journal of Molecular Cell Biology*, 7(1), pp. 35–47. doi: 10.1093/jmcb/mju046.

Lee, J. and Gross, J. M. (2007) 'Laminin β1 and γ1 Containing Laminins Are Essential for Basement Membrane Integrity in the Zebrafish Eye', *Investigative Ophthalmology & Visual Science*, 48(6), pp. 2483–2490. doi: 10.1167/iovs.06-1211.

Lee, J., Lee, B.-K. and Gross, J. M. (2013a) 'Bcl6a function is required during optic cup formation to prevent p53-dependent apoptosis and colobomata', *Human Molecular Genetics*, 22(17), pp. 3568–3582. doi: 10.1093/hmg/ddt211.

Lee, J., Lee, B.-K. and Gross, J. M. (2013b) 'Bcl6a function is required during optic cup formation to prevent p53-dependent apoptosis and colobomata', *Human Molecular Genetics*, 22(17), pp. 3568–3582. doi: 10.1093/hmg/ddt211.

Lian, I. *et al.* (2010) 'The role of YAP transcription coactivator in regulating stem cell self-renewal and differentiation', *Genes & Development*, 24(11), pp. 1106–1118. doi: 10.1101/gad.1903310.

Lister, J. A. *et al.* (2011) 'Embryonic expression of zebrafish MiT family genes tfe3b, tfeb, and tfec', *Developmental dynamics : an official publication of the American Association of Anatomists*, 240(11), pp. 2529–2538. doi: 10.1002/dvdy.22743.

Liu, O. X. *et al.* (2018) 'ZO-2 induces cytoplasmic retention of YAP by promoting a LATS1-ZO-2-YAP complex at tight junctions', *bioRxiv*, p. 355081. doi: 10.1101/355081.

Longbottom, R. *et al.* (2009) 'Genetic ablation of retinal pigment epithelial cells reveals the adaptive response of the epithelium and impact on photoreceptors', *Proceedings of the National Academy of Sciences of the United States of America*, 106(44), pp. 18728–18733. doi: 10.1073/pnas.0902593106.

Loosli, F. *et al.* (2001a) 'Medaka eyeless is the key factor linking retinal determination and eye growth', *Development*, 128(20), pp. 4035–4044.

Loosli, F. *et al.* (2001b) 'Medaka eyeless is the key factor linking retinal determination and eye growth', *Development*, 128(20), pp. 4035–4044.

Loosli, F. *et al.* (2003) 'Loss of eyes in zebrafish caused by mutation of chokh/rx3', *EMBO reports*, 4(9), pp. 894–899. doi: 10.1038/sj.embor.embor919.

Loosli, F., Winkler, S. and Wittbrodt, J. (1999) 'Six3 overexpression initiates the formation of ectopic retina', *Genes & Development*, 13(6), pp. 649–654.

Lovato, T. L. *et al.* (2009) 'A Molecular Mechanism of Temperature Sensitivity for Mutations Affecting the Drosophila Muscle Regulator Myocyte Enhancer Factor-2', *Genetics*, 183(1), pp. 107–117. doi: 10.1534/genetics.109.105056.

Lu, L., Finegold, M. J. and Johnson, R. L. (2018) 'Hippo pathway coactivators Yap and Taz are required to coordinate mammalian liver regeneration', *Experimental & Molecular Medicine*, 50(1), pp. e423–e423. doi: 10.1038/emm.2017.205.

Lupo, G. *et al.* (2005) 'Dorsoventral patterning of the Xenopus eye: a collaboration of Retinoid, Hedgehog and FGF receptor signaling', *Development*, 132(7), pp. 1737–1748. doi: 10.1242/dev.01726.

Lupo, G. *et al.* (2011) 'Retinoic acid receptor signaling regulates choroid fi ssure closure through independent mechanisms in the ventral optic cup and periocular mesenchyme', 108(21), pp. 8698–8703. doi: 10.1073/pnas.1103802108.

Macdonald, R. *et al.* (1995) 'Midline signalling is required for Pax gene regulation and patterning of the eyes', *Development*, 121(10), pp. 3267–3278.

Mana-Capelli, S. *et al.* (2014) 'Angiomotins link F-actin architecture to Hippo pathway signaling', *Molecular Biology of the Cell*, 25(10), pp. 1676–1685. doi: 10.1091/mbc.E13-11-0701.

Martinez-Morales, J. R. *et al.* (2001) 'Otx genes are required for tissue specification in the developing eye', *Development*, 128(11), pp. 2019–2030.

Martinez-Morales, J. R. *et al.* (2009) 'ojoplano-mediated basal constriction is essential for optic cup morphogenesis', *Development*, 136(13), pp. 2165–2175. doi: 10.1242/dev.033563.

Martinez-Morales, J.-R., Cavodeassi, F. and Bovolenta, P. (2017) 'Coordinated Morphogenetic Mechanisms Shape the Vertebrate Eye', *Frontiers in Neuroscience*, 11. doi: 10.3389/fnins.2017.00721.

Matsuo, I. *et al.* (1995) 'Mouse Otx2 functions in the formation and patterning of rostral head', *Genes & Development*, 9(21), pp. 2646–2658. doi: 10.1101/gad.9.21.2646.

McMahon, C. *et al.* (2009) 'Lmx1b is essential for survival of periocular mesenchymal cells and influences Fgf-mediated retinal patterning in zebrafish', *Developmental Biology*, 332(2), pp. 287–298. doi: 10.1016/j.ydbio.2009.05.577.

McNeill, H. and Reginensi, A. (2017) 'Lats1/2 Regulate Yap/Taz to Control Nephron Progenitor Epithelialization and Inhibit Myofibroblast Formation', *Journal of the American Society of Nephrology: JASN*, 28(3), pp. 852–861. doi: 10.1681/ASN.2016060611.

Miesfeld, J. B. *et al.* (2015a) 'Yap and Taz regulate retinal pigment epithelial cell fate', pp. 3021–3032. doi: 10.1242/dev.119008.

Miesfeld, J. B. *et al.* (2015b) 'Yap and Taz regulate retinal pigment epithelial cell fate', pp. 3021–3032. doi: 10.1242/dev.119008.

Miesfeld, J. B. and Link, B. A. (2014) 'Establishment of transgenic lines to monitor and manipulate Yap/Taz-Tead activity in zebrafish reveals both evolutionarily conserved and divergent functions of the Hippo pathway', *Mechanisms of Development*, 133, pp. 177–188. doi: 10.1016/j.mod.2014.02.003.

Miller, M. T. and Strömland, K. (1999) 'Teratogen update: thalidomide: a review, with a focus on ocular findings and new potential uses', *Teratology*, 60(5), pp. 306–321. doi: 10.1002/(SICI)1096-9926(199911)60:5<306::AID-TERA11>3.0.CO;2-Y.

Morcillo, J. *et al.* (2006a) 'Proper patterning of the optic fissure requires the sequential activity of BMP7 and SHH.', *Development*, 133(16), pp. 3179–3190. doi: 10.1242/dev.02493.

Morcillo, J. *et al.* (2006b) 'Proper patterning of the optic fissure requires the sequential activity of BMP7 and SHH.', *Development*, 133(16), pp. 3179–3190. doi: 10.1242/dev.02493.

Moreno-Mármol, T. *et al.* (2020) 'Stretching of the retinal pigment epithelium contributes to zebrafish optic cup morphogenesis', *bioRxiv*, p. 2020.09.23.310631. doi: 10.1101/2020.09.23.310631.

Moreno-Marmol, T., Cavodeassi, F. and Bovolenta, P. (2018a) 'Setting Eyes on the Retinal Pigment Epithelium', *Frontiers in Cell and Developmental Biology*, 6. doi: 10.3389/fcell.2018.00145.

Moreno-Marmol, T., Cavodeassi, F. and Bovolenta, P. (2018b) 'Setting Eyes on the Retinal Pigment Epithelium', *Frontiers in Cell and Developmental Biology*, 6. doi: 10.3389/fcell.2018.00145.

Morgan, J. T., Murphy, C. J. and Russell, P. (2013) 'What do mechanotransduction, Hippo, Wnt, and TGFβ have in common? YAP and TAZ as key orchestrating molecules in ocular health and disease', *Experimental Eye Research*, 115, pp. 1–12. doi: 10.1016/j.exer.2013.06.012.

Morin-Kensicki, E. M. *et al.* (2006) 'Defects in Yolk Sac Vasculogenesis, Chorioallantoic Fusion, and Embryonic Axis Elongation in Mice with Targeted Disruption of Yap65', *Molecular and Cellular Biology*, 26(1), pp. 77–87. doi: 10.1128/MCB.26.1.77-87.2006.

Nakajima, H. *et al.* (2017) 'Flow-Dependent Endothelial YAP Regulation Contributes to Vessel Maintenance', *Developmental Cell*, 40(6), pp. 523-536.e6. doi: 10.1016/j.devcel.2017.02.019.

Nguyen, M. and Arnheiter, H. (2000) 'Signaling and transcriptional regulation in early mammalian eye development: a link between FGF and MITF', *Development*, 127(16), pp. 3581–3591.

Nicolás-Pérez, M. *et al.* (2016) ‘Analysis of cellular behavior and cytoskeletal dynamics reveal a constriction mechanism driving optic cup morphogenesis.’, *eLife*, 5. doi: 10.7554/eLife.15797.

Nikolopoulou, E. *et al.* (2017) ‘Neural tube closure: cellular, molecular and biomechanical mechanisms’, *Development (Cambridge, England)*, 144(4), pp. 552–566. doi: 10.1242/dev.145904.

Nukuda, A. *et al.* (2015) ‘Stiff substrates increase YAP-signaling-mediated matrix metalloproteinase-7 expression’, *Oncogenesis*, 4(9), p. e165. doi: 10.1038/oncsis.2015.24.

Ogilvie, J. M. *et al.* (1999) ‘A reliable method for organ culture of neonatal mouse retina with long-term survival’, *Journal of Neuroscience Methods*, 87(1), pp. 57–65. doi: 10.1016/s0165-0270(98)00157-5.

Ozeki, H. *et al.* (2000) ‘Apoptosis is associated with formation and persistence of the embryonic fissure’, *Current Eye Research*, 20(5), pp. 367–372.

Pan, D. (2007) ‘Hippo signaling in organ size control’, *Genes & Development*, 21(8), pp. 886–897. doi: 10.1101/gad.1536007.

Panciera, T. *et al.* (2016) ‘Induction of Expandable Tissue-Specific Stem/Progenitor Cells through Transient Expression of YAP/TAZ’, *Cell Stem Cell*, 19(6), pp. 725–737. doi: 10.1016/j.stem.2016.08.009.

Parmigiani, C. and McAvoy, J. (1984) ‘Localisation of laminin and fibronectin during rat lens morphogenesis’, *Differentiation; Research in Biological Diversity*, 28(1), pp. 53–61. doi: 10.1111/j.1432-0436.1984.tb00266.x.

Pasquale, E. B. (2008) ‘Eph-Ephrin Bidirectional Signaling in Physiology and Disease’, *Cell*, 133(1), pp. 38–52. doi: 10.1016/j.cell.2008.03.011.

Pearl, E. J., Li, J. and Green, J. B. A. (2017) ‘Cellular systems for epithelial invagination’, *Philosophical Transactions of the Royal Society B: Biological Sciences*, 372(1720). doi: 10.1098/rstb.2015.0526.

Pearson, R. A. *et al.* (2005) ‘ATP Released via Gap Junction Hemichannels from the Pigment Epithelium Regulates Neural Retinal Progenitor Proliferation’, *Neuron*, 46(5), pp. 731–744. doi: 10.1016/j.neuron.2005.04.024.

Perron, M. *et al.* (2003) ‘A novel function for Hedgehog signalling in retinal pigment epithelium differentiation’, *Development*, 130(8), pp. 1565–1577. doi: 10.1242/dev.00391.

Peterson, P. E. *et al.* (1993) ‘Characterization of the extracellular matrix during somitogenesis in the long-tailed monkey (Macaca fascicularis)’, *Acta Anatomica*, 146(4), pp. 223–233. doi: 10.1159/000147460.

Peterson, P. E. *et al.* (1995) 'Localisation of glycoproteins and glycosaminoglycans during early eye development in the macaque.', *Journal of Anatomy*, 186(Pt 1), pp. 31–42.

Piccolo, S., Dupont, S. and Cordenonsi, M. (2014a) 'THE BIOLOGY OF YAP/TAZ: HIPPO SIGNALING AND BEYOND', *Beyond. Physiol Rev*, 94, pp. 1287–1312. doi: 10.1152/physrev.00005.2014.

Piccolo, S., Dupont, S. and Cordenonsi, M. (2014b) 'The biology of YAP/TAZ: hippo signaling and beyond', *Physiological Reviews*, 94(4), pp. 1287–1312. doi: 10.1152/physrev.00005.2014.

Picker, A. *et al.* (2009) 'Dynamic Coupling of Pattern Formation and Morphogenesis in the Developing Vertebrate Retina', *PLOS Biology*, 7(10), p. e1000214. doi: 10.1371/journal.pbio.1000214.

Plouffe, S. W. *et al.* (2018) 'The Hippo pathway effector proteins YAP and TAZ have both distinct and overlapping functions in the cell', *The Journal of Biological Chemistry*, 293(28), pp. 11230–11240. doi: 10.1074/jbc.RA118.002715.

Porazinski, S. *et al.* (2015a) 'YAP is essential for tissue tension to ensure vertebrate 3D body shape', *Nature*, 521(7551), pp. 217–221. doi: 10.1038/nature14215.

Porazinski, S. *et al.* (2015b) 'YAP is essential for tissue tension to ensure vertebrate 3D body shape', *Nature*, 521(7551), pp. 217–221. doi: 10.1038/nature14215.

Porazinski, S. and Ladomery, M. (2018) 'Alternative Splicing in the Hippo Pathway—Implications for Disease and Potential Therapeutic Targets', *Genes*, 9(3). doi: 10.3390/genes9030161.

Rausch, V. and Hansen, C. G. (2020) 'The Hippo Pathway, YAP/TAZ, and the Plasma Membrane', *Trends in Cell Biology*, 30(1), pp. 32–48. doi: 10.1016/j.tcb.2019.10.005.

Raymond, S. M. and Jackson, I. J. (1995) 'The retinal pigmented epithelium is required for development and maintenance of the mouse neural retina', *Current biology: CB*, 5(11), pp. 1286–1295. doi: 10.1016/s0960-9822(95)00255-7.

Rebagliati, M. R. *et al.* (1998) 'Zebrafish nodal-related genes are implicated in axial patterning and establishing left-right asymmetry', *Developmental Biology*, 199(2), pp. 261–272. doi: 10.1006/dbio.1998.8935.

Reis, L. M. and Semina, E. V. (2015) 'Conserved genetic pathways associated with microphthalmia, anophthalmia, and coloboma', *Birth defects research. Part C, Embryo today : reviews*, 105(2), pp. 96–113. doi: 10.1002/bdrc.21097.

Roessler, E. *et al.* (1996) 'Mutations in the human Sonic Hedgehog gene cause holoprosencephaly', *Nature Genetics*, 14(3), pp. 357–360. doi: 10.1038/ng1196-357.

Salah, Z. and Aqeilan, R. I. (2011) 'WW domain interactions regulate the Hippo tumor suppressor pathway', *Cell Death & Disease*, 2(6), p. e172. doi: 10.1038/cddis.2011.53.

Schroeder, M. C. and Halder, G. (2012) 'Regulation of the Hippo pathway by cell architecture and mechanical signals', *Seminars in Cell & Developmental Biology*, 23(7), pp. 803–811. doi: 10.1016/j.semcdb.2012.06.001.

Sedykh, I. *et al.* (2017) 'Zebrafish zic2 controls formation of periocular neural crest and choroid fissure morphogenesis', *Developmental Biology*, 429(1), pp. 92–104. doi: 10.1016/j.ydbio.2017.07.003.

Sidhaye, J. and Norden, C. (2017) 'Concerted action of neuroepithelial basal shrinkage and active epithelial migration ensures efficient optic cup morphogenesis', *eLife*. Edited by D. Y. Stainier, 6, p. e22689. doi: 10.7554/eLife.22689.

Sinn, R. and Wittbrodt, J. (2013) 'An eye on eye development', *Mechanisms of Development*, 130(6–8), pp. 347–358. doi: 10.1016/j.mod.2013.05.001.

Skalicky, S. E. *et al.* (2013) 'Microphthalmia, Anophthalmia, and Coloboma and Associated Ocular and Systemic Features', *JAMA Ophthalmology*, 131(12), p. 1517. doi: 10.1001/jamaophthalmol.2013.5305.

Srivastava, D. *et al.* (2019) 'Modulation of Yorkie activity by alternative splicing is required for developmental stability', *bioRxiv*, p. 2019.12.19.882779. doi: 10.1101/2019.12.19.882779.

Steinfeld, J. *et al.* (2013) 'RPE specification in the chick is mediated by surface ectoderm-derived BMP and Wnt signalling', *Development*, 140(24), pp. 4959–4969. doi: 10.1242/dev.096990.

Stigloher, C. *et al.* (2006) 'Segregation of telencephalic and eye-field identities inside the zebrafish forebrain territory is controlled by Rx3', *Development*, 133(15), pp. 2925–2935. doi: 10.1242/dev.02450.

Strauss, O. (2005) 'The Retinal Pigment Epithelium in Visual Function', *Physiological Reviews*, 85(3), pp. 845–881. doi: 10.1152/physrev.00021.2004.

Tan, G. *et al.* (2009) 'Temperature-Sensitive Mutations Made Easy: Generating Conditional Mutations by Using Temperature-Sensitive Inteins That Function Within Different Temperature Ranges', *Genetics*, 183(1), pp. 13–22. doi: 10.1534/genetics.109.104794.

Tang, C. *et al.* (2018) 'Transcriptional Co-activator Functions of YAP and TAZ Are Inversely Regulated by Tyrosine Phosphorylation Status of Parafibromin', *iScience*, 1, pp. 1–15. doi: 10.1016/j.isci.2018.01.003.

Tibber, M. S., Becker, D. and Jeffery, G. (2007) 'Levels of transient gap junctions between the retinal pigment epithelium and the neuroblastic retina are influenced

by catecholamines and correlate with patterns of cell production', *The Journal of Comparative Neurology*, 503(1), pp. 128–134. doi: 10.1002/cne.21388.

Trede NS, M. N. (2007) *Method for isolation of PCR-ready genomic DNA from zebrafish tissues. - Bio Techniques*. Available at: https://www.ncbi.nlm.nih.gov/pubmed/18072590 (Accessed: 9 January 2020).

Tsuji, N. *et al.* (2012) 'Organogenesis of mild ocular coloboma in FLS mice: Failure of basement membrane disintegration at optic fissure margins', *Experimental Eye Research*, 94(1), pp. 174–178. doi: 10.1016/j.exer.2011.12.004.

Tucker, P. *et al.* (2001) 'The eyeless mouse mutation (ey1) removes an alternative start codon from the Rx/rax homeobox gene', *Genesis (New York, N.Y.: 2000)*, 31(1), pp. 43–53. doi: 10.1002/gene.10003.

Varelas, X. (2014) 'The Hippo pathway effectors TAZ and YAP in development, homeostasis and disease', *Development*, 141(8), pp. 1614–1626. doi: 10.1242/dev.102376.

Varga, Z. M., Wegner, J. and Westerfield, M. (1999) 'Anterior movement of ventral diencephalic precursors separates the primordial eye field in the neural plate and requires cyclops', *Development*, 126(24), pp. 5533–5546.

Vázquez-Marín, J. *et al.* (2019) 'yap1b, a divergent Yap/Taz family member, cooperates with yap1 in survival and morphogenesis via common transcriptional targets', *Development*, 146(13). doi: 10.1242/dev.173286.

Veien, E. S. *et al.* (2008) 'Canonical Wnt signaling is required for the maintenance of dorsal retinal identity', *Development*, 135(24), pp. 4101–4111. doi: 10.1242/dev.027367.

Visetsouk, M. R. *et al.* (2018) 'Basal epithelial tissue folding is mediated by differential regulation of microtubules', *Development (Cambridge, England)*, 145(22). doi: 10.1242/dev.167031.

van de Water, S. *et al.* (2001) 'Ectopic Wnt signal determines the eyeless phenotype of zebrafish masterblind mutant', *Development (Cambridge, England)*, 128(20), pp. 3877–3888.

Weiss, O. *et al.* (2012) 'Abnormal vasculature interferes with optic fissure closure in lmo2 mutant zebrafish embryos', *Developmental Biology*, 369(2), pp. 191–198. doi: 10.1016/j.ydbio.2012.06.029.

Wen, F.-L., Wang, Y.-C. and Shibata, T. (2017) 'Epithelial Folding Driven by Apical or Basal-Lateral Modulation: Geometric Features, Mechanical Inference, and Boundary Effects', *Biophysical Journal*, 112(12), pp. 2683–2695. doi: 10.1016/j.bpj.2017.05.012.

Westenskow, P. D. *et al.* (2010) 'Ectopic Mitf in the embryonic chick retina by co-transfection of β-catenin and Otx2', *Investigative Ophthalmology & Visual Science*, 51(10), pp. 5328–5335. doi: 10.1167/iovs.09-5015.

Westenskow, P., Piccolo, S. and Fuhrmann, S. (2009) 'β-catenin controls differentiation of the retinal pigment epithelium in the mouse optic cup by regulating Mitf and Otx2 expression', *Development (Cambridge, England)*, 136(15), pp. 2505–2510. doi: 10.1242/dev.032136.

Williams, A. L. and Bohnsack, B. L. (2015) 'Neural crest derivatives in ocular development: discerning the eye of the storm', *Birth Defects Research. Part C, Embryo Today: Reviews*, 105(2), pp. 87–95. doi: 10.1002/bdrc.21095.

Williamson, K. A. *et al.* (2014) 'Heterozygous loss-of-function mutations in YAP1 cause both isolated and syndromic optic fissure closure defects', *American Journal of Human Genetics*. doi: 10.1016/j.ajhg.2014.01.001.

Wilson, L. and Maden, M. (2005) 'The mechanisms of dorsoventral patterning in the vertebrate neural tube', *Developmental Biology*, 282(1), pp. 1–13. doi: 10.1016/j.ydbio.2005.02.027.

Wilson, S. W. and Houart, C. (2004) 'Early steps in the development of the forebrain', *Developmental Cell*, 6(2), pp. 167–181. doi: 10.1016/s1534-5807(04)00027-9.

Winkler, S. *et al.* (2000) 'The conditional medaka mutation eyeless uncouples patterning and morphogenesis of the eye', *Development*, 127(9), pp. 1911–1919.

Wu, S. *et al.* (2003) 'hippo encodes a Ste-20 family protein kinase that restricts cell proliferation and promotes apoptosis in conjunction with salvador and warts', *Cell*, 114(4), pp. 445–456. doi: 10.1016/s0092-8674(03)00549-x.

Xu, T. *et al.* (1995) 'Identifying tumor suppressors in genetic mosaics: the Drosophila lats gene encodes a putative protein kinase', *Development*, 121(4), pp. 1053–1063.

Yamamoto, Y., Stock, D. W. and Jeffery, W. R. (2004) 'Hedgehog signalling controls eye degeneration in blind cavefish', *Nature*, 431(7010), pp. 844–847. doi: 10.1038/nature02864.

Yang, C.-C. *et al.* (2015) 'Differential regulation of the Hippo pathway by adherens junctions and apical–basal cell polarity modules', *Proceedings of the National Academy of Sciences*, 112(6), pp. 1785–1790. doi: 10.1073/pnas.1420850112.

Yang, X.-J. (2004) 'Roles of cell-extrinsic growth factors in vertebrate eye pattern formation and retinogenesis', *Seminars in Cell & Developmental Biology*, 15(1), pp. 91–103. doi: 10.1016/j.semcdb.2003.09.004.

Young, R. M. *et al.* (2019) 'Compensatory growth renders Tcf7l1a dispensable for eye formation despite its requirement in eye field specification', *eLife*, 8. doi: 10.7554/eLife.40093.

Yun, S. *et al.* (2009) 'Lhx2 links the intrinsic and extrinsic factors that control optic cup formation', *Development*, 136(23), pp. 3895–3906. doi: 10.1242/dev.041202.

Zeng, Z. *et al.* (2015) 'Temperature-sensitive splicing of mitfa by an intron mutation in zebrafish', *Pigment cell & melanoma research*, 28(2), pp. 229–232. doi: 10.1111/pcmr.12336.

Zhang, J., Smolen, G. A. and Haber, D. A. (2008) 'Negative Regulation of YAP by LATS1 Underscores Evolutionary Conservation of the Drosophila Hippo Pathway', *Cancer Research*, 68(8), pp. 2789–2794. doi: 10.1158/0008-5472.CAN-07-6205.

Zhang, X.-M. and Yang, X.-J. (2001) 'Temporal and Spatial Effects of Sonic Hedgehog Signaling in Chick Eye Morphogenesis', *Developmental biology*, 233(2), pp. 271–290. doi: 10.1006/dbio.2000.0195.

Zhao, B., Li, L., Tumaneng, K., *et al.* (2010) 'A coordinated phosphorylation by Lats and CK1 regulates YAP stability through SCFβ-TRCP', *Genes & Development*, 24(1), pp. 72–85. doi: 10.1101/gad.1843810.

Zhao, B., Li, L., Lei, Q., *et al.* (2010) 'The Hippo–YAP pathway in organ size control and tumorigenesis: an updated version', *Genes & Development*, 24(9), pp. 862–874. doi: 10.1101/gad.1909210.

Zhao, B., Tumaneng, K. and Guan, K.-L. (2011) 'The Hippo pathway in organ size control, tissue regeneration and stem cell self-renewal', *Nature Publishing Group*, 13. doi: 10.1038/ncb2303.

Zhou, C.-J. *et al.* (2008) 'Ocular coloboma and dorsoventral neuroretinal patterning defects in Lrp6 mutant eyes', *Developmental Dynamics*, 237(12), pp. 3681–3689. doi: 10.1002/dvdy.21770.

Zhu, C., Li, L. and Zhao, B. (2015) 'The regulation and function of YAP transcription co-activator', *Acta Biochimica Et Biophysica Sinica*, 47(1), pp. 16–28. doi: 10.1093/abbs/gmu110.

Zou, C. and Levine, E. M. (2012) 'Vsx2 Controls Eye Organogenesis and Retinal Progenitor Identity Via Homeodomain and Non-Homeodomain Residues Required for High Affinity DNA Binding', *PLOS Genetics*, 8(9), p. e1002924. doi: 10.1371/journal.pgen.1002924.

Zuber, M. E. *et al.* (2003) 'Specification of the vertebrate eye by a network of eye field transcription factors', *Development (Cambridge, England)*, 130(21), pp. 5155–5167. doi: 10.1242/dev.00723.